
HIGHER-ORDER ALGORITHMS AND IMPLICIT REGULARIZATION FOR NONLINEARLY PARAMETERIZED ADAPTIVE CONTROL

A PREPRINT

Nicholas M. Boffi and Jean-Jacques E. Slotine

ABSTRACT

Stable concurrent learning and control of dynamical systems is the subject of adaptive control. Adaptive control is a field with many practical applications and a rich theory, but much of the development for nonlinear systems revolves around a few key algorithms. By exploiting strong connections between classical nonlinear adaptive control techniques and recent progress in optimization and machine learning, we show that there exists considerable untapped potential in algorithm development for nonlinear adaptive control. We present a large set of new globally convergent adaptive control algorithms that are applicable both to linearly parameterized systems and to nonlinearly parameterized systems satisfying a certain monotonicity requirement. We adopt a variational formalism based on the Bregman Lagrangian to define a general framework that systematically generates higher-order in-time velocity gradient algorithms. These general algorithms reduce to a recently developed method as a special case, and naturally extend to composite methods that combine perspectives from both adaptive control and system identification. We identify and utilize a provocative connection between adaptive control algorithms for nonlinearly parameterized systems and algorithms for isotonic regression and provable neural network learning to extend these higher-order algorithms to the nonlinearly parameterized realm. Modifications to all presented algorithms inspired by recent progress in distributed stochastic gradient descent algorithms are also developed. We show that time-varying learning rate matrices based on exponential/bounded gain forgetting least squares can be stably employed in the higher-order context, and conditions for their applicability in the nonlinearly parameterized setting are provided. We generalize our algorithms to the non-Euclidean setting and show that the Euler Lagrange equations for the Bregman Lagrangian lead to “natural gradient” and mirror descent-like adaptation laws with momentum that incorporate local geometry through a Hessian metric specified by a convex function. In the infinite friction limit, these higher-order natural adaptation laws reduce to first-order natural laws that have recently been used to respect physical Riemannian constraints during adaptation in robotic applications. We prove that, when the system is in the over-parameterized regime typical of machine learning or is not persistently excited, these non-Euclidean adaptation laws implicitly regularize the system model by minimizing the convex function that specifies the metric throughout adaptation. Local geometry imposed during adaptation thus may be used to select parameter vectors – out of the many that will lead to perfect tracking – for desired properties such as sparsity. We illustrate our analysis with simulations using a higher-order algorithm for nonlinearly parameterized systems to learn regularized hidden layer weights in a three-layer feedforward neural network.

1 Introduction

Adaptation is an online learning problem whose objective is to stably control or predict the dynamics of an unknown nonlinear system. This task is accomplished by constructing an approximation $\hat{\mathbf{f}} = \mathbf{f}(\mathbf{x}, \hat{\mathbf{a}}, t)$ to the true dynamics $\mathbf{f}(\mathbf{x}, \mathbf{a}, t)$ through the adjustment of a set of parameters $\hat{\mathbf{a}}(t)$ under the assumption that there exists a true set of parameters \mathbf{a} that perfectly fits the dynamics. The overarching goal of adaptive control is provably stable concurrent learning and control of dynamical systems.

Adaptive control theory is a mature field, and many results exist tailored to specific system structures (Ioannou & Sun, 2012; Narendra & Annaswamy, 2005; J.-J. Slotine & Li, 1991). An adaptive control algorithm typically consists of a parameter estimator coupled in feedback to the controlled system, and the parameter estimator is often strongly inspired by gradient-based optimization algorithms. A significant difference between standard optimization algorithms and

estimators for adaptive control is that the parameter estimator must not only converge to a set of parameters that leads to perfect tracking, but the system must remain stable throughout adaptation. The additional requirement of stability prevents the immediate application of optimization algorithms as adaptive control algorithms, and stability must be proved by jointly analyzing the closed-loop system and estimator.

Despite the difficulty of the adaptive control problem, significant success has been achieved even for nonlinear systems in the *linearly parameterized* setting, where the dynamics approximation is of the form $\hat{\mathbf{f}} = \mathbf{Y}(\mathbf{x}, t)\hat{\mathbf{a}}$ for some known regressor $\mathbf{Y}(\mathbf{x}, t)$. Examples include the adaptive robot trajectory controller of J.-J. E. Slotine and Li (1987) and the neural network-based controller of Sanner and Slotine (1992), which employs a mathematical expansion in nonlinear physical basis functions to uniformly approximate the unknown dynamics despite linearity in the parameters.

Unlike its linear counterpart, solutions to the adaptive control problem in the general nonlinearly parameterized setting $\hat{\mathbf{f}} = \mathbf{f}(\mathbf{x}, \hat{\mathbf{a}}, t)$ have remained elusive. Intuitively, this is unsurprising: gradient-based algorithms generally have guarantees only for convex loss functions. In the linearly parameterized setting this requirement will be satisfied, but when the parameters appear nonlinearly, the problem is immediately in the difficult realm of non-convex optimization. Nevertheless, progress has been made in specific cases, such as with a convex or concave parameterization (Ai-Poh Loh, Annaswamy, & Skantze, 1999; Annaswamy, Skantze, & Loh, 1998; Kojić & Annaswamy, 2002), with a monotonicity condition (Ortega, Gromov, Nuño, Pyrkin, & Romero, 2019; I. Tyukin, 2011; Tyukin, Prokhorov, & van Leeuwen, 2007), through the Immersion and Invariance (I&I) approach (Astolfi & Ortega, 2003; Liu, Ortega, Su, & Chu, 2010), and through the velocity gradient methodology (A. L. Fradkov, 1999; Fradkov, 1979; Ortega, 1996). Here, we approach the nonlinearly parameterized setting via the velocity gradient approach and through monotonicity assumptions typical of generalized linear models in statistics (Kakade, Kalai, Kanade, & Shamir, 2011).

Our work continues in a recent tradition that utilizes a continuous-time view to analyze optimization algorithms (Bettencourt, Jordan, & Wilson, 2018; Boffi & Slotine, 2020; Diakonikolas & Jordan, 2019; Maddison, Paulin, Teh, O'Donoghue, & Doucet, 2018; Muehlebach & Jordan, 2019; Wibisono, Wilson, & Jordan, 2016). While the continuous-time view of optimization has seen a resurgence after it was used by Su, Boyd, and Candès (2016) to provide an intuitive justification for Nesterov's accelerated gradient method (Nesterov, 1983), continuous-time differential equations were used as early as 1964 by Polyak to derive the classical momentum or "heavy ball" optimization method (B. Polyak, 1964). Given the gradient-based nature of many adaptive control algorithms, the continuous-time view of optimization provides a natural bridge from modern optimization to modern adaptive control.

Continuous-time often affords simpler proofs and it enables the application of physical intuition when reasoning about optimization algorithms, but finding the limiting differential equations for a given discrete-time optimization algorithm may still be a daunting task. The reverse direction – given a continuous-time dynamics, finding a discretization that provably retains the convergence rates of the differential equation – is similarly challenging. In a significant advance, Wibisono et al. (2016) showed that many accelerated methods in optimization can all be derived via a variational point of view from a single mathematical object known as the Bregman Lagrangian. The Bregman Lagrangian leads to second-order mass-spring-damper-like dynamics, and careful discretization provides discrete-time algorithms such as Nesterov's celebrated accelerated gradient method (Nesterov, 1983).

In this paper, we contribute to the linearly and nonlinearly parameterized (under the monotonicity assumptions of (Tyukin et al., 2007)) adaptive control problems. We utilize the Bregman Lagrangian in tandem with the velocity gradient methodology (A. L. Fradkov, 1999; Fradkov, 1979) to define a general formalism that generates higher-order in-time (Morse, 1992) velocity gradient algorithms. Our key insight is that velocity gradient algorithms provide an optimization-like framework that encompasses many well-known adaptive control algorithms, and that the velocity gradient "loss function" can be placed directly in the Euclidean Bregman Lagrangian. This contribution generalizes and extends a recently developed algorithm (Gaudio, Gibson, Annaswamy, & Bolender, 2019), which can be seen as a special case of one of our higher-order velocity gradient laws. Based on the first-order velocity gradient methodology, these higher-order laws lead naturally to the development of composite higher-order adaptation algorithms for linearly parameterized systems (J.-J. Slotine & Li, 1991). By use of a proportional-integral (PI) form, these composite laws are driven directly by the function approximation error $\tilde{\mathbf{f}} = \hat{\mathbf{f}} - \mathbf{f}$ itself, and do not require any explicit filtering of the system dynamics. Much like the well-known reduced-order Luenberger observer, the PI form enables obtaining \mathbf{f} in the adaptation law despite the fact that this signal is not explicitly measured (Luenberger, 1979).

By analogy between the nonlinearly parameterized law presented by Tyukin et al. (2007) and recent results in isotonic regression (Goel & Klivans, 2017; Goel, Klivans, & Meka, 2018; Kakade et al., 2011), we extend these higher-order algorithms to the nonlinearly parameterized setting. In a similar vein, we draw an orthogonal connecting thread to machine learning, and demonstrate a stable modification to our algorithms inspired by the Elastic Averaging Stochastic Gradient Descent (EASGD) algorithm (Zhang, Choromanska, & LeCun, 2014). We then show how to combine all of

our algorithms with time-dependent learning rates through the bounded gain forgetting formalism (J.-J. Slotine & Li, 1991).

It is well known in adaptive control that the true parameters are only recovered when the desired system trajectory satisfies a strong condition known as *persistent excitation* (Narendra & Annaswamy, 2005). In general, an adaptation law need only find a set of parameters that leads to perfect tracking, and hence only needs to approximate the system dynamics along the system trajectory. Herein we ask the question, “*when the system is not persistently excited, what can be said about the parameters that adaptive control converges to, besides $\dot{\mathbf{a}} = 0$?*” This question is strongly related to a line of recent work that analyzes the implicit bias of optimization algorithms in machine learning (Azizan & Hassibi, 2019; Azizan, Lale, & Hassibi, 2019; Gunasekar, Lee, Soudry, & Srebro, 2018a, 2018b; Soudry, Hoffer, Nacson, Gunasekar, & Srebro, 2018). By considering the non-Euclidean Bregman Lagrangian, we find and prove stability of several higher-order “natural gradient” (Amari, 1998) and mirror descent (Beck & Teboulle, 2003; Nemirovski & Yudin, 1983)-like algorithms. We prove that the use of non-Euclidean adaptation laws implicitly regularizes the system model and converges to trajectory-tracking solutions that minimize a given convex function ψ that in part defines the non-Euclidean algorithm. From this perspective, standard Euclidean adaptation laws implicitly utilize l_2 regularization on the parameters. We illustrate our theory with simulations on a system model defined by a three layer neural network.

The paper is organized as follows. In Sec. 2, we present some required mathematical background. This includes a basic review of direct adaptive control (Sec. 2.1), the velocity gradient formalism (Sec. 2.2), and the Bregman Lagrangian. Sec. 3 presents our main contributions, with our higher-order velocity gradient laws in Sec. 3.1, our first-order non-filtered composite laws in Sec. 3.2, our higher-order composite laws and higher-order laws for nonlinearly parameterized systems in Sec. 3.3, the elastic modification in Sec. 3.4, and our extension to time-dependent learning rates in Sec. 3.5. We extend our results to the non-Euclidean setting and discuss implicit regularization in Sec. 4. We illustrate our implicit regularization results via simulation in Sec. 5. We conclude with some closing remarks and future directions in Sec. 6.

2 Preliminaries

2.1 Direct adaptive control

We begin with an introduction to the formalism of direct adaptive control, and describe the systems to which our results apply. For simplicity, we restrict ourselves to the class of n^{th} -order nonlinear systems

$$x^{(n)} + f(\mathbf{x}, \mathbf{a}, t) = u \quad (1)$$

where $x^{(i)} \in \mathbb{R}$ denotes the i^{th} derivative of x , $\mathbf{x} = (x, x^{(1)}, \dots, x^{(n-1)})^T \in \mathbb{R}^n$ is the system state, $\mathbf{a} \in \mathbb{R}^p$ is a vector of unknown parameters, $f : \mathbb{R}^n \times \mathbb{R}^p \times \mathbb{R}_+ \rightarrow \mathbb{R}$ is of known functional form but is unknown due to its dependence on \mathbf{a} , and $u \in \mathbb{R}$ is the control input. The goal of adaptive control is stable concurrent learning and control. In other words, we seek to design a feedback control law $u = u(\mathbf{x}, \hat{\mathbf{a}})$ that depends on a set of adjustable parameters $\hat{\mathbf{a}} \in \mathbb{R}^p$ and ensures that $\mathbf{x}(t) \rightarrow \mathbf{x}_d(t)$ where $\mathbf{x}_d(t) \in \mathbb{R}^n$ is a known desired trajectory with all system signals remaining bounded. The estimated parameters $\hat{\mathbf{a}}$ are updated according to a learning rule or adaptation law

$$\dot{\hat{\mathbf{a}}} = \mathbf{g}(\mathbf{a}, \hat{\mathbf{a}}, \mathbf{x}) \quad (2)$$

where $\mathbf{g} : \mathbb{R}^p \times \mathbb{R}^p \times \mathbb{R}^n \rightarrow \mathbb{R}^p$ must be implementable solely in terms of known system signals despite its potential dependence on \mathbf{a} . Like reinforcement learning, adaptive control is fundamentally an online learning problem where the data-generating process is a nonlinear dynamical system coupled in feedback to the learning process, though it typically involves much faster convergence. For n^{th} order systems as considered in (1), a common approach is to define the *sliding variable* (J.-J. Slotine & Li, 1991)

$$s = \left(\frac{d}{dt} + \lambda \right)^{n-1} \tilde{x} = \tilde{x}^{(n-1)} - \tilde{x}_r^{(n-1)} \quad (3)$$

where we have defined $\tilde{x}^{(i)}(t) = x^{(i)}(t) - x_d^{(i)}(t)$ and $\tilde{x}_r^{(n-1)}$ as the remainder based on the definition of s . According to the definition (3), s obeys the differential equation

$$\dot{s} = u - f(\mathbf{x}, \mathbf{a}, t) - \tilde{x}_r^{(n-1)}. \quad (4)$$

Hence, from (4), we may choose

$$u = f(\mathbf{x}, \hat{\mathbf{a}}, t) + \tilde{x}_r^{(n-1)} - \eta s \quad (5)$$

to obtain the stable first-order linear filter

$$\dot{s} = -\eta s + f(\mathbf{x}, \hat{\mathbf{a}}, t) - f(\mathbf{x}, \mathbf{a}, t). \quad (6)$$

For future convenience, we define $\tilde{f}(\mathbf{x}, \hat{\mathbf{a}}, \mathbf{a}, t) = f(\mathbf{x}, \hat{\mathbf{a}}, t) - f(\mathbf{x}, \mathbf{a}, t)$ and we will omit its arguments when clear from the context. From the definition of s in (3), $s = 0$ defines the *dynamics*

$$\left(\frac{d}{dt} + \lambda \right)^{n-1} \tilde{x} = 0. \quad (7)$$

Equation (7) is a stable $(n-1)^{\text{th}}$ -order filter which ensures that $\tilde{x} \rightarrow 0$ exponentially. For systems of the form (1), it is thus sufficient to consider the two first-order dynamics (2) and (6), and the adaptive control problem has been reduced to finding a learning algorithm that ensures $s \rightarrow 0$.

Remark 2.1. Systems in the matched uncertainty form

$$\dot{\mathbf{x}} = \mathbf{A}\mathbf{x} + \mathbf{b}(u - f(\mathbf{x}, \mathbf{a}, t)),$$

where the constant pair (\mathbf{A}, \mathbf{b}) is controllable and the constant parameter vector \mathbf{a} in the nonlinear function $f(\mathbf{x}, \mathbf{a}, t)$ is unknown, can always be put in the form (1) by using a state transformation to the second controllability canonical form – see Luenberger (1979), Chapter 8.8. After such a transformation, the new state variables \mathbf{z} satisfy $\dot{z}_i = z_{i+1}$ for $i < n$ and $\dot{z}_n = -\sum_{i=1}^{n-1} a_i z_i + u - f(\mathbf{x}, \mathbf{a}, t)$. Defining s as in (3) and correctly computing u leads to (6). Hence, all results in this paper extend immediately to such systems. \diamond

Remark 2.2. The fundamental utility of defining the variable s is its conversion of the adaptive control problem for the n^{th} -order system (1) to an adaptive control problem for the first-order system (6). Our results may be simply extended to other error models (Ai-Poh Loh et al., 1999; Narendra & Annaswamy, 2005) of the form (6), or error models with similar input-output guarantees, as summarized by Lemma A.1. \diamond

Remark 2.3. We will use \mathbf{f} to denote the equivalent first-order system to (1), $\dot{\mathbf{x}} = \mathbf{f}(\mathbf{x}, \mathbf{a}, t) + \mathbf{u}$, where $\mathbf{f} = (x_2, x_3, \dots, f(\mathbf{x}, \mathbf{a}, t))$ and $\mathbf{u} = (0, 0, \dots, u)$. \diamond

A classic setting for adaptive control is when the unknown nonlinear dynamics depends linearly on the set of unknown parameters, that is

$$f(\mathbf{x}, \mathbf{a}, t) = \mathbf{Y}(\mathbf{x}, t)\mathbf{a},$$

with $\mathbf{Y} : \mathbb{R}^n \times \mathbb{R}_+ \rightarrow \mathbb{R}^{1 \times p}$ a known function. In this setting, a well-known algorithm is the adaptive controller of J.-J. Slotine and Coetsee (1986), given by

$$\dot{\mathbf{a}} = -\mathbf{P}\mathbf{Y}^T s, \quad (8)$$

and its extension to multi-input adaptive robot control (J.-J. E. Slotine & Li, 1987), where $\mathbf{P} = \mathbf{P}^T > 0 \in \mathbb{R}^{p \times p}$ is a constant positive definite matrix of learning rates. Consideration of the Lyapunov-like function $V = \frac{1}{2}s^2 + \frac{1}{2}\tilde{\mathbf{a}}^T \mathbf{P}^{-1} \tilde{\mathbf{a}}$ shows stability of the feedback interconnection of (6) and (8) and convergence to the desired trajectory via an application of Barbalat's Lemma (J.-J. Slotine & Li, 1991). We will refer to (8) as the Slotine and Li controller.

Example 2.1. Online parameter estimation may also be used within an observer-like framework for dynamic prediction. This allows one, for instance, to design provably stable online learning rules for the weights of a recurrent neural network in the dynamics approximation context (Alemi, Machens, Deneve, & Slotine, 2018; Gilra & Gerstner, 2017; Sussillo & Abbott, 2009). Consider a nonlinear system dynamics

$$\dot{\mathbf{x}} = \mathbf{f}(\mathbf{x}) + \mathbf{c}(t),$$

where $\mathbf{x} \in \mathbb{R}^n$ is the system state, $\mathbf{f} : \mathbb{R}^n \rightarrow \mathbb{R}^n$ is the system dynamics and $\mathbf{c} : \mathbb{R}_+ \rightarrow \mathbb{R}^n$ is a system input. Define the observer-like system

$$\dot{\hat{\mathbf{x}}} = -k(\hat{\mathbf{x}} - \mathbf{x}) + \mathbf{Y}(\hat{\mathbf{x}})\hat{\mathbf{a}} + \mathbf{c}(t),$$

where $\mathbf{Y} : \mathbb{R}^n \rightarrow \mathbb{R}^{n \times p}$, $\hat{\mathbf{a}} \in \mathbb{R}^p$ and $k > 0$ is a scalar gain. Assume that there exists a fixed parameter vector \mathbf{a} such that for all $\mathbf{x} \in \mathbb{R}^n$, $\mathbf{Y}(\mathbf{x})\mathbf{a} = \mathbf{f}(\mathbf{x})$. By adding and subtracting $\mathbf{f}(\hat{\mathbf{x}}) = \mathbf{Y}(\hat{\mathbf{x}})\hat{\mathbf{a}}$, the error $\mathbf{e} = \hat{\mathbf{x}} - \mathbf{x}$ has dynamics

$$\dot{\mathbf{e}} = -k\mathbf{e} + \mathbf{Y}(\hat{\mathbf{x}})\tilde{\mathbf{a}} + \mathbf{f}(\hat{\mathbf{x}}) - \mathbf{f}(\mathbf{x}).$$

Coupling the above error dynamics with an adaptation law

$$\dot{\hat{\mathbf{a}}} = -\gamma \mathbf{Y}(\hat{\mathbf{x}})^T \mathbf{e},$$

for $\gamma > 0$ a scalar learning rate, and consideration of the virtual system (Wang & Slotine, 2005)

$$\dot{\mathbf{e}}_v = -k\mathbf{e}_v + \mathbf{Y}(\hat{\mathbf{x}})\tilde{\mathbf{a}}_v + \mathbf{f}(\mathbf{e}_v + \mathbf{x}) - \mathbf{f}(\mathbf{x}),$$

$$\dot{\tilde{\mathbf{a}}}_v = -\gamma \mathbf{Y}^T(\hat{\mathbf{x}})\mathbf{e}_v,$$

where both \mathbf{x} and $\dot{\mathbf{x}}$ are viewed as external inputs (Chung & Slotine, 2009; Jouffroy & Slotine, 2004) shows that $\mathbf{e} \rightarrow 0$ if k is chosen so that the dynamics of \mathbf{e}_v is contracting (Lohmiller & Slotine, 1998), i.e.,

$$k > \sup_{\mathbf{x}} \left(\lambda_{\max} \left[\left(\frac{\partial \mathbf{f}(\mathbf{x})}{\partial \mathbf{x}} \right)_s \right] \right).$$

Above, \mathbf{A}_s denotes the symmetric part of a matrix. More generally, rather than the proportional term $-k\mathbf{e}$, any term of the form $\mathbf{g}(\dot{\mathbf{x}}) - \mathbf{g}(\mathbf{x})$ may be used in $\dot{\mathbf{x}}$, leading to the error dynamics

$$\dot{\mathbf{e}} = \mathbf{g}(\dot{\mathbf{x}}) - \mathbf{g}(\mathbf{x}) + \mathbf{Y}(\dot{\mathbf{x}})\tilde{\mathbf{a}} + \mathbf{f}(\dot{\mathbf{x}}) - \mathbf{f}(\mathbf{x}).$$

For the above dynamics, the condition on k may be replaced by the more general condition that $\mathbf{g}(\mathbf{e}_v + \mathbf{x}) + \mathbf{f}(\mathbf{e}_v + \mathbf{x})$ is contracting with respect to \mathbf{e}_v in a constant diagonal metric. \triangle

In this work, we make a mild additional assumption that simplifies some of the proofs.

Assumption 2.1. The dynamics $\hat{f}(\mathbf{x}, \hat{\mathbf{a}}, t)$ is locally bounded in $\dot{\mathbf{x}}$ and $\hat{\mathbf{a}}$ uniformly in t . That is, if $\|\mathbf{x}\| \leq \infty$ and $\|\hat{\mathbf{a}}\| < \infty$, then $\forall t \geq 0$, $|\hat{f}(\mathbf{x}, \hat{\mathbf{a}}, t)| < \infty$. \diamond

2.2 Velocity gradient algorithms

We now provide a brief introduction to a class of adaptive control methods known as velocity gradient algorithms (A. L. Fradkov, 1999; Fradkov, 1979; Ortega, 1996). Velocity gradient algorithms are applicable to nonlinearly parameterized systems that satisfy a convexity requirement described in Assumption 2.4. In their most basic form, these algorithms are specified by a “local” goal functional $Q(\mathbf{x}, t)$ where $Q : \mathbb{R}^n \times \mathbb{R}_+ \rightarrow \mathbb{R}$. Q is required to satisfy three main assumptions.

Assumption 2.2. $Q(\mathbf{x}, t)$ is non-negative and radially unbounded: $Q \geq 0$ for all \mathbf{x} , t and $Q(\mathbf{x}, t) \rightarrow \infty$ when $\|\mathbf{x}\| \rightarrow \infty$. $Q(\mathbf{x}, t)$ is also uniformly continuous in t whenever \mathbf{x} is bounded. \diamond

Assumption 2.3. There exists an ideal set of control parameters \mathbf{a} such that the origin of the system (1) is globally asymptotically stable when the control is evaluated at \mathbf{a} . Furthermore, Q is a Lyapunov function for the system when the control is evaluated at \mathbf{a} . That is, there exists a strictly increasing function ρ such that $\rho(0) = 0$ with $\dot{Q}(\mathbf{x}, \mathbf{a}, t) \leq -\rho(Q)$. \diamond

Assumption 2.4. The time derivative of Q is convex in the control parameters $\hat{\mathbf{a}}$. The first-order condition for convexity

$$\dot{Q}(\mathbf{x}, \mathbf{a}_1, t) \geq \dot{Q}(\mathbf{x}, \mathbf{a}_2, t) + (\mathbf{a}_1 - \mathbf{a}_2)^T \nabla_{\mathbf{a}_2} \dot{Q}(\mathbf{x}, \mathbf{a}_2, t), \quad (9)$$

must be satisfied for all \mathbf{a}_1 and \mathbf{a}_2 . \diamond

When Assumptions 2.2-2.4 are satisfied, the velocity gradient adaptive control law is defined as

$$\dot{\mathbf{a}} = -\mathbf{P} \nabla_{\mathbf{a}} \dot{Q}(\mathbf{x}, \hat{\mathbf{a}}, t). \quad (10)$$

where $\mathbf{P} = \mathbf{P}^T > 0$ is a positive definite matrix of learning rates. Its properties are summarized in the following proposition (A. L. Fradkov, 1999).

Proposition 2.1. Consider the velocity gradient algorithm (10) with local goal functional $Q(\mathbf{x}, t)$ satisfying Assumptions 2.2-2.4. Then, all solutions $(\mathbf{x}(t), \dot{\mathbf{a}}(t))$ given by (1) and (10) remain bounded, and

$$\lim_{t \rightarrow \infty} Q(\mathbf{x}(t), t) = 0$$

for all $\mathbf{x}(0) \in \mathbb{R}^n$.

The proof follows by consideration of the Lyapunov function $V = Q + \frac{1}{2} \tilde{\mathbf{a}}^T \mathbf{P}^{-1} \tilde{\mathbf{a}}$. Intuitively, while the goal functional Q may only depend on the control parameters $\hat{\mathbf{a}}$ indirectly through \mathbf{x} , its time derivative will depend explicitly on $\hat{\mathbf{a}}$ through $\dot{\mathbf{x}}$. The adaptation law (10) ensures that $\hat{\mathbf{a}}$ moves in a direction to decrease \dot{Q} . Under the conditions specified by Assumptions 2.2-2.4, this causes \dot{Q} to be negative for long enough to accomplish the desired goal (A. L. Fradkov, 1999).

Remark 2.4. If Q is chosen so that \dot{Q} depends on $\hat{\mathbf{a}}$ only through $f(\mathbf{x}, \hat{\mathbf{a}}, t)$ and f is linearly parameterized, then Assumption 2.4 will immediately be satisfied by convexity of affine functions. Indeed, consider defining the goal functional $Q = \frac{1}{2}s^2$ for system (1). It is clear that this proposed goal functional satisfies Assumptions 2.2 and 2.3¹.

¹Strictly speaking, $\frac{1}{2}s^2$ does not have to be uniformly continuous in t for bounded \mathbf{x} . This is a technical condition useful for the proof, but in many cases stability may still be shown via other means.

Then $\dot{Q} = -\eta s^2 + s\tilde{f}$, and (10) exactly recovers the Slotine and Li controller (8), originally derived based on Lyapunov considerations². In this sense, velocity gradient algorithms represent a flexible class of methods that contain as particular cases some pre-existing approaches. \diamond

Rather than a local functional, one may instead specify an integral goal functional of the form $Q(\mathbf{x}, \hat{\mathbf{a}}, t) = \int_0^t R(\mathbf{x}(t'), \hat{\mathbf{a}}(t'), t') dt'$. In this case, (10) takes the form

$$\dot{\hat{\mathbf{a}}} = -\mathbf{P} \nabla_{\hat{\mathbf{a}}} R(\mathbf{x}, \hat{\mathbf{a}}, t). \quad (11)$$

Equation (11) is a gradient flow algorithm on the loss function $R(\mathbf{x}, \hat{\mathbf{a}}, t)$. Replacing Assumptions 2.2 and 2.3 by the slightly modified setting:

Assumption 2.5. R is a non-negative function: $R(\mathbf{x}(t), \hat{\mathbf{a}}(t), t) \geq 0$ for all t . \diamond

Assumption 2.6. There exists an ideal set of controller parameters \mathbf{a} and a scalar function μ such that $\int_0^\infty \mu(t') dt' < \infty$, $\lim_{t \rightarrow \infty} \mu(t) = 0$, and $R(\mathbf{x}(t), \mathbf{a}, t) \leq \mu(t)$ for all t . \diamond

The properties of algorithm (11) are summarized in the following proposition (A. L. Fradkov, 1999).

Proposition 2.2. *Consider the velocity gradient algorithm (11) where the goal functional Q satisfies Assumptions 2.4-2.6. Then $Q(t) \leq \alpha$ where*

$$\alpha = \frac{1}{2} \tilde{\mathbf{a}}(0)^T \mathbf{P}^{-1} \tilde{\mathbf{a}}(0) + \int_0^\infty \mu(t') dt'$$

and $R \rightarrow 0$ for any bounded solution $\mathbf{x}(t)$.

Integral functionals allow the specification of a control goal that depends on all past data and that may have an explicit dependence on $\hat{\mathbf{a}}$. R is chosen so that it does not necessarily depend on the structure of the dynamics. Local functionals, on the other hand, result in adaptation laws that *do* have an explicit dependence on the dynamics through the appearance of the term $\left(\frac{\partial Q}{\partial \mathbf{x}}\right)^T \dot{\mathbf{x}}$ in \dot{Q} .

Integral functionals can be particularly useful if $R \rightarrow 0$ implies the desired control goal, and in this work, we will generally focus on the setting where $R = \frac{1}{2} \tilde{f}^2$ is the function approximation error. In particular, note that for this choice of R the result of Prop. 2.2 implies that $\tilde{f} \in \mathcal{L}_2$, which may be enough to ensure that $\mathbf{x} \in \mathcal{L}_\infty$, and hence that $\tilde{f} \rightarrow 0$ and $\mathbf{x} \rightarrow \mathbf{x}_d$. However, even when proved to be stable, this kind of law clearly cannot be implemented directly as it depends on the unknown \tilde{f} .

While \tilde{f} itself is unknown, it is contained in \dot{s} . Intuitively, unknown quantities contained in \dot{s} can thus be obtained in the adaptation dynamics through a proportional term in $\hat{\mathbf{a}}$ that contains s . This idea of gaining a “free” derivative is the basis of the reduced-order Luenberger observer for linear systems (Luenberger, 1979), and has been used in adaptive control, with particular success when applied to nonlinear parameterizations. Similar concepts can be extended to nonlinear observers; see Lohmiller and Slotine (1998), Sec. 4.1. Proportional-integral adaptive laws of this type have been known as algorithms in finite form (A. L. Fradkov, 1999; I. Y. Tyukin, 2003) and appear in the well-known I&I framework (Astolfi & Ortega, 2003; Liu et al., 2010). This approach will be the basis for our algorithms for nonlinearly parameterized systems.

Goal functionals can also be written as a sum of local and integral functionals with similar guarantees, and these approaches will lead to composite algorithms in the subsequent sections. The interested reader is referred to A. L. Fradkov (1999), Chapter 3 for more details.

2.3 The Bregman Lagrangian and accelerated optimization algorithms

In a continuous-time framework, the analysis of an optimization algorithm can be broken into two steps: first, an understanding of the quantitative convergence rates of the continuous-time differential equation, and second, a search over numerical discretization techniques that preserve these convergence rates. In Wibisono et al. (2016), the *Bregman Lagrangian* was shown to generate a suite of accelerated optimization algorithms by appealing to the Euler Lagrange equations through the principle of least action. In its original form, the Bregman Lagrangian is given by

$$\mathcal{L}(\mathbf{x}, \dot{\mathbf{x}}, t) = e^{\bar{\alpha} + \bar{\gamma}} \left(d_\psi \left(\mathbf{x} + e^{-\bar{\alpha}} \dot{\mathbf{x}} \parallel \mathbf{x} \right) - e^{\bar{\beta}} f(\mathbf{x}) \right). \quad (12)$$

²Note that $s\tilde{f}$ is still convex in $\hat{\mathbf{a}}$ despite the fact that s may change sign because \tilde{f} is linear in $\hat{\mathbf{a}}$ by assumption.

In (12), $f(\mathbf{x})$ is the loss function, and $d_\psi(\cdot \parallel \cdot)$ is the Bregman divergence

$$d_\psi(\mathbf{y} \parallel \mathbf{x}) = \psi(\mathbf{y}) - \psi(\mathbf{x}) - (\mathbf{y} - \mathbf{x})^T \nabla \psi(\mathbf{x}),$$

where $\psi(\mathbf{x})$ is a strictly convex *distance generating function*. ψ may be taken to be the Euclidean norm in \mathbb{R}^n for simplicity, or instead may be chosen to define a local optimization geometry. We will utilize the Euclidean norm for much of this work, and will consider the non-Euclidean case in Sec. 4.

The Bregman divergence may be understood as the error made when approximating $\psi(\mathbf{y})$ by a first-order Taylor expansion around \mathbf{x} . It is guaranteed to be non-negative for strictly convex functions by the first-order characterization of convexity (9). While it is not a norm in general, it defines a distance-like function for ψ strictly convex related to the *Hessian metric* $\frac{1}{2}\|\mathbf{x}\|_{\nabla^2\psi}^2 = \frac{1}{2}\mathbf{x}^T \nabla^2\psi(\mathbf{x})\mathbf{x}$. As two simple examples, for $\psi(\mathbf{x}) = \frac{1}{2}\|\mathbf{x}\|^2$, $d_\psi(\mathbf{x} \parallel \mathbf{y}) = \|\mathbf{x} - \mathbf{y}\|^2$. For $\psi(\mathbf{x}) = \frac{1}{2}\mathbf{x}^T \mathbf{Q}\mathbf{x}$ for $\mathbf{Q} > 0$ a positive definite matrix, $d_\psi(\mathbf{x} \parallel \mathbf{y}) = (\mathbf{x} - \mathbf{y})^T \mathbf{Q}(\mathbf{x} - \mathbf{y})$. For more general convex functions ψ , there may not exist a simple algebraic form for $d_\psi(\cdot \parallel \cdot)$.

The quantities $\bar{\alpha}(t) : \mathbb{R}_+ \rightarrow \mathbb{R}$, $\bar{\beta}(t) : \mathbb{R}_+ \rightarrow \mathbb{R}$, and $\bar{\gamma}(t) : \mathbb{R}_+ \rightarrow \mathbb{R}$ in (12) are arbitrary time-dependent functions that ultimately set the damping and learning rates. To generate accelerated optimization algorithms, Wibisono, Wilson, and Jordan required two *ideal scaling conditions*: $\dot{\bar{\beta}} \leq e^{\bar{\alpha}}$ and $\dot{\bar{\gamma}} = e^{\bar{\alpha}}$. These conditions come out of the Euler Lagrange equations, where the second is used to eliminate an unwanted term, and a Lyapunov argument, where the first is used to ensure negativity of a chosen Lyapunov function. This work was continued by Wilson, Recht, and Jordan (2016), where a second Bregman Lagrangian was defined and used to analyze momentum algorithms via Lyapunov arguments, and extended to the Hamiltonian setting where a surprising connection between discrete-time optimization algorithms and symplectic integration was noted by Betancourt et al. (2018).

Gaudio et al. (2019) recently utilized the Bregman Lagrangian to derive a momentum-like adaptive control algorithm. To do so, they defined $\bar{\alpha} = \log(\beta\mathcal{N})$, $\bar{\beta} = \log\left(\frac{\gamma}{\beta\mathcal{N}}\right)$, and $\bar{\gamma} = \int e^{\bar{\alpha}} dt^3$. Here, $\gamma \geq 0$ and $\beta \geq 0$ are non-negative scalar hyperparameters and $\mathcal{N} = \mathcal{N}(t)$ is a context-dependent normalizing signal. With these definitions, choosing the Euclidean norm $\psi(\cdot) = \frac{1}{2}\|\cdot\|^2$, and in the adaptive control framework defined in Sec. 2.1, (12) becomes

$$\mathcal{L}\left(\hat{\mathbf{a}}, \dot{\hat{\mathbf{a}}}, t\right) = e^{\int_0^t \beta\mathcal{N}(t) dt} \frac{1}{\beta\mathcal{N}} \left(\frac{1}{2} \dot{\hat{\mathbf{a}}}^T \dot{\hat{\mathbf{a}}} - \gamma\beta\mathcal{N} \frac{d}{dt} \left[\frac{1}{2} s^2 \right] \right). \quad (13)$$

Comparing (12) and (13), it is clear that the loss function $f(\mathbf{x})$ in (12) has been replaced by $\frac{1}{2}s^2$ in (13). Following Remark 2.4, this is precisely the \dot{Q} velocity gradient functional that gives rise to the Slotine and Li controller. For (13), the Euler-Lagrange equations lead to the adaptation law

$$\ddot{\hat{\mathbf{a}}} + \dot{\hat{\mathbf{a}}} \left(\beta\mathcal{N} - \frac{\dot{\mathcal{N}}}{\mathcal{N}} \right) = -\gamma\beta\mathcal{N} \mathbf{Y}^T s. \quad (14)$$

(14) may be understood as a higher-order in-time version of the Slotine and Li adaptive controller. In effect, the Slotine and Li controller is endowed with momentum and state-dependent damping. (14) may also be re-written as two first-order systems

$$\dot{\hat{\mathbf{v}}} = -\gamma \mathbf{Y}^T s, \quad (15)$$

$$\dot{\hat{\mathbf{a}}} = \beta\mathcal{N}(\hat{\mathbf{v}} - \hat{\mathbf{a}}), \quad (16)$$

which are useful for proving stability. The properties of (14) are summarized in the following proposition.

Proposition 2.3. *Consider the higher-order adaptation algorithm (14) or its equivalent representation (15) & (16) with $\mathcal{N} = 1 + \mu\|\mathbf{Y}\|^2$ and $\mu > \frac{\gamma}{\eta\beta}$. Then, all trajectories $(\mathbf{x}, \hat{\mathbf{v}}, \hat{\mathbf{a}})$ remain bounded, $s \in \mathcal{L}_\infty \cap \mathcal{L}_2$, $(\hat{\mathbf{a}} - \hat{\mathbf{v}}) \in \mathcal{L}_2$, $s \rightarrow 0$ and $\mathbf{x} \rightarrow \mathbf{x}_d$.*

The proof follows by consideration of the Lyapunov function $V = \frac{1}{2} \left(s^2 + \frac{1}{\gamma} \|\tilde{\mathbf{v}}\|^2 + \frac{1}{\gamma} \|\hat{\mathbf{v}} - \hat{\mathbf{a}}\|^2 \right)$ (Gaudio et al., 2019).

Remark 2.5. This transformation to a system of two first-order systems may seem somewhat *ad-hoc*, but it follows immediately by consideration of the non-Euclidean Bregman Lagrangian (12). Indeed, it is easy to check that

³Note that these conditions validate the second ideal scaling condition but not the first. As mentioned above, the first ideal scaling condition is required only by the choice of Lyapunov function in the original work, which was used to derive convergence rates for optimization algorithms (Wibisono et al., 2016). In this sense, it is not strictly required for adaptive control.

$\hat{\mathbf{v}} = \hat{\mathbf{a}} + \frac{\dot{\hat{\mathbf{a}}}}{\beta\mathcal{N}}$, which is precisely $\mathbf{x} + e^{-\bar{\alpha}}\dot{\mathbf{x}}$ in the first argument of $d_\psi(\cdot \parallel \cdot)$ in (12). The transformation is also readily apparent by use of the *Bregman Hamiltonian*

$$\mathcal{H}(\hat{\mathbf{a}}, \mathbf{p}) = \frac{1}{2}\beta Ne^{-\bar{\gamma}}\|\mathbf{p}\|^2 + \gamma e^{\bar{\gamma}} \left[\frac{d}{dt} \frac{1}{2}s^2 \right], \quad (17)$$

which, via Hamilton's equations, leads to

$$\begin{aligned} \dot{\mathbf{p}} &= -\frac{\partial \mathcal{H}}{\partial \hat{\mathbf{a}}} = -\gamma e^{\bar{\gamma}} s \mathbf{Y}^T, \\ \dot{\hat{\mathbf{a}}} &= \frac{\partial \mathcal{H}}{\partial \mathbf{p}} = \beta Ne^{-\bar{\gamma}} \mathbf{p}. \end{aligned}$$

Defining $\hat{\mathbf{v}} = e^{-\bar{\gamma}}\mathbf{p} + \hat{\mathbf{a}}$ leads immediately to (15) & (16). As is typical in classical mechanics, the Bregman Hamiltonian may be obtained from a Legendre transform of the Bregman Lagrangian. The Hamiltonian equations may be useful for discrete-time algorithm development through application of symplectic discretization techniques (Betancourt et al., 2018; França, Sulam, Robinson, & Vidal, 2019; Shi, Du, Su, & Jordan, 2019). \diamond

Remark 2.6. It is well known, for example from a passivity interpretation of the Lyapunov-like analysis (see, e.g., (J.-J. Slotine & Li, 1991)), that the pure integrator in the standard Slotine and Li adaptation law (8) can be replaced by any linear positive real transfer function containing a pure integrator. The higher-order algorithms presented in this work are distinct from this approach, as most clearly seen by the state-dependent damping term in (14). \diamond

3 Main contributions

In this section, we present the main contributions of this work. We begin by noting that the Bregman Lagrangian generates higher-order velocity gradient algorithms, of which the adaptation law (14) is a special case. We prove some general conditions under which these higher-order algorithms will achieve tracking. By analogy with integral velocity gradient functionals, we derive a proportional-integral scheme to implement a first-order composite adaptation law (J.-J. Slotine & Li, 1991) driven directly by the function approximation error rather than its filtered version. We subsequently fuse the generating functional for the composite law with the Bregman Lagrangian to construct a higher-order composite algorithm.

Combining a connection between the techniques of isotonic regression (Goel & Klivans, 2017; Goel et al., 2018; Kakade et al., 2011) and adaptive control algorithms for monotone nonlinear parameterizations (I. Tyukin, 2011; Tyukin et al., 2007), we demonstrate how to modify our higher-order velocity gradient framework to derive higher-order algorithms for nonlinearly parameterized systems. We follow this development by discussing a new form of high-order algorithm inspired by the Elastic Averaging Stochastic Gradient Descent (EASGD) algorithm (Boffi & Slotine, 2020; Zhang et al., 2014) and extensions to distributed adaptation (Wensing & Slotine, 2017). We subsequently demonstrate how to use time-varying learning rates based on the bounded gain forgetting technique with our presented algorithms (J.-J. Slotine & Li, 1991).

3.1 Accelerated velocity gradient algorithms

As noted in Sec. 2.3, the Bregman Lagrangian (13) that generates the higher-order algorithm (14) contains the local velocity gradient functional $Q = \frac{1}{2}s^2$ that gives rise to the Slotine and Li controller (8). Based on this observation, we define local and integral higher-order velocity gradient algorithms via the Euclidean Bregman Lagrangian. We begin with the local functional

$$\mathcal{L}(\hat{\mathbf{a}}, \dot{\hat{\mathbf{a}}}, t) = e^{\int_0^t \beta\mathcal{N}(t)dt} \frac{1}{\beta\mathcal{N}(t)} \left(\frac{1}{2} \dot{\hat{\mathbf{a}}}^T \dot{\hat{\mathbf{a}}} - \gamma \beta \mathcal{N}(t) \frac{d}{dt} Q(\mathbf{x}, t) \right),$$

which generates the higher-order law

$$\ddot{\hat{\mathbf{a}}} + \dot{\hat{\mathbf{a}}} \left(\beta\mathcal{N} - \frac{\dot{\mathcal{N}}}{\mathcal{N}} \right) = -\gamma \beta \mathcal{N} \frac{\partial \dot{Q}(\mathbf{x}, \hat{\mathbf{a}}, t)}{\partial \hat{\mathbf{a}}}. \quad (18)$$

Algorithm (18) can be re-written as two first-order systems

$$\dot{\hat{\mathbf{v}}} = -\gamma \frac{\partial \dot{Q}(\mathbf{x}, \hat{\mathbf{a}}, t)}{\partial \hat{\mathbf{a}}}, \quad (19)$$

$$\dot{\hat{\mathbf{a}}} = \beta\mathcal{N}(\hat{\mathbf{v}} - \hat{\mathbf{a}}). \quad (20)$$

To achieve the control goal, we require the following technical assumption in addition to Assumptions 2.2 & 2.4. This assumption replaces Assumption 2.3 for first-order velocity gradient algorithms.

Assumption 3.1. There exists a time-varying normalizing signal $N(t)$ and non-negative scalar values $\beta \geq 0, \mu \geq 0$ such that the time-derivative of the goal functional evaluated at the true parameters, $\dot{Q}(\mathbf{x}, \mathbf{a}, t)$, satisfies the following inequality

$$\dot{Q}(\mathbf{x}, \mathbf{a}, t) - \frac{\beta\mu}{\gamma}N(t)\|\hat{\mathbf{a}} - \hat{\mathbf{v}}\|^2 + 2(\hat{\mathbf{a}} - \hat{\mathbf{v}})^T \frac{\partial \dot{Q}}{\partial \hat{\mathbf{a}}} \leq -\rho(Q). \quad (21)$$

In (21), $\rho(\cdot)$ is positive definite, uniformly continuous in Q , and satisfies $\rho(0) = 0$. \diamond

With Assumption 3.1 in hand, we can state the following proposition.

Proposition 3.1. Consider the algorithm (18) or its equivalent form (19) & (20), and assume Q satisfies Assumptions 2.2, 2.4, and 3.1. Then, all solutions $(\mathbf{x}(t), \hat{\mathbf{v}}(t), \hat{\mathbf{a}}(t))$ remain bounded, $(\hat{\mathbf{a}} - \hat{\mathbf{v}}) \in \mathcal{L}_2$, and $\lim_{t \rightarrow \infty} Q = 0$.

Proof. Consider the Lyapunov-like function

$$V = Q(\mathbf{x}, t) + \frac{1}{2\gamma}\tilde{\mathbf{v}}^T\tilde{\mathbf{v}} + \frac{1}{2\gamma}(\hat{\mathbf{a}} - \hat{\mathbf{v}})^T(\hat{\mathbf{a}} - \hat{\mathbf{v}}). \quad (22)$$

Equation (22) implies that, with $\mathcal{N}(t) = 1 + \mu N(t)$,

$$\begin{aligned} \dot{V} &= \dot{Q}(\mathbf{x}, \hat{\mathbf{a}}, t) - \hat{\mathbf{a}}^T \frac{\partial \dot{Q}}{\partial \hat{\mathbf{a}}} - \frac{\beta}{\gamma}\|\hat{\mathbf{a}} - \hat{\mathbf{v}}\|^2 - \frac{\beta\mu}{\gamma}N(t)\|\hat{\mathbf{a}} - \hat{\mathbf{v}}\|^2 + 2(\hat{\mathbf{a}} - \hat{\mathbf{v}})^T \frac{\partial \dot{Q}}{\partial \hat{\mathbf{a}}} \\ &\leq \dot{Q}(\mathbf{x}, \mathbf{a}, t) - \frac{\beta}{\gamma}\|\hat{\mathbf{a}} - \hat{\mathbf{v}}\|^2 - \frac{\beta\mu}{\gamma}N(t)\|\hat{\mathbf{a}} - \hat{\mathbf{v}}\|^2 + 2(\hat{\mathbf{a}} - \hat{\mathbf{v}})^T \frac{\partial \dot{Q}}{\partial \hat{\mathbf{a}}} \\ &\leq -\rho(Q) - \frac{\beta}{\gamma}\|\hat{\mathbf{a}} - \hat{\mathbf{v}}\|^2. \end{aligned} \quad (23)$$

By radial unboundedness of $Q(\mathbf{x}, t)$ in \mathbf{x} , (22) & (23) show that \mathbf{x} remains bounded. Similarly, radial unboundedness of V in $\tilde{\mathbf{v}}$ and $\hat{\mathbf{a}} - \hat{\mathbf{v}}$ show that $\hat{\mathbf{v}}$ and $\hat{\mathbf{a}}$ remain bounded. Integrating (23) shows that $\frac{\beta}{\gamma} \int_0^\infty \|\hat{\mathbf{a}} - \hat{\mathbf{v}}\|^2 dt \leq V(0) - V(\infty) < \infty$, so that $(\hat{\mathbf{a}} - \hat{\mathbf{v}}) \in \mathcal{L}_2$. An identical argument shows that $\int_0^\infty \rho(Q) dt < \infty$. Now, because \mathbf{x} and $\hat{\mathbf{a}}$ are bounded, and because $\tilde{\mathbf{f}}(\mathbf{x}, \hat{\mathbf{a}}, t)$ is locally bounded in \mathbf{x} and $\hat{\mathbf{a}}$ uniformly in t by assumption, writing $\mathbf{x}(t) - \mathbf{x}(s) = \int_s^t \tilde{\mathbf{f}}(\mathbf{x}, \hat{\mathbf{a}}, t) dt$ shows that $\mathbf{x}(t)$ is uniformly continuous in t . Because $Q(\mathbf{x}, t)$ is uniformly continuous when \mathbf{x} is bounded, and because ρ is uniformly continuous in Q , ρ is uniformly continuous in t and $\lim_{t \rightarrow \infty} \rho(t) = \lim_{t \rightarrow \infty} \rho(Q(\mathbf{x}(t), t)) = 0$ by Barbalat's lemma. This shows that $\lim_{t \rightarrow \infty} Q(\mathbf{x}(t), t) = 0$. \square

Remark 3.1. The uniform continuity assumptions on $\rho(\cdot)$ and Q used in the general setting handled by the proof of Prop. 3.1 are not strictly necessary. Without them, we can conclude existence of the integral $\int_0^\infty \rho(Q)$ but not that $Q \rightarrow 0$. In many cases, signal chasing arguments based on the finiteness of this integral are sufficient, as will be shown in the coming sections. \diamond

By taking $Q = \frac{1}{2}s^2$ in Prop. 3.1, we immediately recover Prop. 2.3⁴. In this sense, Prop. 3.1 elucidates the underlying structure exploited by the Bregman Lagrangian to generate higher-order algorithms.

We now consider the integral functional

$$\mathcal{L}(\hat{\mathbf{a}}, \dot{\hat{\mathbf{a}}}, t) = e^{\int_0^t \beta \mathcal{N}(t') dt} \frac{1}{\beta \mathcal{N}(t)} \left(\frac{1}{2} \dot{\hat{\mathbf{a}}}^T \dot{\hat{\mathbf{a}}} - \gamma \beta \mathcal{N}(t) \frac{d}{dt} \int_0^t R(\mathbf{x}(t'), \hat{\mathbf{a}}(t'), t') dt' \right),$$

which generates the higher-order law

$$\ddot{\hat{\mathbf{a}}} + \dot{\hat{\mathbf{a}}} \left(\beta \mathcal{N} - \frac{\dot{\mathcal{N}}}{\mathcal{N}} \right) = -\gamma \beta \mathcal{N} \frac{\partial R(\mathbf{x}, \hat{\mathbf{a}}, t)}{\partial \hat{\mathbf{a}}}. \quad (24)$$

We again re-write (24) as two first-order systems

$$\dot{\hat{\mathbf{v}}} = -\gamma \frac{\partial R(\mathbf{x}, \hat{\mathbf{a}}, t)}{\partial \hat{\mathbf{a}}}, \quad (25)$$

$$\dot{\hat{\mathbf{a}}} = \beta \mathcal{N}(\hat{\mathbf{v}} - \hat{\mathbf{a}}). \quad (26)$$

We now require a modified version of Assumption 3.1.

⁴Following Remark 3.1, we conclude that $s \in \mathcal{L}_2 \cap \mathcal{L}_\infty$, and $\dot{s} \in \mathcal{L}_\infty$ by local boundedness of $\tilde{\mathbf{f}}$ in \mathbf{x} and $\hat{\mathbf{a}}$ uniformly in t , showing $s \rightarrow 0$ by Barbalat's lemma.

Assumption 3.2. R is a non-negative function: $R(\mathbf{x}, \hat{\mathbf{a}}, t) \geq 0$ for all $\mathbf{x}, \hat{\mathbf{a}}$, and t . Furthermore, there exists a time-dependent normalizing signal $N(t)$ and non-negative scalar values $\beta \geq 0, \mu \geq 0$ such that

$$R(\mathbf{x}, \mathbf{a}, t) - R(\mathbf{x}, \hat{\mathbf{a}}, t) - \frac{\beta\mu}{\gamma} N(t) \|\hat{\mathbf{a}} - \hat{\mathbf{v}}\|^2 + 2(\hat{\mathbf{a}} - \hat{\mathbf{v}})^T \nabla_{\hat{\mathbf{a}}} R(\mathbf{x}, \hat{\mathbf{a}}, t) \leq -kR(\mathbf{x}, \hat{\mathbf{a}}, t)$$

for some constant $k > 0$. \diamond

With Assumption 3.2, we can state the following proposition.

Proposition 3.2. Consider algorithm (24) or its equivalent form (25) & (26) along with Assumptions 2.4 & 3.2. Then, for any bounded trajectory $\mathbf{x}(t)$ of (1), $\hat{\mathbf{v}}$ and $\hat{\mathbf{a}}$ remain bounded, $(\hat{\mathbf{a}} - \hat{\mathbf{v}}) \in \mathcal{L}_2$, and $\int_0^\infty R(\mathbf{x}(t'), \hat{\mathbf{a}}(t'), t') dt' < \infty$.

Proof. Consider the Lyapunov-like function

$$V = \frac{1}{2\gamma} \tilde{\mathbf{v}}^T \tilde{\mathbf{v}} + \frac{1}{2\gamma} (\hat{\mathbf{a}} - \hat{\mathbf{v}})^T (\hat{\mathbf{a}} - \hat{\mathbf{v}}). \quad (27)$$

Equation (27) implies that, with $\mathcal{N}(t) = 1 + \mu N(t)$,

$$\begin{aligned} \dot{V} &= -\hat{\mathbf{a}}^T \frac{\partial R(\mathbf{x}, \hat{\mathbf{a}}, t)}{\partial \hat{\mathbf{a}}} - \frac{\beta}{\gamma} \|\hat{\mathbf{a}} - \hat{\mathbf{v}}\|^2 - \frac{\beta\mu}{\gamma} N(t) \|\hat{\mathbf{a}} - \hat{\mathbf{v}}\|^2 + 2(\hat{\mathbf{a}} - \hat{\mathbf{v}})^T \frac{\partial R(\mathbf{x}, \hat{\mathbf{a}}, t)}{\partial \hat{\mathbf{a}}} \\ &\leq R(\mathbf{x}, \mathbf{a}, t) - R(\mathbf{x}, \hat{\mathbf{a}}, t) - \frac{\beta}{\gamma} \|\hat{\mathbf{a}} - \hat{\mathbf{v}}\|^2 - \frac{\beta\mu}{\gamma} N(t) \|\hat{\mathbf{a}} - \hat{\mathbf{v}}\|^2 + 2(\hat{\mathbf{a}} - \hat{\mathbf{v}})^T \frac{\partial R(\mathbf{x}, \hat{\mathbf{a}}, t)}{\partial \hat{\mathbf{a}}} \\ &\leq -kR(\mathbf{x}, \hat{\mathbf{a}}, t) - \frac{\beta}{\gamma} \|\hat{\mathbf{a}} - \hat{\mathbf{v}}\|^2 \end{aligned} \quad (28)$$

(27) & (28) show that, for any bounded solution $\mathbf{x}, \hat{\mathbf{v}}$ and $\hat{\mathbf{a}}$ remain bounded. Furthermore, integrating (28) shows that $\int_0^\infty R(\mathbf{x}(t'), \hat{\mathbf{a}}(t'), t') dt' < \infty$ and $(\hat{\mathbf{a}} - \hat{\mathbf{v}}) \in \mathcal{L}_2$. \square

As mentioned in Sec. 2.2, we will be particularly interested in Prop. 3.2 when $R = \frac{1}{2} \tilde{f}^2$, which will generate composite adaptation algorithms.

Remark 3.2. Classically, Lyapunov functions used in adaptive control consist of a sum of tracking and parameter estimation error terms, with $\dot{\hat{\mathbf{a}}}$ chosen to cancel a term of unknown sign. Several Lyapunov functions in this work consist only of parameter estimation error terms, such as (27). From a mathematical point of view, all that matters is that \dot{V} is negative semi-definite and contains signals related to the tracking error. Integrating \dot{V} allows the application of tools from functional analysis to ensure that the control goal is accomplished. \diamond

3.2 Composite adaptation laws

Here we consider the linearly parameterized setting $f(\mathbf{x}, \mathbf{a}, t) = \mathbf{Y}(\mathbf{x}, t)\mathbf{a}$, and derive new first- and second-order composite adaptation laws. Composite adaptation laws are driven by two sources of error: the tracking error itself, as summarized by s in the Slotine and Li controller, and a prediction error generally obtained from an algebraic relation which is itself constructed by filtering the dynamics (J.-J. Slotine & Li, 1991). A starting point for our first proposed algorithm is to consider a hybrid local and integral velocity gradient functional

$$Q(\mathbf{x}, \mathbf{x}_d, t) = \frac{\gamma}{2} s^2(\mathbf{x}, \mathbf{x}_d) + \frac{\kappa}{2} \int_0^t \tilde{f}^2(\mathbf{x}(t'), \hat{\mathbf{a}}(t'), t') dt', \quad (29)$$

where $\kappa > 0$ and $\gamma > 0$ are positive learning rates weighting the contributions of each term. As discussed in Sec. 2.2, the first term leads to the Slotine and Li controller. The second can be clearly seen to satisfy Assumptions 2.5 and 2.6 with $\mu(t) = 0$. It also satisfies Assumption 2.4, as \tilde{f}^2 is a quadratic function of $\hat{\mathbf{a}}$ for linear \tilde{f} . Following the velocity gradient formalism, the resulting adaptation law is given by

$$\dot{\hat{\mathbf{a}}} = -\mathbf{P} \mathbf{Y}^T (\gamma s + \kappa \mathbf{Y} \hat{\mathbf{a}}), \quad (30)$$

which is a composite adaptation law simultaneously driven by s and the instantaneous function approximation error $\mathbf{Y} \hat{\mathbf{a}} = \tilde{f}$. Equation (30) depends on the function approximation error \tilde{f} , which is not measured and hence cannot be

used directly in an adaptation law. Nevertheless, it can be obtained through a proportional-integral form for $\hat{\mathbf{a}}$. To do so, we define

$$\xi(\mathbf{x}, \mathbf{x}_d, t) = -\kappa \mathbf{P} s(\mathbf{x}, \mathbf{x}_d) \mathbf{Y}^T(\mathbf{x}, t) \quad (31)$$

$$\rho(\mathbf{x}, \mathbf{x}_d, t) = \kappa \mathbf{P} \int_{x_n(t_0)}^{x_n(t)} s(\mathbf{x}, \mathbf{x}_d) \frac{\partial \mathbf{Y}(\mathbf{x}, t)^T}{\partial x_n} dx_n \quad (32)$$

$$\hat{\mathbf{a}} = \bar{\mathbf{a}} + \xi(\mathbf{x}, \mathbf{x}_d, t) + \rho(\mathbf{x}, \mathbf{x}_d, t) \quad (33)$$

$$\begin{aligned} \dot{\hat{\mathbf{a}}} = & -(\kappa\eta + \gamma) s \mathbf{P} \mathbf{Y}^T + \kappa s \sum_{i=1}^{n-1} \mathbf{P} \frac{\partial \mathbf{Y}}{\partial x_i} \dot{x}_i - \sum_{i=1}^{n-1} \left(\frac{\partial \rho}{\partial x_i} \right)^T \dot{x}_i \\ & - \left(\frac{\partial \rho}{\partial \mathbf{x}_d} \right)^T \dot{\mathbf{x}}_d - \frac{\partial \xi}{\partial t} - \frac{\partial \rho}{\partial t} \end{aligned} \quad (34)$$

Computing $\dot{\hat{\mathbf{a}}}$ demonstrates that (30) is obtained despite its dependence on $\mathbf{Y}\hat{\mathbf{a}}$ through only the known signals contained in (31)-(34). A few remarks concerning the algorithm (30)-(34) are in order.

Remark 3.3. The $\mathbf{Y}\hat{\mathbf{a}}$ term may also be obtained by following the I&I formalism (Astolfi & Ortega, 2003; Liu et al., 2010). To our knowledge, this discussion is the first that demonstrates the possibility of using a PI law in combination with a standard Lyapunov-stability motivated adaptation law to obtain a composite law. \diamond

Remark 3.4. More error signals may be used for additional terms in the adaptation law. For example, a prediction error obtained by filtering the dynamics may also be employed, leading to a three-term composite algorithm. \diamond

Remark 3.5. Much like the standard composite law obtained by filtering the dynamics, rearranging (30) shows that $\dot{\hat{\mathbf{a}}} + \mathbf{P} \mathbf{Y}^T \mathbf{Y} \hat{\mathbf{a}} = -\mathbf{P} \mathbf{Y}^T s$, so that the additional term can be seen to add a damping term that smooths adaptation (J.-J. Slotine & Li, 1991). \diamond

Remark 3.6. As mentioned in Sec. 2.1, for clarity of presentation we have restricted our discussion to the n^{th} -order system (1). In general, the PI form (33) leads to *unwanted* unknown terms contained in $\left(\frac{\partial \xi(\mathbf{x}, \mathbf{x}_d)}{\partial \mathbf{x}} \right)^T \dot{\mathbf{x}}$ in addition to the *desired* unknown term. In this case, the desired unknown term is $-\kappa \mathbf{P} \mathbf{Y}^T \mathbf{Y} \hat{\mathbf{a}}$ while the undesired unknown term is $-\kappa \mathbf{P} \frac{\partial \mathbf{Y}}{\partial x_n} \dot{x}_n s$. Indeed, the purpose of introducing the additional proportional term $\rho(\mathbf{x}, \mathbf{x}_d)$ in (31) is to cancel this undesired unknown term. In general, cancellation of the undesired terms can be obtained by choosing ρ to solve a PDE, and solutions to this PDE will only exist if the undesired term is the gradient of an auxiliary function. ρ is then chosen to be exactly this auxiliary function. In some cases, the PDE can be avoided, such as through dynamic scaling techniques (Karagiannis, Sassano, & Astolfi, 2009) or the similar embedding technique of Tyukin (I. Tyukin, 2011). \diamond

The properties of the adaptive law (30) may be summarized with the following proposition.

Proposition 3.3. Consider the adaptation algorithm (30) with a linearly parameterized unknown, $f(\mathbf{x}, \mathbf{a}, t) = \mathbf{Y}(\mathbf{x}, t) \mathbf{a}$. Then all trajectories $(\mathbf{x}, \hat{\mathbf{a}})$ remain bounded, $s \in L_2 \cap L_\infty$, $\tilde{f} \in L_2$, $s \rightarrow 0$, and $\mathbf{x} \rightarrow \mathbf{x}_d$.

Proof. Consider the Lyapunov-like function

$$V = \frac{1}{2} s^2 + \frac{1}{2\gamma} \hat{\mathbf{a}}^T \mathbf{P}^{-1} \hat{\mathbf{a}},$$

which has time derivative

$$\dot{V} = -\eta s^2 - \frac{\kappa}{\gamma} \tilde{f}^2.$$

This immediately shows $s \in L_\infty$ and $\hat{\mathbf{a}} \in L_\infty$. Because $s \in L_\infty$, $\mathbf{x} \in L_\infty$ by definition of the sliding variable (J.-J. Slotine & Li, 1991). Integrating \dot{V} shows that $s \in L_2$ and $\tilde{f} \in L_2$. The result follows by application of Lemma A.1 or directly by Barbalat's Lemma. \square

Following the accelerated velocity gradient approach of Sec. 3.1, we now obtain a higher-order composite algorithm, and give a PI implementation. We again consider a hybrid local and integral velocity gradient functional, so that (12) takes the form

$$\mathcal{L}(\hat{\mathbf{a}}, \dot{\hat{\mathbf{a}}}, t) = e^{\int_0^t \beta \mathcal{N}(t') dt} \frac{1}{\beta \mathcal{N}(t)} \left(\frac{1}{2} \dot{\hat{\mathbf{a}}}^T \dot{\hat{\mathbf{a}}} - \beta \mathcal{N}(t) \frac{d}{dt} \left[\frac{\gamma}{2} s^2 + \frac{\kappa}{2} \int_0^t \tilde{f}^2(\mathbf{x}(t'), \hat{\mathbf{a}}(t'), t') dt' \right] \right) \quad (35)$$

where $\gamma > 0$ and $\kappa > 0$ are positive constants weighting the two error terms. The Euler-Lagrange equations then lead to the higher-order composite system

$$\ddot{\mathbf{a}} + \left(\beta \mathcal{N} - \frac{\dot{\mathcal{N}}}{\mathcal{N}} \right) \dot{\mathbf{a}} = -\beta \mathcal{N} \mathbf{Y}^T (\gamma s + \kappa \mathbf{Y} \tilde{\mathbf{a}}). \quad (36)$$

As in Sec. 2.3, (36) may be implemented as two first-order systems

$$\dot{\tilde{\mathbf{v}}} = -\mathbf{Y}^T (\gamma s + \kappa \mathbf{Y} \tilde{\mathbf{a}}), \quad (37)$$

$$\dot{\mathbf{a}} = \beta \mathcal{N} (\tilde{\mathbf{v}} - \mathbf{a}), \quad (38)$$

where now (37) is obtained through the PI form $\tilde{\mathbf{v}} = \bar{\mathbf{v}} + \xi(\mathbf{x}, \mathbf{x}_d, t) + \rho(\mathbf{x}, \mathbf{x}_d, t)$ with ξ , ρ , and $\bar{\mathbf{v}}$ given by (31), (32), and (34) respectively with $\mathbf{P} = \mathbf{I}$. The properties of the higher-order composite adaptation law (36) are stated in the following proposition.

Proposition 3.4. *Consider the higher-order composite adaptation algorithm (36) or its equivalent (37) & (38) for a linearly parameterized unknown, $f(\mathbf{x}, \mathbf{a}, t) = \mathbf{Y}(\mathbf{x}, t) \mathbf{a}$. Set $\mathcal{N} = 1 + \mu \|\mathbf{Y}\|^2$ and $\mu > \frac{\gamma}{\beta} \left(\frac{1}{\eta} + \frac{\kappa}{\gamma} \right)$. Then all trajectories $(\mathbf{x}, \tilde{\mathbf{v}}, \mathbf{a})$ remain bounded, $\|\tilde{\mathbf{v}} - \mathbf{a}\| \in L_2$, $s \in L_\infty \cap L_2$, $\tilde{f} \in L_\infty \cap L_2$, $s \rightarrow 0$, and $\mathbf{x} \rightarrow \mathbf{x}_d$.*

The proof is given in App. A.2.

Remark 3.7. By following the proof, the normalizing signal \mathcal{N} may be chosen alternatively to be matrix-valued as $\mathbf{N} = \mathbf{I} + \mu \mathbf{Y}^T \mathbf{Y}$. \diamond

Remark 3.8. The new $\mathbf{Y} \tilde{\mathbf{a}}$ term may be used in isolation, by considering the Lyapunov function $V = \frac{1}{2} \tilde{\mathbf{v}}^T \mathbf{P}^{-1} \tilde{\mathbf{v}} + \frac{1}{2} (\mathbf{a} - \tilde{\mathbf{v}})^T \mathbf{P}^{-1} (\mathbf{a} - \tilde{\mathbf{v}})$. \diamond

3.3 Higher-order algorithms for nonlinearly parameterized adaptive control

We now utilize the development in Sec. 3.2 to present a new higher-order algorithm applicable when the unknown parameters appear nonlinearly in the dynamics. Significant progress has been made in this direction with the assumption of *monotonicity*, and several notions of monotonicity have appeared in the literature (Astolfi & Ortega, 2003; Liu et al., 2010; Ortega et al., 2019; I. Tyukin, 2011; Tyukin et al., 2007). We consider one notion of monotonicity presented by Tyukin, which is captured in the following assumption.

Assumption 3.3. There exists a known time- and state-dependent function $\alpha : \mathbb{R}^n \times \mathbb{R}_{\geq 0} \rightarrow \mathbb{R}^p$ such that

$$\tilde{\mathbf{a}}^T \alpha(\mathbf{x}, t) (f(\mathbf{x}, \tilde{\mathbf{a}}, t) - f(\mathbf{x}, \mathbf{a}, t)) \geq 0, \quad (39)$$

$$|\alpha(\mathbf{x}, t)^T \tilde{\mathbf{a}}| \geq \frac{1}{D_1} |f(\mathbf{x}, \tilde{\mathbf{a}}, t) - f(\mathbf{x}, \mathbf{a}, t)|. \quad (40)$$

where $D_1 > 0$ is a positive scalar. \diamond

This assumption is satisfied, for example, by all functions f of the form

$$f(\mathbf{x}, \mathbf{a}, t) = \lambda(\mathbf{x}, t) f_m(\mathbf{x}, \phi(\mathbf{x}, t)^T \mathbf{a}, t), \quad (41)$$

where $\lambda : \mathbb{R}^n \times \mathbb{R}_{\geq 0} \rightarrow \mathbb{R}$, $\phi : \mathbb{R}^n \times \mathbb{R}_{\geq 0} \rightarrow \mathbb{R}^p$, $f_m : \mathbb{R}^n \times \mathbb{R} \times \mathbb{R}_{\geq 0} \rightarrow \mathbb{R}$, and where f_m is monotonic and Lipschitz in $\phi(\mathbf{x})^T \mathbf{a}$. In this setting, $\alpha(\mathbf{x}, t)$ may be taken as $\alpha(\mathbf{x}, t) = (-1)^p D_1 \lambda(\mathbf{x}, t) \phi(\mathbf{x}, t)$ where $p = 0$ if f_m is non-decreasing in $\phi^T \mathbf{a}$ and $p = 1$ if f_m is non-increasing in $\phi^T \mathbf{a}$ (I. Tyukin, 2011; Tyukin et al., 2007).

Under Assumption 3.3, Tyukin showed that the adaptation law

$$\dot{\tilde{\mathbf{a}}} = -\tilde{f}(\mathbf{x}, \tilde{\mathbf{a}}, t) \mathbf{P} \alpha(\mathbf{x}, t) \quad (42)$$

with $\mathbf{P} = \mathbf{P}^T > 0$ ensures that $\tilde{f} \in L_2 \cap \mathcal{L}_\infty$ and that all trajectories $(\mathbf{x}, \tilde{\mathbf{a}})$ remain bounded. Equation (42) may be implemented in a manner similar to (31)-(34)

$$\xi(\mathbf{x}, \mathbf{x}_d, t) = -\mathbf{P} s(\mathbf{x}, \mathbf{x}_d) \alpha(\mathbf{x}, t), \quad (43)$$

$$\rho(\mathbf{x}, \mathbf{x}_d, t) = \mathbf{P} \int_{x_n(t_0)}^{x_n(t)} s(\mathbf{x}, \mathbf{x}_d) \frac{\partial \alpha(\mathbf{x}, t)}{\partial x_n} dx_n, \quad (44)$$

$$\tilde{\mathbf{a}} = \bar{\mathbf{a}} + \xi(\mathbf{x}, \mathbf{x}_d, t) + \rho(\mathbf{x}, \mathbf{x}_d, t), \quad (45)$$

$$\dot{\tilde{\mathbf{a}}} = -\eta s \mathbf{P} \alpha + \mathbf{P} s \sum_{i=1}^{n-1} \frac{\partial \alpha}{\partial x_i} x_{i+1} - \sum_{i=1}^{n-1} \frac{\partial \rho}{\partial x_i} x_{i+1} - \left(\frac{\partial \rho}{\partial \mathbf{x}_d} \right)^T \dot{\mathbf{x}}_d - \frac{\partial \xi}{\partial t} - \frac{\partial \rho}{\partial t}. \quad (46)$$

Algorithm (42) is similar to a gradient flow algorithm. If $f(\mathbf{x}, \mathbf{a}, t)$ has the form (41) and is non-decreasing, gradient flow on the loss function $L(\mathbf{x}, \hat{\mathbf{a}}, t) = \frac{1}{2} \tilde{f}^2(\mathbf{x}, \hat{\mathbf{a}}, t)$ with a gain matrix $D_1 \mathbf{P}$ leads to

$$\dot{\hat{\mathbf{a}}} = -\tilde{f}(\mathbf{x}, \hat{\mathbf{a}}, t) f'_m(\mathbf{x}, \boldsymbol{\phi}^T \hat{\mathbf{a}}, t) \mathbf{P} \boldsymbol{\alpha}$$

where $'$ denotes differentiation with respect to the second argument. $f'_m(\mathbf{x}, \boldsymbol{\phi}^T \hat{\mathbf{a}}, t)$ is of unknown sign, but by monotonicity of \tilde{f} in the sense of (39), it is sufficient to set it to one to ensure that the search proceeds in the correct direction despite non-convexity of the square loss in this setting. Similarly, if f is non-increasing, we find

$$\dot{\hat{\mathbf{a}}} = \tilde{f}(\mathbf{x}, \hat{\mathbf{a}}, t) f'_m(\mathbf{x}, \boldsymbol{\phi}^T \hat{\mathbf{a}}, t) \mathbf{P} \boldsymbol{\alpha}$$

and it is sufficient to set f'_m to negative one to ensure the search proceeds in the correct direction.

In machine learning, specifically the area of isotonic regression, remarkably similar methods have been used to estimate generalized linear models (GLMs). GLM regression is an extension of linear regression where the data is assumed to be generated by a function of the form $f(\mathbf{x}) = u(\mathbf{w}^T \mathbf{x})$ for known ‘link function’ u and unknown parameters \mathbf{w} . The first computationally and statistically efficient algorithm for this problem – the GLM-Tron of Kakade et al. (2011) – assumes that u is Lipschitz and monotonic, much like Assumption 3.3.

The GLM-Tron algorithm was recently extended to the setting of kernel methods and was subsequently used to provably learn two hidden layer neural networks by Goel and Klivans (2017); this extension is known as the Alphatron. In the kernel GLM setting handled by the Alphatron, the function to be approximated is assumed to be of the form $f(\mathbf{x}) = u(\sum_{i=1}^m w_i \mathcal{K}(\mathbf{x}, \mathbf{x}_i))$ where \mathcal{K} is the kernel function for a Reproducing Kernel Hilbert Space (RKHS) \mathcal{H} . \mathcal{K} is thus given by the RKHS inner product of a feature map ψ , $\mathcal{K}(\mathbf{x}, \mathbf{y}) = \langle \psi(\mathbf{x}), \psi(\mathbf{y}) \rangle_{\mathcal{H}}$. As in the setting handled by the GLM-Tron, u is assumed to be monotonic and Lipschitz. The Alphatron initializes all weights to zero, and given a batch of labeled training data $(\mathbf{x}_i, f(\mathbf{x}_i))_{i=1}^m$, updates them with a learning rate $\lambda > 0$ according to the iteration

$$\hat{w}_i^{t+1} = \hat{w}_i^t - \frac{\lambda}{m} \left(\hat{f}(\hat{\mathbf{w}}^t, \mathbf{x}_i) - f(\mathbf{x}_i) \right). \quad (47)$$

We now demonstrate a surprising equivalence between Tyukin’s adaptation law (42) and the Alphatron weight update (47) in the following proposition.

Proposition 3.5. *The adaptation law (42) is an online variant of the Alphatron algorithm (47).*

Proof. Defining the vector $\hat{\mathbf{v}}^t = \sum_{i=1}^m \hat{w}_i^t \psi(\mathbf{x}_i)$, (47) implies the iteration on $\hat{\mathbf{v}}$,

$$\hat{\mathbf{v}}^{t+1} = \hat{\mathbf{v}}^t - \frac{\lambda}{m} \sum_{i=1}^m \left(\hat{f}(\hat{\mathbf{w}}^t, \mathbf{x}_i) - f(\mathbf{x}_i) \right) \psi(\mathbf{x}_i). \quad (48)$$

(48) shows that at time t ,

$$\hat{\mathbf{v}}^t = -\frac{\lambda}{m} \sum_{i=1}^m \left(\sum_{j=1}^{t-1} \tilde{f}_i^j \right) \psi(\mathbf{x}_i), \quad (49)$$

where \tilde{f}_i^j in (49) is the function approximation error on the i^{th} input example at iteration j , $\tilde{f}_i^j = \hat{f}(\hat{\mathbf{w}}^j, \mathbf{x}_i) - f(\mathbf{x}_i)$.

Now, assuming that for the adaptive control problem $f(\mathbf{x}, \mathbf{a}, t) = u(\boldsymbol{\alpha}^T(\mathbf{x}, t) \mathbf{a})$, setting $\mathbf{P} = \lambda \mathbf{I}$, $\hat{\mathbf{a}}(0) = \mathbf{0}$, and integrating both sides of (42), we see that at time t ,

$$\hat{\mathbf{a}}(t) = -\lambda \int_0^t \tilde{f}(\mathbf{x}(t'), \mathbf{a}, t') \boldsymbol{\alpha}(\mathbf{x}(t'), t') dt'. \quad (50)$$

Comparison of (49) to (50) shows that in (50) the data appears continuously, the batch size m is one, and the data is not revisited. The current function approximation \hat{f} at time t for the parameters in (50) can then be written

$$\begin{aligned} \hat{f}(t) &= u(\boldsymbol{\alpha}^T(\mathbf{x}, t) \hat{\mathbf{a}}(t)) = u \left(\int_0^t -\lambda \tilde{f}(\mathbf{x}(t'), \hat{\mathbf{a}}(t'), t') \boldsymbol{\alpha}^T(\mathbf{x}(t'), t) \boldsymbol{\alpha}(\mathbf{x}(t'), t') dt' \right) \\ &= u \left(\int_0^t c(t') \mathcal{K}(t, t') dt' \right) \end{aligned} \quad (51)$$

where we have defined $c(t') = -\lambda \tilde{f}(\mathbf{x}(t'), \hat{\mathbf{a}}(t'), t')$ and $\mathcal{K}(t, t') = \boldsymbol{\alpha}^T(\mathbf{x}(t), t) \boldsymbol{\alpha}(\mathbf{x}(t'), t')$. Similarly, in the case of the Alphatron, the current approximation at iteration t is given by

$$\begin{aligned}\hat{f}(\hat{\mathbf{w}}^t, \mathbf{x}) &= u \left(\langle \hat{\mathbf{v}}^t, \boldsymbol{\psi}(\mathbf{x}) \rangle_{\mathcal{H}} \right) = u \left(\sum_{i=1}^m \left(\sum_{j=1}^{t-1} -\frac{\lambda}{m} \tilde{f}_i^j \right) \langle \boldsymbol{\psi}(\mathbf{x}), \boldsymbol{\psi}(\mathbf{x}_i) \rangle \right) \\ &= u \left(\sum_{i=1}^m \hat{w}_i^t \mathcal{K}(\mathbf{x}, \mathbf{x}_i) \right),\end{aligned}\quad (52)$$

where we have noted that with $\hat{w}_i^0 = 0$ for all i , $\hat{w}_i^t = \sum_{j=1}^{t-1} -\frac{\lambda}{m} \tilde{f}_i^j$. The correspondence between (51) and (52) is clear. \square

Proposition 3.5 demonstrates an equivalence between techniques in nonlinearly parameterized adaptive control and non-convex learning. Given the well-recognized importance of momentum in non-convex learning problems (Attouch, Goudou, & Redont, 2000; Jin, Netrapalli, & Jordan, 2017; O'Neill & Wright, 2017), this correspondence immediately suggests the higher-order version of (42)

$$\ddot{\hat{\mathbf{a}}} + \left(\beta \mathcal{N} - \frac{\dot{\mathcal{N}}}{\mathcal{N}} \right) \dot{\hat{\mathbf{a}}} = -\gamma \beta \mathcal{N} \tilde{f} \boldsymbol{\alpha}, \quad (53)$$

which, as before, admits an equivalent representation in terms of two first-order systems,

$$\dot{\hat{\mathbf{v}}} = -\gamma \tilde{f} \boldsymbol{\alpha}, \quad (54)$$

$$\dot{\hat{\mathbf{a}}} = \beta \mathcal{N} (\hat{\mathbf{v}} - \hat{\mathbf{a}}). \quad (55)$$

Equation (53) may be implemented through (54) & (55) via the PI form (43)-(46) applied to the $\hat{\mathbf{v}}$ variable. Equation (53) may be obtained via the Bregman Lagrangian (35) for higher-order velocity gradient laws by choosing only the integral term. It is then necessary to modify the resulting Euler-Lagrange equations by setting f'_m to ± 1 based on monotonicity of \tilde{f} . (54) and (55) can also be obtained from the corresponding Bregman Hamiltonian, following Remark 2.5 and again setting f'_m according to the monotonicity properties of f . The following proposition summarizes the properties of (54) and (55).

Proposition 3.6. *Consider the algorithm (53) or its equivalent form (54) & (55) under Assumption 3.3 with $\mathcal{N} = 1 + \mu \|\boldsymbol{\alpha}(\mathbf{x}, t)\|^2$ and $\mu > \frac{\gamma D_1}{\beta}$. Then, all trajectories $(\mathbf{x}, \hat{\mathbf{a}}, \hat{\mathbf{v}})$ remain bounded, $\tilde{f} \in L_2$, $(\hat{\mathbf{a}} - \hat{\mathbf{v}}) \in \mathcal{L}_2$, $s \in \mathcal{L}_2 \cap \mathcal{L}_\infty$, $s \rightarrow 0$ and $\mathbf{x} \rightarrow \mathbf{x}_d$.*

The proof is given in App. A.3.

Remark 3.9. As noted in Remark 3.7, by following the proof of Prop. 3.6, one may also take \mathcal{N} to be matrix-valued as $\mathbf{N} = 1 + \mu \boldsymbol{\alpha}(\mathbf{x}, t) \boldsymbol{\alpha}(\mathbf{x}, t)^T$. \diamond

Proposition 3.6 shows that the Bregman Lagrangian-based framework for generating higher-order algorithms is quite general, and may also be applied to the nonlinearly parameterized setting, despite non-convexity of the corresponding optimization problems.

Predominantly inspired by deep learning, there has recently been strong interest in non-convex models that are nevertheless amenable to gradient-based or gradient-inspired optimization. The development in this section suggests that progress in learning algorithm development for these models should be followed by the adaptive control community and used to develop new adaptive control algorithms. In the reverse direction, our higher-order algorithm (53) can immediately be converted into an online or batch learning algorithm with momentum for kernel-based GLMs by assuming that \tilde{f} is measured, rather than differentially related to s as in (6).

3.4 The elastic modification

We now consider a modification to the previously discussed adaptive control laws inspired by the Elastic Averaging SGD (EASGD) algorithm (Boffi & Slotine, 2020; Zhang et al., 2014). EASGD is an algorithm intended for distributed training of deep neural networks across p graphics processing units (GPUs). Each GPU is used to train a local copy of the deep network model, and each local copy maintains its own set of parameters $\hat{\mathbf{a}}^{(i)}$. These parameters are updated

according to the iteration

$$\hat{\mathbf{a}}_{t+1}^{(i)} = \hat{\mathbf{a}}_t^{(i)} - \lambda \mathbf{g}_t^{(i)} + \lambda k \left(\bar{\mathbf{a}}_t - \hat{\mathbf{a}}_t^{(i)} \right), \quad (56)$$

$$\bar{\mathbf{a}}_{t+1} = \bar{\mathbf{a}}_t + \lambda k \left(\frac{1}{p} \sum_{i=1}^p \hat{\mathbf{a}}_t^{(i)} - \bar{\mathbf{a}}_t \right), \quad (57)$$

where λ is the learning rate, $\mathbf{g}_t^{(i)}$ is the stochastic gradient approximation computed by the i^{th} agent at timestep t , k is the coupling strength, and $\bar{\mathbf{a}}$ is the *quorum* variable (Russo & Slotine, 2011; Tabareau, Slotine, & Pham, 2010). Equation (57) takes the form of a low-pass filter of the instantaneous average of the set of local parameters.

It was observed by Boffi and Slotine (2020) that in the non-distributed ($p = 1$) case, (56) & (57) do not reduce to standard stochastic gradient descent, and that application of EASGD in this setting has different generalization properties than standard SGD when used to train deep neural networks. In this sense, the $p = 1$ reduction of EASGD is a new higher-order in-time optimization algorithm. In a similar vein, by construction of suitable Lyapunov functions, we now show that adding a quorum-like variable to the adaptive laws considered in previous sections maintains their stability. This immediately gives rise to a new class of higher-order adaptive control algorithms. Interestingly, these algorithms do not seem to admit an equivalent representation in terms of a single second-, third-, or fourth-order system for $\hat{\mathbf{a}}$, but must be written as a system of first-order equations.

Remark 3.10. The algorithms considered in this subsection immediately extend to the case of cloud-based adaptation for networked robotic systems (Wensing & Slotine, 2017), where the quorum variable is allowed to have its own dynamics as in (57) rather than simply representing the instantaneous spatial average of the distributed parameters. \diamond

3.4.1 Elastic modification for the Slotine & Li controller

We first apply the elastic modification to the Slotine & Li adaptive controller (8) for linearly parameterized unknown dynamics $\tilde{f} = \mathbf{Y}\tilde{\mathbf{a}}$. These results extend trivially to the non-filtered composite algorithm of Sec. 3.2. To this end, we define the adaptation law

$$\dot{\hat{\mathbf{a}}} = -\mathbf{P}\mathbf{Y}^T s + k (\bar{\mathbf{a}} - \hat{\mathbf{a}}), \quad (58)$$

$$\dot{\bar{\mathbf{a}}} = k (\hat{\mathbf{a}} - \bar{\mathbf{a}}), \quad (59)$$

whose basic stability properties are summarized in the following proposition.

Proposition 3.7. *Consider the adaptation law (58) & (59). Then all trajectories $(\mathbf{x}, \hat{\mathbf{a}}, \bar{\mathbf{a}})$ remain bounded, $s \in \mathcal{L}_2 \cap \mathcal{L}_\infty$, $(\hat{\mathbf{a}} - \bar{\mathbf{a}}) \in \mathcal{L}_2$, $s \rightarrow 0$ and $\mathbf{x} \rightarrow \mathbf{x}_d$.*

Proof. The Lyapunov-like function

$$V = \frac{1}{2} \left(\tilde{\mathbf{a}}^T \mathbf{P}^{-1} \tilde{\mathbf{a}} + \tilde{\mathbf{a}}^T \mathbf{P}^{-1} \tilde{\mathbf{a}} + s^2 \right)$$

has time derivative

$$\dot{V} = -\eta s^2 - k (\bar{\mathbf{a}} - \hat{\mathbf{a}})^T \mathbf{P}^{-1} (\bar{\mathbf{a}} - \hat{\mathbf{a}}).$$

This shows that s , $\hat{\mathbf{a}}$, and $\bar{\mathbf{a}}$ remain bounded. The remaining conclusions of the proposition are immediately drawn by integrating \dot{V} and applying Barbalat's lemma. \square

3.4.2 Elastic modification for nonlinearly parameterized systems

We now apply the elastic modification to the algorithm (42) for nonlinearly parameterized unknown dynamics satisfying Assumption 3.3. As in (58) & (59), we define

$$\dot{\tilde{\mathbf{a}}} = -\tilde{f} \mathbf{P} \alpha + k (\bar{\mathbf{a}} - \tilde{\mathbf{a}}), \quad (60)$$

$$\dot{\bar{\mathbf{a}}} = k (\tilde{\mathbf{a}} - \bar{\mathbf{a}}). \quad (61)$$

Proposition 3.8. *Consider the adaptation law (60) & (61) implemented with appropriate modifications to (43)-(46). Then all trajectories $(\mathbf{x}, \hat{\mathbf{a}}, \bar{\mathbf{a}})$ remain bounded, $\tilde{f} \in \mathcal{L}_2 \cap \mathcal{L}_\infty$, $(\hat{\mathbf{a}} - \bar{\mathbf{a}}) \in \mathcal{L}_2$, $s \in \mathcal{L}_\infty \cap \mathcal{L}_2$, $s \rightarrow 0$ and $\mathbf{x} \rightarrow \mathbf{x}_d$.*

Proof. The Lyapunov-like function

$$V = \frac{1}{2} \left(\tilde{\mathbf{a}}^T \mathbf{P}^{-1} \tilde{\mathbf{a}} + \tilde{\mathbf{a}}^T \mathbf{P}^{-1} \tilde{\mathbf{a}} \right)$$

has time derivative

$$\dot{V} \leq -\frac{1}{D_1} \tilde{f}^2 - k(\hat{\mathbf{a}} - \bar{\mathbf{a}})^T \mathbf{P}^{-1}(\hat{\mathbf{a}} - \bar{\mathbf{a}}).$$

This shows that $\hat{\mathbf{a}}$ and $\bar{\mathbf{a}}$ remain bounded. Integration of \dot{V} shows $\tilde{f} \in \mathcal{L}_2$ and $(\hat{\mathbf{a}} - \bar{\mathbf{a}}) \in \mathcal{L}_2$. Application of Lemma A.1 completes the proof. \square

3.4.3 Elastic modification for higher-order algorithms

We now turn to consider the higher-order algorithms presented in Secs. 3.2 and 3.3. In the higher-order setting, there are three clear possibilities for the elastic modification: coupling to a quorum variable for the $\hat{\mathbf{a}}$ variable, coupling to a quorum variable for the $\hat{\mathbf{v}}$ variable, or coupling to quorum variables in both $\hat{\mathbf{a}}$ and $\hat{\mathbf{v}}$. We prove stability for all three possibilities only in the nonlinearly parameterized setting described by Assumption 3.3. The results extend naturally to the higher-order composite algorithm for linearly parameterized systems presented in Sec. 3.2 by suitable adjustments to the proofs. We begin with the first possibility,

$$\dot{\hat{\mathbf{v}}} = -\gamma \tilde{f} \boldsymbol{\alpha}, \quad (62)$$

$$\dot{\hat{\mathbf{a}}} = \beta \mathcal{N}(\hat{\mathbf{v}} - \hat{\mathbf{a}}) + k \beta \mathcal{N}(\bar{\mathbf{a}} - \hat{\mathbf{a}}), \quad (63)$$

$$\dot{\bar{\mathbf{a}}} = k \beta \mathcal{N}(\hat{\mathbf{a}} - \bar{\mathbf{a}}). \quad (64)$$

The basic stability properties of the algorithm (62)-(64) are summarized in the following proposition.

Proposition 3.9. *Consider the higher-order algorithm with elastic modification in the $\hat{\mathbf{a}}$ variable (62)-(64) under Assumption 3.3. Set $\frac{1}{3} \leq k < 1$, $\mathcal{N} = 1 + \mu \|\boldsymbol{\alpha}(\mathbf{x}, t)\|^2$, and $\mu > \frac{2D_1\gamma}{\beta(1-k)}$. Then all trajectories $(\mathbf{x}, \hat{\mathbf{a}}, \hat{\mathbf{v}}, \bar{\mathbf{a}})$ remain bounded, $\tilde{f} \in \mathcal{L}_2 \cap \mathcal{L}_\infty$, $s \in \mathcal{L}_2 \cap \mathcal{L}_\infty$, $(\hat{\mathbf{a}} - \hat{\mathbf{v}}) \in \mathcal{L}_2$, $(\hat{\mathbf{a}} - \bar{\mathbf{a}}) \in \mathcal{L}_2$, $s \rightarrow 0$ and $\mathbf{x} \rightarrow \mathbf{x}_d$.*

The proof is given in App. A.4. We now consider the second possibility of adding a quorum variable in the $\hat{\mathbf{v}}$ variable,

$$\dot{\hat{\mathbf{v}}} = -\gamma \tilde{f} \boldsymbol{\alpha} + \rho(\bar{\mathbf{v}} - \hat{\mathbf{v}}), \quad (65)$$

$$\dot{\bar{\mathbf{v}}} = \rho(\hat{\mathbf{v}} - \bar{\mathbf{v}}), \quad (66)$$

$$\dot{\hat{\mathbf{a}}} = \beta \mathcal{N}(\hat{\mathbf{v}} - \hat{\mathbf{a}}). \quad (67)$$

The basic stability properties of (65)-(67) are summarized in the following proposition.

Proposition 3.10. *Consider the higher-order algorithm with elastic modification in the $\hat{\mathbf{v}}$ variable (65)-(67) under Assumption 3.3. Set $\rho < 2\beta$, $\mathcal{N} = 1 + \mu \|\boldsymbol{\alpha}(\mathbf{x}, t)\|^2$, and $\mu > \frac{\gamma D_1}{\beta}$. Then all trajectories $(\mathbf{x}, \hat{\mathbf{a}}, \hat{\mathbf{v}}, \bar{\mathbf{v}})$ remain bounded, $\tilde{f} \in \mathcal{L}_2 \cap \mathcal{L}_\infty$, $s \in \mathcal{L}_2 \cap \mathcal{L}_\infty$, $(\hat{\mathbf{v}} - \bar{\mathbf{v}}) \in \mathcal{L}_2$, $(\hat{\mathbf{v}} - \hat{\mathbf{a}}) \in \mathcal{L}_2$, $s \rightarrow 0$ and $\mathbf{x} \rightarrow \mathbf{x}_d$.*

The proof is given in App. A.5. Finally, we consider adding coupling to quorum variables in both $\hat{\mathbf{a}}$ and $\hat{\mathbf{v}}$,

$$\dot{\hat{\mathbf{v}}} = -\gamma \tilde{f} \boldsymbol{\alpha} + \rho(\bar{\mathbf{v}} - \hat{\mathbf{v}}), \quad (68)$$

$$\dot{\bar{\mathbf{v}}} = \rho(\hat{\mathbf{v}} - \bar{\mathbf{v}}), \quad (69)$$

$$\dot{\hat{\mathbf{a}}} = \beta \mathcal{N}(\hat{\mathbf{v}} - \hat{\mathbf{a}}) + k \beta \mathcal{N}(\bar{\mathbf{a}} - \hat{\mathbf{a}}), \quad (70)$$

$$\dot{\bar{\mathbf{a}}} = k \beta \mathcal{N}(\hat{\mathbf{a}} - \bar{\mathbf{a}}). \quad (71)$$

The basic stability properties of (68)-(71) are summarized in the following proposition.

Proposition 3.11. *Consider the higher-order algorithm with the elastic modification in both the $\hat{\mathbf{v}}$ and $\hat{\mathbf{a}}$ variables (68)-(71) under Assumption 3.3. Set $\rho < \beta(1-k)$, $\frac{1}{3} \leq k < 1$, $\mathcal{N} = 1 + \mu \|\boldsymbol{\alpha}(\mathbf{x}, t)\|^2$ and $\mu > \frac{2\gamma D_1}{\beta(1-k)}$. Then, all trajectories $(\mathbf{x}, \hat{\mathbf{v}}, \bar{\mathbf{v}}, \hat{\mathbf{a}}, \bar{\mathbf{a}})$ remain bounded, $\tilde{f} \in \mathcal{L}_2 \cap \mathcal{L}_\infty$, $s \in \mathcal{L}_2 \cap \mathcal{L}_\infty$, $(\hat{\mathbf{v}} - \bar{\mathbf{v}}) \in \mathcal{L}_2$, $(\hat{\mathbf{a}} - \bar{\mathbf{a}}) \in \mathcal{L}_2$, $(\hat{\mathbf{v}} - \hat{\mathbf{a}}) \in \mathcal{L}_2$, $s \rightarrow 0$ and $\mathbf{x} \rightarrow \mathbf{x}_d$.*

The proof is given in App. A.6. We have thus shown that all adaptive control algorithms presented in this paper, as well as the classic algorithm of Slotine and Li, can be modified to include feedback coupling to a low-pass filtered (exponentially weighted average) version of the adaptation variables. It is well known that iterate averaging for stochastic optimization algorithms such as stochastic gradient descent can improve convergence rates via variance reduction (B. T. Polyak & Juditsky, 1992). The elastic modification is similar in spirit, but employs feedback rather than series coupling. This suggests that adding the elastic term may improve robustness of adaptation algorithms, and we leave a theoretical investigation of this conjecture for future work.

3.5 Exponential forgetting least squares and bounded gain forgetting

We now demonstrate how to apply the techniques of exponential forgetting and bounded gain forgetting least squares (J.-J. Slotine & Li, 1991) to the adaptation algorithms presented thus far. These techniques are useful for estimation of time-varying parameters, as they rapidly discard previous information used for parameter estimation. Exponential forgetting least squares is described by a time-dependent learning-rate matrix $\mathbf{P}(t)$, which, in the linearly parameterized case $\tilde{f} = \mathbf{Y}\tilde{\mathbf{a}}$ takes the form

$$\dot{\mathbf{P}} = \begin{cases} \lambda\mathbf{P} - \mathbf{P}\mathbf{Y}^T\mathbf{Y}\mathbf{P} & \text{if } \|\mathbf{P}\| \leq P_0 \\ 0 & \text{else,} \end{cases} \quad (72)$$

where $\lambda > 0$ is a constant forgetting factor, P_0 is a maximum bound on the norm, and $\|\mathbf{P}\|$ is a matrix norm such as the induced matrix 2-norm. Equation (72) implies for the inverse matrix

$$\frac{d}{dt}\mathbf{P}^{-1} = \begin{cases} -\lambda\mathbf{P}^{-1} + \mathbf{Y}^T\mathbf{Y} & \text{if } \|\mathbf{P}\| \leq P_0 \\ 0 & \text{else.} \end{cases} \quad (73)$$

In the nonlinearly parameterized case described by Assumption 3.3, we will replace \mathbf{Y}^T in (72) & (73) by $\alpha(\mathbf{x}, t)$. In the bounded gain forgetting technique, λ is a time-dependent function

$$\lambda(t) = \lambda_0 \left(1 - \frac{\|\mathbf{P}\|}{P_0} \right) \quad (74)$$

where $\lambda_0 > 0$ sets the forgetting factor when the norm of \mathbf{P} is small. It can be shown that this choice of $\lambda(t)$ ensures that $\|\mathbf{P}\| \leq P_0$, and thus we may drop the case statement in (72) & (73) (J.-J. Slotine & Li, 1991). The choice of $\lambda(t)$ in bounded gain forgetting and the case statement used in (72) & (73) are both employed to prevent unboundedness of the learning rate matrix.

We focus on algorithms without the elastic modification of Sec. 3.4; extension to the elastic modification is simple. We also focus on the bounded gain forgetting technique: proofs for the exponential forgetting least squares technique are identical, with the addition of an appropriate case statement in the time derivative of the Lyapunov function. For simplicity, we include only the time-dependent gain $\mathbf{P}(t)$ and set the scalar gains $\kappa = \gamma = 1$ where applicable.

3.5.1 First-order non-filtered composite

We begin with the first-order non-filtered composite (30) with \mathbf{P} given by (72). In this case, the composite algorithm may be implemented via the PI form (31)-(34) where now $\mathbf{P} = \mathbf{P}(t)$.

Proposition 3.12. *Consider the adaptation algorithm (30) with $\mathbf{P}(t)$ given by (72), $\lambda(t)$ given by (74), and $\kappa = \gamma = 1$. Then all trajectories $(\mathbf{x}, \tilde{\mathbf{a}})$ remain bounded, $\tilde{f} \in \mathcal{L}_2 \cap \mathcal{L}_\infty$, $s \in \mathcal{L}_2 \cap \mathcal{L}_\infty$, $s \rightarrow 0$ and $\mathbf{x} \rightarrow \mathbf{x}_d$.*

Proof. The Lyapunov-like function

$$V = \frac{1}{2}s^2 + \frac{1}{2}\tilde{\mathbf{a}}^T\mathbf{P}^{-1}\tilde{\mathbf{a}},$$

has time derivative

$$\dot{V} = -\eta s^2 - \frac{1}{2}\tilde{f}^2 - \frac{\lambda}{2}\tilde{\mathbf{a}}^T\mathbf{P}^{-1}\tilde{\mathbf{a}},$$

which shows that s and $\tilde{\mathbf{a}}$ remain bounded. Because s remains bounded, \mathbf{x} remains bounded. Integrating \dot{V} shows that $s \in \mathcal{L}_2$ and $\tilde{f} \in \mathcal{L}_2$. The proof is completed by application of Lemma A.1 or directly by Barbalat's Lemma. \square

3.5.2 Higher-order non-filtered composite

We can state a similar result for the higher-order non-filtered composite with time-dependent $\mathbf{P}(t)$ given by (72),

$$\ddot{\mathbf{a}} + \left(\beta\mathcal{N} - \frac{\dot{\mathcal{N}}}{\mathcal{N}} - \dot{\mathbf{P}}\mathbf{P}^{-1} \right) \dot{\mathbf{a}} = -\beta\mathcal{N}\mathbf{P}(t)\mathbf{Y}^T(s + \tilde{f}), \quad (75)$$

which admits the equivalent representation as two first-order systems,

$$\dot{\mathbf{v}} = -\mathbf{P}(t)\mathbf{Y}^T(s + \tilde{f}), \quad (76)$$

$$\dot{\mathbf{a}} = \beta\mathcal{N}\mathbf{P}(t)(\mathbf{v} - \hat{\mathbf{a}}). \quad (77)$$

Equation (76) can be implemented via the PI form $\hat{\mathbf{v}} = \bar{\mathbf{v}} + \xi(\mathbf{x}, \mathbf{x}_d, t) + \rho(\mathbf{x}, \mathbf{x}_d, t)$ where ξ , ρ , and $\bar{\mathbf{v}}$ are given by (31), (32), and (34) respectively with $\gamma = \kappa = 1$.

Proposition 3.13. Consider the adaptation algorithm (75) or its equivalent form (76) & (77) with $\mathbf{P}(t)$ given by (72), $\lambda(t)$ given by (74), $\mathcal{N}(t) = 1 + \mu \|\mathbf{Y}\|^2$ and $\mu > \frac{3\eta+2}{2\eta\beta}$. Then all trajectories $(\mathbf{x}, \hat{\mathbf{v}}, \hat{\mathbf{a}})$ remain bounded, $\tilde{f} \in \mathcal{L}_2 \cap \mathcal{L}_\infty$, $s \in \mathcal{L}_2 \cap \mathcal{L}_\infty$, $s \rightarrow 0$ and $\mathbf{x} \rightarrow \mathbf{x}_d$.

The proof is given in App. A.7.

Remark 3.11. Because $\mathbf{P}(t)$ is uniformly bounded in t , it is not necessary to include $\mathbf{P}(t)$ in (77); by a slight modification of the proof, it is easy to show that the modified higher-order law

$$\ddot{\hat{\mathbf{a}}} + \left(\beta \mathcal{N} - \frac{\dot{\mathcal{N}}}{\mathcal{N}} \right) \dot{\hat{\mathbf{a}}} = -\beta \mathcal{N} \mathbf{P}(t) \mathbf{Y}^T (s + \tilde{f}),$$

is also a stable adaptive law with a suitable choice of gains. \diamond

3.5.3 First-order algorithm for nonlinearly parameterized systems

We now consider Tyukin's first-order algorithm for nonlinearly parameterized systems (42) with $\mathbf{P} = \mathbf{P}(t)$ given by (72). To do so, we require an additional assumption

Assumption 3.4. For the same function $\boldsymbol{\alpha}(\mathbf{x}, t)$ as in Assumption 3.3, there exists a constant D_2 such that

$$|\tilde{f}(\mathbf{x}, \hat{\mathbf{a}}, t)| \geq D_2 |\boldsymbol{\alpha}(\mathbf{x}, t)^T \tilde{\mathbf{a}}|. \quad (78)$$

Assumption 3.4 requires the existence of a known lower bounding linear function for the function approximation error \tilde{f} . Together with Assumption 3.3, it states that \tilde{f} lies between two linear functions. Given that the update (72) is derived based on recursive *linear* least squares considerations, it is unsurprising that such an assumption is required in the nonlinearly parameterized setting. We are now in a position to state the following proposition.

Proposition 3.14. Consider the adaptation algorithm (42) with $\mathbf{P}(t)$ given by (72) and $\lambda(t)$ given by (74) for \tilde{f} satisfying Assumptions 3.3 and 3.4. Further assume that $D_1 < 2D_2^2$ or that $D_2 > \frac{1}{2}$. Then, all trajectories $(\mathbf{x}, \hat{\mathbf{a}})$ remain bounded, $\tilde{f} \in \mathcal{L}_2$, $s \in \mathcal{L}_2 \cap \mathcal{L}_\infty$, $s \rightarrow 0$ and $\mathbf{x} \rightarrow \mathbf{x}_d$.

Proof. Consider the Lyapunov-like function

$$V = \frac{1}{2} \tilde{\mathbf{a}}^T \mathbf{P}^{-1} \tilde{\mathbf{a}}, \quad (79)$$

which has time derivative

$$\begin{aligned} \dot{V} &= -\tilde{f} \boldsymbol{\alpha}^T \tilde{\mathbf{a}} + \frac{1}{2} (\tilde{\mathbf{a}}^T \boldsymbol{\alpha})^2 - \frac{\lambda}{2} \tilde{\mathbf{a}}^T \mathbf{P}^{-1} \tilde{\mathbf{a}}, \\ &\leq -\frac{1}{D_1} \tilde{f}^2 + \frac{1}{2D_2^2} \tilde{f}^2 = -\left(\frac{1}{D_1} - \frac{1}{2D_2^2} \right) \tilde{f}^2. \end{aligned}$$

For $D_1 < 2D_2^2$, $\dot{V} \leq 0$ and $\tilde{f}^2 \in \mathcal{L}_2$. Alternatively, using the same Lyapunov function,

$$\dot{V} \leq -(\boldsymbol{\alpha}^T \tilde{\mathbf{a}})^2 \left(D_2 - \frac{1}{2} \right).$$

For $D_2 > \frac{1}{2}$, $\dot{V} \leq 0$ and $\boldsymbol{\alpha}^T \tilde{\mathbf{a}} \in \mathcal{L}_2$. By Assumption 3.3, this implies that $\tilde{f} \in \mathcal{L}_2$. Hence, both approaches demonstrate that $\hat{\mathbf{a}}$ remains bounded and that $\tilde{f} \in \mathcal{L}_2$. By Lemma A.1, the proposition is proved. \square

3.5.4 Higher-order algorithm for nonlinearly parameterized systems

Last, we consider the higher-order algorithm for nonlinearly parameterized systems

$$\ddot{\hat{\mathbf{a}}} + \left(\beta \mathcal{N} - \frac{\dot{\mathcal{N}}}{\mathcal{N}} - \dot{\mathbf{P}} \mathbf{P}^{-1} \right) \dot{\hat{\mathbf{a}}} = -\beta \mathcal{N} \tilde{f} \mathbf{P}(t) \boldsymbol{\alpha}(\mathbf{x}, t), \quad (80)$$

which admits the equivalent representation as two first-order systems,

$$\dot{\hat{\mathbf{v}}} = -\tilde{f} \mathbf{P}(t) \boldsymbol{\alpha}(\mathbf{x}, t) \quad (81)$$

$$\dot{\hat{\mathbf{a}}} = \beta \mathcal{N} \mathbf{P}(t) (\hat{\mathbf{v}} - \hat{\mathbf{a}}) \quad (82)$$

Proposition 3.15. Consider the adaptation algorithm (80) or its equivalent form (81) & (82) with $\mathbf{P}(t)$ given by (72), $\lambda(t)$ given by (74), $\mathcal{N} = 1 + \mu \|\boldsymbol{\alpha}\|^2$, and $\mu > \frac{4D_2 - 2 + (2D_1 + 1)^2}{\beta(4D_2 - 1)}$. Let \tilde{f} satisfy Assumptions 3.3 and 3.4. Further assume that $D_2 > \frac{1}{2}$. Then, all trajectories $(\mathbf{x}, \hat{\mathbf{v}}, \hat{\mathbf{a}})$ remain bounded, $\tilde{f} \in \mathcal{L}_2$, $s \in \mathcal{L}_2 \cap \mathcal{L}_\infty$, $s \rightarrow 0$ and $\mathbf{x} \rightarrow \mathbf{x}_d$.

The proof is given in App. A.8.

Remark 3.12. As in Sec. 3.5.2, because $\mathbf{P}(t)$ is uniformly bounded in t , it is not necessary to include $\mathbf{P}(t)$ in (82). It is simple to show by modification of the proof that

$$\ddot{\hat{\mathbf{a}}} + \left(\beta\mathcal{N} - \frac{\dot{\mathcal{N}}}{\mathcal{N}} \right) \dot{\hat{\mathbf{a}}} = -\beta\mathcal{N}\tilde{f}\mathbf{P}(t)\boldsymbol{\alpha}(\mathbf{x}, t)$$

is also a stable adaptive law with a suitable choice of gains.

4 Natural gradient adaptation and implicit regularization

4.1 The Bregman divergence and natural adaptation laws

Lee, Kwon, and Park (2018) introduced an elegant modification of the Slotine and Li adaptive robot controller, later generalized by Wensing and Slotine (2018). It consists of replacing the usual parameter estimation error term $\frac{1}{2}\|\tilde{\mathbf{a}}\|^2$ in the Lyapunov-like function $V = \frac{1}{2}s^2 + \frac{1}{2}\|\tilde{\mathbf{a}}\|^2$ with the Bregman divergence $d_\psi(\mathbf{a} \parallel \tilde{\mathbf{a}})$ (introduced in Sec. 2.3), to obtain the new “non-Euclidean” Lyapunov-like function

$$V = \frac{1}{2}s^2 + d_\psi(\mathbf{a} \parallel \tilde{\mathbf{a}}), \quad (83)$$

for an arbitrary strictly convex function ψ . Indeed, a quick calculation shows that the derivative of the Bregman divergence is simply

$$\frac{d}{dt}d_\psi(\mathbf{a} \parallel \tilde{\mathbf{a}}) = \tilde{\mathbf{a}}^T \nabla^2 \psi(\tilde{\mathbf{a}}) \dot{\tilde{\mathbf{a}}}. \quad (84)$$

Taking $\psi(\mathbf{x}) = \frac{1}{2}\mathbf{x}^T \mathbf{P}^{-1} \mathbf{x}$ results in the usual weighted quadratic term $\frac{1}{2}\tilde{\mathbf{a}}^T \mathbf{P}^{-1} \tilde{\mathbf{a}}$ in the Lyapunov function. More generally, this procedure effectively replaces the gain matrix \mathbf{P} in the adaptation law by the $\tilde{\mathbf{a}}$ -dependent *inverse Hessian* $[\nabla^2 \psi(\tilde{\mathbf{a}})]^{-1}$ of the strictly convex function ψ .

As discussed in Wensing and Slotine (2018), in essence, this procedure replaces the gradient of the velocity-gradient functional \dot{Q} by the *natural gradient* in the sense of Amari (1998), so that the resulting adaptation law respects the underlying Riemannian geometry captured by the *Hessian metric* $\nabla^2 \psi(\tilde{\mathbf{a}})$. The standard adaptation law $\dot{\tilde{\mathbf{a}}} = -\mathbf{P} \mathbf{Y}^T s$ uses the constant metric \mathbf{P}^{-1} , which in turn explains the appearance of \mathbf{P} in the natural gradient-like system.

The setting of a general strictly convex function ψ enables designing adaptation algorithms that respect physical Riemannian constraints (Lee et al., 2018; Lee, Wensing, & Park, 2019) that the parameters must obey, as in the estimation of mass properties in robotics (Wensing, Kim, & Slotine, 2018), or allows one to introduce a priori bounds on parameter estimates without resorting to parameter projection techniques through the choice of a log-barrier function for ψ (Lee et al., 2018; Wensing & Slotine, 2018). In Sec. 4.3, we further prove that the choice of ψ imposes implicit regularization of the resulting parameter estimates in adaptive control.

4.2 The Bregman Lagrangian and natural higher-order algorithms

The Bregman Lagrangian easily allows for the introduction of non-Euclidean metrics. In Sec. 2.3, we took the distance generating function ψ to be the Euclidean norm, $\psi(\mathbf{x}) = \frac{1}{2}\|\mathbf{x}\|^2$. We now show that taking an arbitrary strictly convex function leads to a more general class of algorithms that can be seen as the higher-order variants of those discussed in the previous subsection. With the same definitions of $\bar{\alpha}$, $\bar{\gamma}$, and $\bar{\beta}$ as in Sec. 2.3, but now taking the more general Bregman divergence $d_\psi(\cdot \parallel \cdot)$, the Bregman Lagrangian (13) takes the form

$$\mathcal{L} = e^{\int_0^t \beta\mathcal{N}(t)dt} \left(\beta\mathcal{N}d_\psi\left(\hat{\mathbf{a}} + \frac{\dot{\hat{\mathbf{a}}}{\beta\mathcal{N}}}{\mathcal{N}} \parallel \hat{\mathbf{a}}\right) - \gamma \frac{d}{dt} \left[\frac{1}{2}s^2 \right] \right). \quad (85)$$

The Euler-Lagrange equations for (85) lead to the higher-order adaptation law

$$\ddot{\hat{\mathbf{a}}} + \left(\beta\mathcal{N} - \frac{\dot{\mathcal{N}}}{\mathcal{N}} \right) \dot{\hat{\mathbf{a}}} + \gamma\beta\mathcal{N} \left(\nabla^2 \psi \left(\hat{\mathbf{a}} + \frac{\dot{\hat{\mathbf{a}}}{\beta\mathcal{N}}}{\mathcal{N}} \right) \right)^{-1} \mathbf{Y}^T s = 0. \quad (86)$$

As in the previous subsection, the usual adaptive law $\mathbf{Y}^T s$ is pre-multiplied by the inverse Hessian of ψ , now evaluated at $\hat{\mathbf{a}} + \frac{\dot{\hat{\mathbf{a}}}}{\beta\mathcal{N}}$. As discussed in Sec. 2.3, this quantity is precisely $\hat{\mathbf{v}}$. The resulting adaptation law can be written in the equivalent form

$$\dot{\hat{\mathbf{v}}} = -\gamma (\nabla^2 \psi(\hat{\mathbf{v}}))^{-1} \mathbf{Y}^T s, \quad (87)$$

$$\dot{\hat{\mathbf{a}}} = \beta\mathcal{N}(\hat{\mathbf{v}} - \hat{\mathbf{a}}). \quad (88)$$

Equations (87) & (88) demonstrate that using the general Bregman divergence in the Bregman Lagrangian leads to higher-order variants of the “natural” algorithms of Sec. 4.1. Taking the $\beta \rightarrow \infty$ limit immediately recovers the first-order laws discussed in Sec. 4.1. The stability of the above laws for *strongly* convex ψ is stated in the following proposition.

Proposition 4.1. *Consider the higher-order “natural” adaptation law (86) or its equivalent (87) & (88). Assume that ψ is l -strongly convex so that $\nabla^2 \psi(\cdot) \geq l \mathbf{I}$ globally. Take $\mathcal{N} = 1 + \mu \|\mathbf{Y}\|^2$ and $\mu > \frac{\gamma(1+l^{-1})^2}{4\beta\eta}$. Then all trajectories $(\mathbf{x}, \hat{\mathbf{v}}, \hat{\mathbf{a}})$ remain bounded, $s \in \mathcal{L}_2 \cap \mathcal{L}_\infty$, $s \rightarrow 0$ and $\mathbf{x} \rightarrow \mathbf{x}_d$.*

The proof is given in App. A.9. A second, related variant is given by

$$\dot{\hat{\mathbf{v}}} = -\gamma (\nabla^2 \psi(\hat{\mathbf{v}}))^{-1} \mathbf{Y}^T s, \quad (89)$$

$$\dot{\hat{\mathbf{a}}} = \beta\mathcal{N} (\nabla^2 \psi(\hat{\mathbf{a}}))^{-1} (\nabla \psi(\hat{\mathbf{v}}) - \nabla \psi(\hat{\mathbf{a}})). \quad (90)$$

Algorithm (89) & (90) is equivalent to algorithm (14) *entirely in the mirrored domain*. Indeed, it may be re-written

$$\begin{aligned} \frac{d}{dt} \nabla \psi(\hat{\mathbf{v}}) &= -\gamma \mathbf{Y}^T s, \\ \frac{d}{dt} \nabla \psi(\hat{\mathbf{a}}) &= \beta\mathcal{N} (\nabla \psi(\hat{\mathbf{v}}) - \nabla \psi(\hat{\mathbf{a}})), \end{aligned}$$

which shows that $\nabla \psi(\hat{\mathbf{a}})$ obtains the same values over time as $\hat{\mathbf{a}}$ computed via algorithm (14). In effect, as shown by Prop. 4.2, the stability of this adaptive law shows that the parameters obtained by the higher-order algorithm (14) may be transformed via the inverse of the gradient of an l -strongly convex and L -smooth function, and the resulting transformed parameters will still ensure stability and tracking for the closed-loop system.

A modification of (89) & (90) that just incorporates the Hessian metric in $\hat{\mathbf{a}}$ is given by

$$\dot{\hat{\mathbf{v}}} = -\gamma (\nabla^2 \psi(\hat{\mathbf{v}}))^{-1} \mathbf{Y}^T s, \quad (91)$$

$$\dot{\hat{\mathbf{a}}} = \beta\mathcal{N} (\nabla^2 \psi(\hat{\mathbf{a}}))^{-1} (\hat{\mathbf{v}} - \hat{\mathbf{a}}). \quad (92)$$

The properties of these two possible adaptation laws are given in the following proposition.

Proposition 4.2. *Consider the adaptation algorithm (89) & (90) or the adaptation algorithm (91) & (92). Assume that ψ is l -strongly convex and L -smooth, so that $l\mathbf{I} \leq \nabla^2 \psi(\cdot) \leq L\mathbf{I}$. Take $\mathcal{N} = 1 + \mu \|\mathbf{Y}\|^2$ and choose $\mu > \frac{\gamma(l+\gamma L)^2}{4\beta\eta l^3}$ in the former case and $\mu > \frac{\gamma(l+\gamma L)^2}{4\beta\eta l^2}$ in the latter. Then all trajectories $(\mathbf{x}, \hat{\mathbf{v}}, \hat{\mathbf{a}})$ remain bounded, $s \in \mathcal{L}_2 \cap \mathcal{L}_\infty$, $s \rightarrow 0$ and $\mathbf{x} \rightarrow \mathbf{x}_d$.*

The proof is presented in App. A.10.

Remark 4.1. For efficient implementation of the proposed higher-order algorithms, as well as for their first-order equivalents, ψ should be chosen so that $[\nabla^2 \psi(\cdot)]^{-1}$ is efficiently computable and ideally sparse. Alternatively, if the inverse function of the gradient $(\nabla \psi^{-1})(\cdot)$ is efficiently computable, $\nabla \psi(\hat{\mathbf{a}})$ or $\nabla \psi(\hat{\mathbf{v}})$ may be updated directly and subsequently inverted to arrive at the parameter values. Discretization of these algorithms is a subtle issue, and discretization of the $\dot{\hat{\mathbf{a}}}$ and $\dot{\hat{\mathbf{v}}}$ dynamics directly results in a natural gradient-like update (Amari, 1998), while discretization of the $\frac{d}{dt} \nabla \psi(\hat{\mathbf{a}})$ and $\frac{d}{dt} \nabla \psi(\hat{\mathbf{v}})$ dynamics leads to a mirror descent-like update (Beck & Teboulle, 2003; Nemirovski & Yudin, 1983); these discrete-time algorithms have the same continuous-time limit (Krichene, Bayen, & Bartlett, 2015). \diamond

4.3 Implicit regularization and adaptive control

With deep networks as the predominant example, modern machine learning often considers highly over-parameterized models that are capable of interpolating the training data (achieving zero error on the training set) while still generalizing well to unseen examples. The classical principles of statistical learning theory emphasize a trade-off between

generalization performance and model capacity, and predict that in the highly over-parameterized regime, generalization performance should be poor due to a tendency of the model to fit noise in the training data. Nevertheless, empirical evidence indicates that neural networks and other modern machine learning models do not obey classical statistical learning wisdom (Belkin, Hsu, Ma, & Mandal, 2019). More surprisingly, the ability to simultaneously fit label noise in the training data yet generalize to new examples has been observed even in over-parameterized linear models (Bartlett, Long, Lugosi, & Tsigler, 2019; Muthukumar, Vodrahalli, & Sahai, 2019) and has led to the study of *implicit bias* of optimization algorithms – that is, the tendency of an algorithm to converge to a particular (e.g. minimum norm) solution when there are many that interpolate the training data (Azizan & Hassibi, 2019; Azizan et al., 2019; Gunasekar et al., 2018a, 2018b; Soudry et al., 2018).

In adaptive control, the possibility of there being many possible parameter vectors $\hat{\mathbf{a}}$ that lead to zero tracking error is not unique to the over-parameterized case. Unless the trajectory is *persistently exciting* (Narendra & Annaswamy, 2005; J.-J. Slotine & Li, 1991), it is well-known that $\hat{\mathbf{a}}$ will not converge to the true parameters \mathbf{a} in general. Depending on the complexity of the trajectory, there may even be many solutions in the *under-parameterized* case where $\dim(\hat{\mathbf{a}}) < \dim(\mathbf{a})$. This occurs because, to achieve perfect tracking, the adaptation algorithm need only fit the unknown dynamics $f(\mathbf{x}(t), \mathbf{a}, t)$ along the trajectory rather than the whole state space, so that the *effective* number of parameters may be less than $\dim(\mathbf{a})$. The wealth of possible solutions is captured by the time-dependent null-space of $\mathbf{Y}(\mathbf{x}(t), t)$: when $\mathbf{x} \rightarrow \mathbf{x}_d$, we can conclude that $\mathbf{Y}(\mathbf{x}_d(t), t)\hat{\mathbf{a}}(t) = 0$, and hence that $\hat{\mathbf{a}}(t) = \mathbf{a} + \hat{\mathbf{n}}(t)$ where $\mathbf{Y}(\mathbf{x}_d(t), t)\hat{\mathbf{n}}(t) = 0$ for all t . In the over-parameterized case when $\dim(\hat{\mathbf{a}}) > \dim(\mathbf{a})$, the set of parameters that achieve zero tracking error is not unique regardless of the complexity of the desired trajectory.

By deriving and extending continuous-time versions of recent results considering implicit bias of mirror descent algorithms (Azizan & Hassibi, 2019; Azizan et al., 2019), we now show how the “natural” adaptive laws of the previous two subsections impose implicit regularization on the solution $\hat{\mathbf{a}}$. This implicit regularization provides an answer to the question, *when there are infinitely many solutions that achieve zero tracking error, which one does adaptive control “choose”?*

To answer this question, we define the set

$$\mathcal{A} = \{\boldsymbol{\theta} \mid \mathbf{Y}(\mathbf{x}(t), t)\boldsymbol{\theta} = f(\mathbf{x}(t), \mathbf{a}, t) \quad \forall t\} \quad (93)$$

i.e., (93) contains only parameters that interpolate the dynamics $f(\mathbf{x}(t), t)$ along the entire trajectory. We are now in a position to state the following proposition.

Proposition 4.3. *Consider the “natural gradient”-like adaptation law*

$$\dot{\hat{\mathbf{a}}} = -[\nabla^2\psi(\hat{\mathbf{a}})]^{-1}\mathbf{Y}^Ts, \quad (94)$$

where $\psi(\cdot)$ is a strictly convex function. Assume that $\hat{\mathbf{a}}(t) \rightarrow \hat{\mathbf{a}}_\infty \in \mathcal{A}$. Then

$$\hat{\mathbf{a}}_\infty = \arg \min_{\boldsymbol{\theta} \in \mathcal{A}} d_\psi(\boldsymbol{\theta} \parallel \hat{\mathbf{a}}(0)). \quad (95)$$

Proof. Let $\boldsymbol{\theta}$ be any constant vector of parameters. The Bregman divergence $d_\psi(\boldsymbol{\theta} \parallel \hat{\mathbf{a}}) = \psi(\boldsymbol{\theta}) - \psi(\hat{\mathbf{a}}) - \nabla\psi(\hat{\mathbf{a}})^T(\boldsymbol{\theta} - \hat{\mathbf{a}})$ has time derivative

$$\frac{d}{dt}d_\psi(\boldsymbol{\theta} \parallel \hat{\mathbf{a}}) = \left(\frac{d}{dt}\nabla\psi(\hat{\mathbf{a}})\right)^T(\boldsymbol{\theta} - \hat{\mathbf{a}}).$$

From (94), $\frac{d}{dt}\nabla\psi(\hat{\mathbf{a}}) = -\mathbf{Y}^Ts$, so that

$$\frac{d}{dt}d_\psi(\boldsymbol{\theta} \parallel \hat{\mathbf{a}}) = -s\mathbf{Y}(\boldsymbol{\theta} - \hat{\mathbf{a}}).$$

Integrating both sides of the above shows that

$$d_\psi(\boldsymbol{\theta} \parallel \hat{\mathbf{a}}(0)) = d_\psi(\boldsymbol{\theta} \parallel \hat{\mathbf{a}}(t)) + \int_0^t s(\tau)\mathbf{Y}(\mathbf{x}(\tau), \tau)(\boldsymbol{\theta} - \hat{\mathbf{a}}(\tau))d\tau.$$

If we now take $\boldsymbol{\theta} \in \mathcal{A}$, $\mathbf{Y}(\mathbf{x}(\tau), \tau)\boldsymbol{\theta} = f(\mathbf{x}(\tau), \mathbf{a}, \tau)$ and the integral term is independent of $\boldsymbol{\theta}$. Assuming that $\hat{\mathbf{a}} \rightarrow \hat{\mathbf{a}}_\infty \in \mathcal{A}$, we can take the limit as $t \rightarrow \infty$ and say that for any $\boldsymbol{\theta} \in \mathcal{A}$, $\hat{\mathbf{a}}_\infty \in \mathcal{A}$,

$$d_\psi(\boldsymbol{\theta} \parallel \hat{\mathbf{a}}(0)) = d_\psi(\boldsymbol{\theta} \parallel \hat{\mathbf{a}}_\infty) + \int_0^\infty s(\tau)(f(\mathbf{x}(\tau), \mathbf{a}, \tau) - \mathbf{Y}(\mathbf{x}(\tau), \tau)\hat{\mathbf{a}}(\tau))d\tau.$$

Because the only dependence of the right-hand side on $\boldsymbol{\theta}$ is in the first term, the arg min of the two Bregman divergences must be identical. The minimum of the right-hand side over $\boldsymbol{\theta}$ is clearly obtained at $\hat{\mathbf{a}}_\infty$, while the minimum of the left-hand side is by definition obtained at $\arg \min_{\boldsymbol{\theta} \in \mathcal{A}} d_\psi(\boldsymbol{\theta}, \hat{\mathbf{a}}(0))$. From this, we conclude that

$$\hat{\mathbf{a}}_\infty = \arg \min_{\boldsymbol{\theta} \in \mathcal{A}} d_\psi(\boldsymbol{\theta} \parallel \hat{\mathbf{a}}(0)).$$

□

A few discussion points related to this proposition are now provided.

Remark 4.2. The assumptions of Prop. 4.3 provide a setting where theoretical insight may be gained into the implicit regularization of adaptive control algorithms, but they are stronger than needed. In general, the parameters $\hat{\mathbf{a}}(t)$ found by an adaptive controller need not converge to a constant despite the fact that $\dot{\hat{\mathbf{a}}} \rightarrow 0^5$. Similarly, even in the case that the parameters converge, it is not strictly required that $\mathbf{Y}(\mathbf{x}(t), t)\hat{\mathbf{a}}_\infty = f(\mathbf{x}(t), \mathbf{a}, t)$ along the entire trajectory, only asymptotically. In the following section, numerical simulations will demonstrate the implicit regularization of parameters $\hat{\mathbf{a}}(t)$ found by adaptive control along the entire trajectory. ◇

Remark 4.3. As a corollary, if $\hat{\mathbf{a}}(0) = \arg \min_{\boldsymbol{\theta} \in \mathbb{R}^p} \psi(\boldsymbol{\theta})$, then we conclude that $\hat{\mathbf{a}}_\infty = \arg \min_{\boldsymbol{\theta} \in \mathcal{A}} \psi(\boldsymbol{\theta})$. This is a form of implicit regularization imposed by the adaptation algorithm (94): out of all possible interpolating parameters, it chooses the $\hat{\mathbf{a}}$ that achieves the minimum value of ψ . ◇

As shown in Prop. 4.4, our argument for implicit regularization also holds in the nonlinearly parameterized setting captured by Assumption 3.3 with an additional Assumption 4.1.

Assumption 4.1. For any vector of parameters $\boldsymbol{\theta}$ and the true parameters \mathbf{a} , $f(\mathbf{x}(t), \boldsymbol{\theta}, t) = f(\mathbf{x}(t), \mathbf{a}, t)$ implies that $\boldsymbol{\alpha}(\mathbf{x}(t), t)^T \boldsymbol{\theta} = \boldsymbol{\alpha}(\mathbf{x}(t), t)^T \mathbf{a}$. ◇

For the class of systems (41), a sufficient condition for Assumption 4.1 is that $\lambda(\mathbf{x}(t), t) \neq 0$ and that the map $\phi(\mathbf{x}, t)^T \mathbf{a} \rightarrow f_m(\mathbf{x}(t), \phi(\mathbf{x}, t)^T \mathbf{a})$ is invertible at every t . We may now state our implicit regularization result for nonlinearly parameterized systems.

Proposition 4.4. Consider the adaptation algorithm

$$\dot{\hat{\mathbf{a}}} = -[\nabla^2 \psi(\hat{\mathbf{a}})]^{-1} \tilde{f}(\mathbf{x}(t), t) \boldsymbol{\alpha}(\mathbf{x}(t), t) \quad (96)$$

under Assumptions 3.3 & 4.1. Assume $\hat{\mathbf{a}}(t) \rightarrow \hat{\mathbf{a}}_\infty \in \mathcal{A}$. Then

$$\hat{\mathbf{a}}_\infty = \arg \min_{\boldsymbol{\theta} \in \mathcal{A}} d_\psi(\boldsymbol{\theta} \parallel \hat{\mathbf{a}}(0)).$$

Proof. The proof is much the same as Prop. 4.3. The Bregman divergence $d_\psi(\boldsymbol{\theta} \parallel \hat{\mathbf{a}})$ for any fixed vector of parameters $\boldsymbol{\theta}$ verifies

$$\frac{d}{dt} d_\psi(\boldsymbol{\theta} \parallel \hat{\mathbf{a}}) = -\tilde{f}(\mathbf{x}(t), t) \boldsymbol{\alpha}(\mathbf{x}(t), t)^T (\boldsymbol{\theta} - \hat{\mathbf{a}}),$$

so that, integrating both sides,

$$d_\psi(\boldsymbol{\theta} \parallel \hat{\mathbf{a}}(0)) = d_\psi(\boldsymbol{\theta} \parallel \hat{\mathbf{a}}(t)) + \int_0^t \tilde{f}(\mathbf{x}(\tau), \tau) \boldsymbol{\alpha}(\mathbf{x}(\tau), \tau)^T (\boldsymbol{\theta} - \hat{\mathbf{a}}(\tau)) d\tau.$$

Now take $\boldsymbol{\theta} \in \mathcal{A}$. By the assumptions of the proposition, $\boldsymbol{\alpha}(\mathbf{x}(\tau), \tau)^T \boldsymbol{\theta} = \boldsymbol{\alpha}(\mathbf{x}(\tau), \tau)^T \mathbf{a}$ is independent of $\boldsymbol{\theta}$. Hence, assuming that $\hat{\mathbf{a}}(t) \rightarrow \hat{\mathbf{a}}_\infty \in \mathcal{A}$, we can write

$$d_\psi(\boldsymbol{\theta} \parallel \hat{\mathbf{a}}(0)) = d_\psi(\boldsymbol{\theta} \parallel \hat{\mathbf{a}}_\infty) + \int_0^\infty \tilde{f}(\mathbf{x}(\tau), \tau) \boldsymbol{\alpha}(\mathbf{x}(\tau), \tau)^T (\mathbf{a} - \hat{\mathbf{a}}(\tau)) d\tau.$$

Optimizing both sides over $\boldsymbol{\theta} \in \mathcal{A}$ as in Prop. 4.3 yields the result. □

Remark 4.4. Algorithm (96) must be implemented in PI form due to the appearance of \tilde{f} , but the use of the usual PI form in $\hat{\mathbf{a}}$ is complicated by the presence of the inverse Hessian of ψ . To implement (42), the Euclidean variant may be implemented through the usual PI form for an auxiliary variable $\hat{\mathbf{v}} = -\tilde{f}(\mathbf{x}(t), t) \boldsymbol{\alpha}(\mathbf{x}(t), t)$, and then the controller parameters may be computed by inverting the gradient of ψ , $\hat{\mathbf{a}}(t) = (\nabla \psi^{-1})(\hat{\mathbf{v}}(t))$. ◇

⁵Lyapunov function arguments based on a parameter estimation error term generally lead to the conclusion that the parameters remain bounded, and it is generally the case that $\dot{\hat{\mathbf{a}}} \rightarrow 0$ as it is driven by an error term. Nevertheless, $\hat{\mathbf{a}}$ may stay time-varying for all t . For instance, the function $f(t) = \sin(\sqrt{t})$ remains bounded and time-varying for all t , but has $f'(t) = \frac{1}{2\sqrt{t}} \cos(\sqrt{t}) \rightarrow 0$.

Remark 4.5. Our results also extend to the higher-order setting captured by algorithm (86). The assumption that $\hat{\mathbf{a}} \rightarrow \hat{\mathbf{a}}_\infty$ also implies $\dot{\hat{\mathbf{a}}} \rightarrow 0$. As noted in Sec. 2.3, $\hat{\mathbf{v}} = \hat{\mathbf{a}} + \frac{\dot{\hat{\mathbf{a}}}}{\beta\mathcal{N}}$ and we thus conclude that under this assumption $\hat{\mathbf{v}} \rightarrow \hat{\mathbf{a}}_\infty$. Because $\dot{\hat{\mathbf{v}}}$ in (87) is identical to algorithm (94), the result follows. \diamond

Props. 4.3 & 4.4 demonstrate an implicit regularization imposed by adaptation algorithms that has thus far not been noticed in the literature. In doing so, they identify an additional design choice that may be exploited for the application of interest. Prop. 4.3 implies that the Slotine and Li controller, when initialized with the parameters at $\hat{\mathbf{a}}(0) = \mathbf{0}$, finds the interpolating parameter vector of minimum l_2 norm. Other norms, such as the l_1, l_∞, l_p for arbitrary p , or group norms will find alternative parameter vectors that may have desirable properties such as sparsity⁶. The usual Euclidean geometry-based adaptive laws can be seen as a form of ridge regression, while imposing l_1, l_2 and l_1 simultaneously, or l_p regularization through the choice of ψ can be seen as the adaptive control equivalents of LASSO or compressed sensing, elastic net, and bridge regression respectively.

4.4 Non-Euclidean measure of the tracking error

The usual Lyapunov function incorporates a Euclidean tracking error term given by $\frac{1}{2}s^2$. In a similar vein to the derivation of the “natural” adaptive laws, for any strictly convex function $\phi : \mathbb{R} \rightarrow \mathbb{R}$, we may instead replace this tracking error term by the Bregman divergence $d_\phi(0 \parallel s)$. This quantity has time derivative

$$\frac{d}{dt}d_\phi(0 \parallel s) = -\eta s^2 \phi''(s) + \phi''(s) \mathbf{Y} \tilde{\mathbf{a}}$$

in the linearly parameterized case. Because $\phi''(s) \geq 0$ for strictly convex ϕ , it is simple to see that this modification to the usual Lyapunov function in combination with a non-Euclidean measure of the parameter estimation error leads to a family of stable adaptation laws parameterized by ϕ and ψ of the form $\dot{\hat{\mathbf{a}}} = -[\nabla^2\psi(\hat{\mathbf{a}})]^{-1} \mathbf{Y}^T \phi''(s) s$. This shows, for example, that any odd power of s may be stably employed in the adaptation law by taking $\phi = s^p$ for some even power p . Surprisingly, more exotic adaptation laws such as $\dot{\hat{\mathbf{a}}} = -[\nabla^2\psi(\hat{\mathbf{a}})]^{-1} \mathbf{Y}^T e^{\lambda|s|} s$ for $\lambda > 0$ may also be used. Similar reasoning applies to the proposed elastic modifications and to the higher-order algorithms that utilize a term proportional to s by taking $\mathcal{N} = 1 + \mu \|\mathbf{Y}\|^2 \phi''(s)$.

In the single-input case, all of these laws could be more simply obtained by replacing the $\frac{1}{2}s^2$ term in the Lyapunov-like function with a term of the form $g(s)$ where $g'(s)s \geq 0$ and $g'(s)$ is known. In the multi-input case, these two approaches differ. Taking g to be a strongly convex function with minimum attained at $s = 0$ and a known gradient, the Lyapunov-like function

$$V = g(\mathbf{s}) - \inf_{\mathbf{s}} g(\mathbf{s}) + d_\psi(\mathbf{a} \parallel \hat{\mathbf{a}})$$

shows that the adaptation law

$$\dot{\hat{\mathbf{a}}} = -[\nabla^2\psi(\hat{\mathbf{a}})]^{-1} \mathbf{Y}^T \nabla g(\mathbf{s})$$

is globally convergent. On the other hand, the Lyapunov-like function

$$V = d_\phi(0 \parallel \mathbf{s}) + d_\psi(\mathbf{a} \parallel \hat{\mathbf{a}})$$

shows that the distinct adaptation law

$$\dot{\hat{\mathbf{a}}} = -[\nabla^2\psi(\hat{\mathbf{a}})]^{-1} \mathbf{Y}^T [\nabla^2\phi(\mathbf{s})] \mathbf{s}$$

is also globally convergent.

5 Simulations

In this section, we empirically verify the global convergence and implicit regularization of our higher-order algorithm for nonlinearly parameterized systems (53). In particular, we consider a second order system

$$\begin{aligned} \dot{x}_1 &= x_2, \\ \dot{x}_2 &= u - f(\mathbf{x}, t, \mathbf{a}), \end{aligned}$$

with an unknown system dynamics of the form

$$f(\mathbf{x}, \mathbf{a}, t) = \sigma \left(\tanh(\mathbf{V} \mathbf{x})^T \mathbf{a} \right). \quad (97)$$

⁶Because the l_1 norm is not strictly convex, it may be replaced with a suitable approximation such as the $l_{1+\epsilon}$ norm for $\epsilon > 0$ and small (Azizan & Hassibi, 2019; Azizan et al., 2019).

Equation (97) represents a three-layer neural network with input layer \mathbf{x} , hidden layer weights \mathbf{V} , hidden layer nonlinearity $\tanh(\cdot)$, hidden layer weights \mathbf{a} , and elementwise output nonlinearity $\sigma(\mathbf{x}) = e^{\cdot \mathbf{x}}$. The system model (97) can clearly be seen to satisfy Assumption 3.3 with $\alpha(\mathbf{x}) = \tanh(\mathbf{V}\mathbf{x})^7$. The PI form of algorithm (53) is given by

$$\nabla\psi(\hat{\mathbf{v}}) = \bar{v} + \xi(\mathbf{x}, \mathbf{x}_d) + \rho(\mathbf{x}, \mathbf{x}_d), \quad (98)$$

$$\xi(\mathbf{x}, \mathbf{x}_d) = -\gamma s(\mathbf{x}, \mathbf{x}_d) \tanh(\mathbf{V}\mathbf{x}), \quad (99)$$

$$\rho(\mathbf{x}, \mathbf{x}_d) = \gamma [\tanh(\mathbf{V}\mathbf{x}) x_2 - \log(\cosh(\mathbf{V}\mathbf{x})) \oslash \mathbf{V}_2 + (\lambda \tilde{x} - x_{2,d}) \tanh(\mathbf{V}\mathbf{x})], \quad (100)$$

$$\dot{\bar{v}} = \gamma (\dot{x}_{2,d} - \lambda (x_2 - x_{2,d}) - \eta s) \tanh(\mathbf{V}\mathbf{x}) + \gamma x_2 \tanh(\mathbf{V}\mathbf{x}) \circ \mathbf{V}_1 \oslash \mathbf{V}_2, \quad (101)$$

$$\dot{\hat{\mathbf{a}}} = \beta (1 + \mu \|\tanh(\mathbf{V}\mathbf{x})\|^2) (\hat{\mathbf{v}} - \hat{\mathbf{a}}), \quad (102)$$

where \circ and \oslash denote elementwise multiplication and division respectively, where \mathbf{V}_i is the i^{th} column of \mathbf{V} , and where $\hat{\mathbf{v}}$ is obtained from $\nabla\psi(\hat{\mathbf{v}})$ by inverting $\nabla\psi$. For the squared p norm $\psi(\cdot) = \frac{1}{2} \|\cdot\|_p^2$, the inverse function can be analytically computed as

$$(\nabla\psi^{-1})(\mathbf{y}) = \|\mathbf{y}\|_q^{2-q} |\mathbf{y}|^{q-1} \text{sign}(\mathbf{y}) \quad (103)$$

where $\frac{1}{q} + \frac{1}{p} = 1$, $|\cdot|$ denotes elementwise absolute value and $\text{sign}(\cdot)$ denotes elementwise sign (Gentile, 2003). We consider the l_1, l_2, l_4, l_6 , and l_{10} norms for ψ . To approximate the l_1 norm, (103) is used with $p = 1.1$. All other p norms can be used directly.

In all simulations we take $\lambda = .5$ in the definition of s (4) and $\eta = .5$ in the control input (5). For the adaptation hyperparameters, we choose $\gamma = 1.5$ for the l_2, l_4 , and l_6 norms. We take $\gamma = 50$ for the l_1 norm and $\gamma = .5$ for the l_{10} norm⁸. In all cases, $\beta = 1$ and $\mu = \frac{3\gamma}{2\eta\beta}$. We set $\text{dim}(\mathbf{a}) = \text{dim}(\hat{\mathbf{a}}) = 500$ and randomly initialize $\hat{\mathbf{a}}$ and $\hat{\mathbf{v}}$ around zero from a normal distribution with standard deviation 10^{-3} . The true parameter vector \mathbf{a} is drawn from a normal distribution with mean zero and standard deviation 7.5. The matrix \mathbf{V} is set to have normally distributed elements with standard deviation $\frac{1}{\sqrt{\text{dim}(\mathbf{a})}}$. The state vector is initialized to have $\mathbf{x}(0) = \mathbf{x}_d(0)$. The desired trajectory is taken to be

$$x_d(t) = \sin\left(\frac{\sqrt{2}\pi}{12}t + \cos\left(\frac{\sqrt{3}\pi}{12}t\right)\right)$$

The tracking error for each choice of ψ along with a baseline comparison to fixed $\hat{\mathbf{a}}(t) = \hat{\mathbf{a}}(0)$ is shown in Fig. 1A. Figs. 1B-F show trajectories for 100 out of the 500 parameters. The timescale on each axis is set to show the trajectories approximately until the parameters converge for the given algorithm. Each case results in remarkably different dynamics and resulting converged parameter vectors $\hat{\mathbf{a}}_\infty^\psi$, and the tracking performance is good for each algorithm.

Further insight can be gained into the structure of the parameter vector $\hat{\mathbf{a}}_\infty^\psi$ found by each adaptation algorithm by consideration of the histograms (rug plots shown on x axis) for $\hat{\mathbf{a}}$ at the end of the simulation in Figs. 2A-F. Fig. 2A shows the true parameter vector. The choice of $\psi(\cdot) = \frac{1}{2} \|\cdot\|_{1.1}^2$ in Fig. 2B leads to an incredibly sparse solution with most of the weight placed on a few parameters. This is consistent with l_1 regularized solutions found by the LASSO algorithm. The inset displays a closer view around zero. The choice of $\psi(\cdot) = \frac{1}{2} \|\cdot\|_2^2$ in Fig. 2C (Euclidean adaptation law) leads to a parameter vector $\hat{\mathbf{a}}_\infty^{\frac{1}{2} \|\cdot\|_2^2} \neq \mathbf{a}$ that is roughly Gaussian distributed. This distribution highlights the implicit l_2 regularization of standard adaptation laws. The progression from $\psi(\cdot) = \frac{1}{2} \|\cdot\|_4^2$ to $\psi(\cdot) = \frac{1}{2} \|\cdot\|_{10}^2$ displays a trend towards approximate l_∞ -norm regularization: the distribution of parameters is pushed to be bimodal and peaked around ± 1 , and the l_∞ norm of $\hat{\mathbf{a}}_\infty$ decreases as p is increased.

Fig. 3A shows the function approximation error $\tilde{f}^2(\mathbf{x}(t), \hat{\mathbf{a}}(t))$ for each algorithm along with a reference value for fixed $\hat{\mathbf{a}}(t) = \hat{\mathbf{a}}(0)$. Each algorithm, as expected by our theory and seen by the low tracking error in Fig. 1A, pushes \tilde{f}^2 to zero despite the different forms of regularization imposed on the parameter vectors. Figs. 3B-F show the control input as a function of time along with the unique “ideal” control law $u(t) = \ddot{x}_d + f(\mathbf{x}_d(t), \mathbf{a}(t))$ valid when $\mathbf{x}(0) = \mathbf{x}_d(0)$. All control inputs can be seen to converge to the ideal law, though the rate of convergence depends on the choice of algorithm. The control input is of reasonable magnitude throughout adaptation for each algorithm.

⁷While the exponential is not globally Lipschitz continuous, it is locally. \mathbf{x} remains bounded due to the proportional control term $-\eta s$ and hence the assumption is satisfied.

⁸These values of γ were chosen to ensure good control performance without excessively high control inputs or fast parameter adaptation. In particular, adaptation occurs very slowly with l_1 regularization, as small parameters are quickly eliminated to promote sparsity. A high adaptation gain was needed to ensure adaptation on a similar timescale to the other norms.

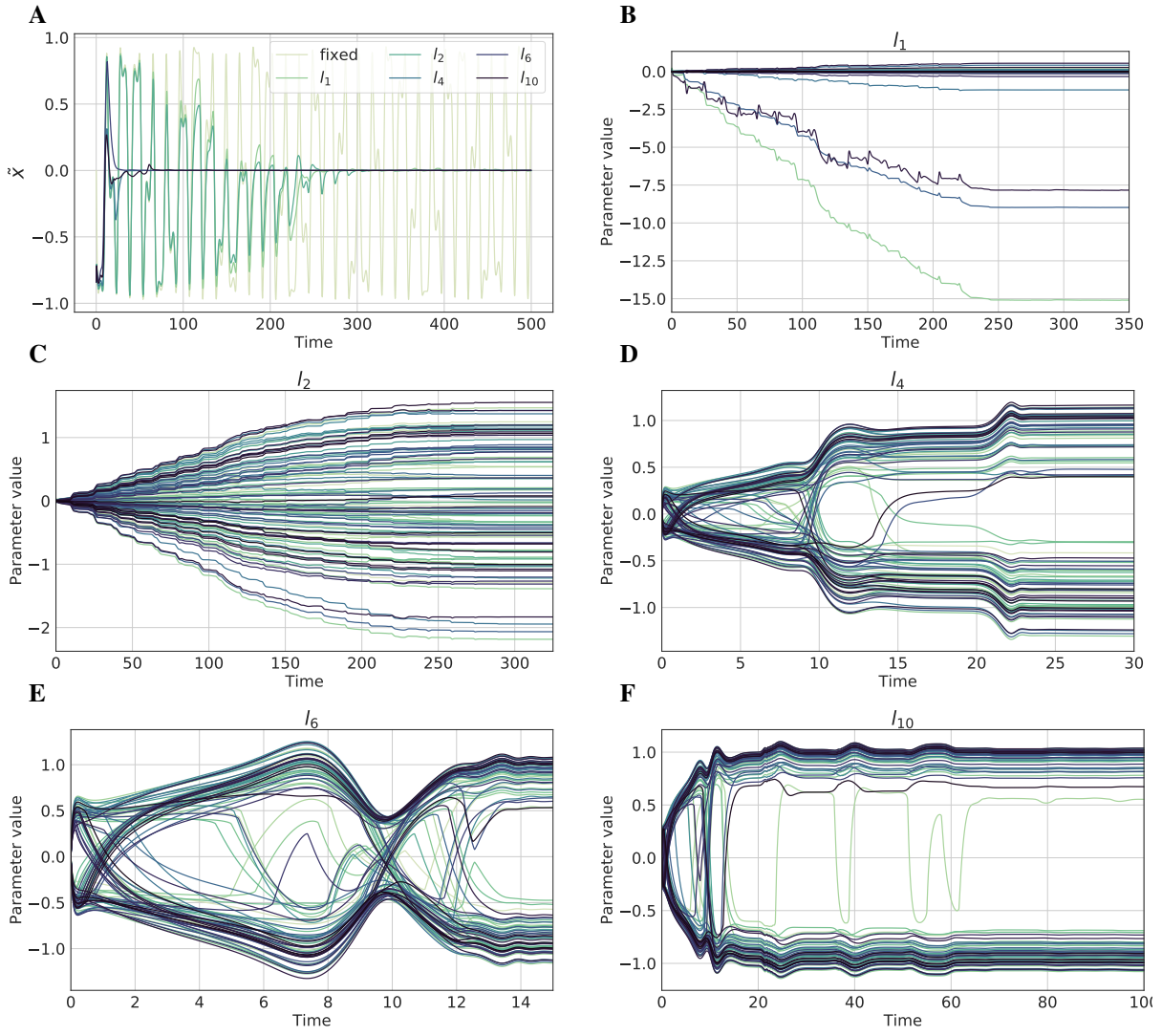


Figure 1: (A) Trajectory tracking error. All algorithms result in convergence $\mathbf{x} \rightarrow \mathbf{x}_d$, though transient performance differs between the algorithms. (B-F) Parameter trajectories for 100/500 of the total parameters. Each algorithm results in remarkably different parameter trajectories and final values $\hat{\mathbf{a}}_\infty^\psi$.

6 Concluding remarks and future directions

It is somewhat unusual in nonlinear control to have a choice between a large variety of algorithms that can all be proven to globally converge. Nevertheless, in this paper, we have presented a suite of new globally convergent adaptive control algorithms. The algorithms combine the velocity gradient methodology (A. L. Fradkov, 1999; Fradkov, 1979) with the Bregman Lagrangian (Betancourt et al., 2018; Wibisono et al., 2016) to systematically generate higher-order velocity gradient algorithms, of which the recent algorithm due to Gaudio et al. (2019) is a special case. Based on analogies between isotonic regression (Goel & Klivans, 2017; Goel et al., 2018; Kakade et al., 2011) and algorithms for nonlinearly parameterized adaptive control (I. Tyukin, 2011; Tyukin et al., 2007), we extended our higher-order velocity gradient algorithms to the nonlinearly parameterized setting. Using a similar parallel to distributed stochastic gradient descent algorithms (Boffi & Slotine, 2020; Zhang et al., 2014), we developed a stable modification of all of our algorithms. We subsequently fused our developments with time-dependent learning rates based on the bounded gain forgetting formalism (J.-J. Slotine & Li, 1991).

By consideration of the non-Euclidean Bregman Lagrangian, we derived natural gradient (Amari, 1998) and mirror descent (Beck & Teboulle, 2003; Nemirovski & Yudin, 1983)-like algorithms with momentum. Taking the infinite friction limit of these algorithms recovers a recent algorithm for adaptive robot control (Lee et al., 2018) that respects

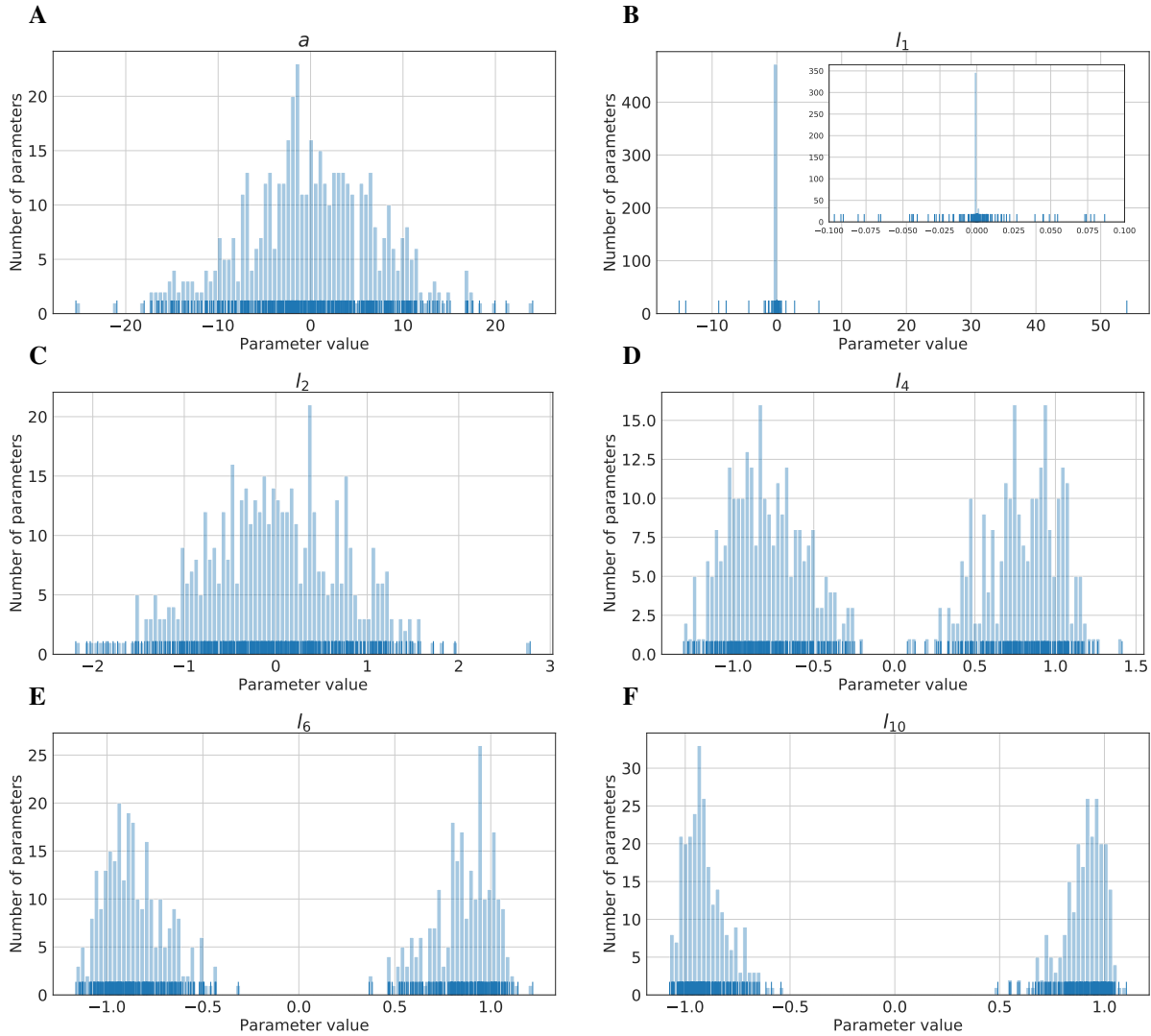


Figure 2: Parameter histograms. (A) True parameters a . (B) Parameter vector found by the algorithm with $\psi(\cdot) = \frac{1}{2} \|\cdot\|_{1,1}^2$. The resulting solution is extremely sparse, and has a few parameters with large magnitude, indicative of implicit l_1 regularization. (C) Parameter vector found by the standard Euclidean algorithm with $\psi(\cdot) = \frac{1}{2} \|\cdot\|_2^2$. The resulting parameter vector looks approximately Gaussian distributed, indicating l_2 regularization. (C)-(F) Parameter vectors found by $\psi(\cdot) = \frac{1}{2} \|\cdot\|_p^2$ with $p = 4, 6$, and 10 respectively. The transition clearly indicates a trend towards l_∞ -norm regularization, with two bimodal peaks forming around ± 1 . The l_∞ norm of the parameter vector decreases with increasing p .

physical Riemannian constraints on the parameters throughout adaptation. By extending recent results on implicit regularization of optimization algorithms in machine learning (Azizan & Hassibi, 2019; Azizan et al., 2019) to the continuous-time setting, we proved that these mirror descent like-algorithms – in the first-order, second-order, and nonlinearly parameterized settings – impose implicit regularization on the parameter vectors found by adaptive control. We illustrated these results through simulation, and demonstrated how approximations of the l_1 norm can be used to find sparse controls, showed that the usual Euclidean adaptation laws impose l_2 regularization, and showed interpretable regularization for higher-order p norms. As discussed in Example 2.1, all of the algorithms presented herein may also be used for dynamic prediction, and hence our results on implicit regularization and our new adaptation algorithms may immediately be transferred to this setting, for example for use in training recurrent networks (Alemi et al., 2018; Gilra & Gerstner, 2017; Sussillo & Abbott, 2009). In particular, an extension of our nonlinearly parameterized algorithms to the case where $\alpha(x, t)$ is a matrix would enable learning weights underneath typical recurrent network activation functions.

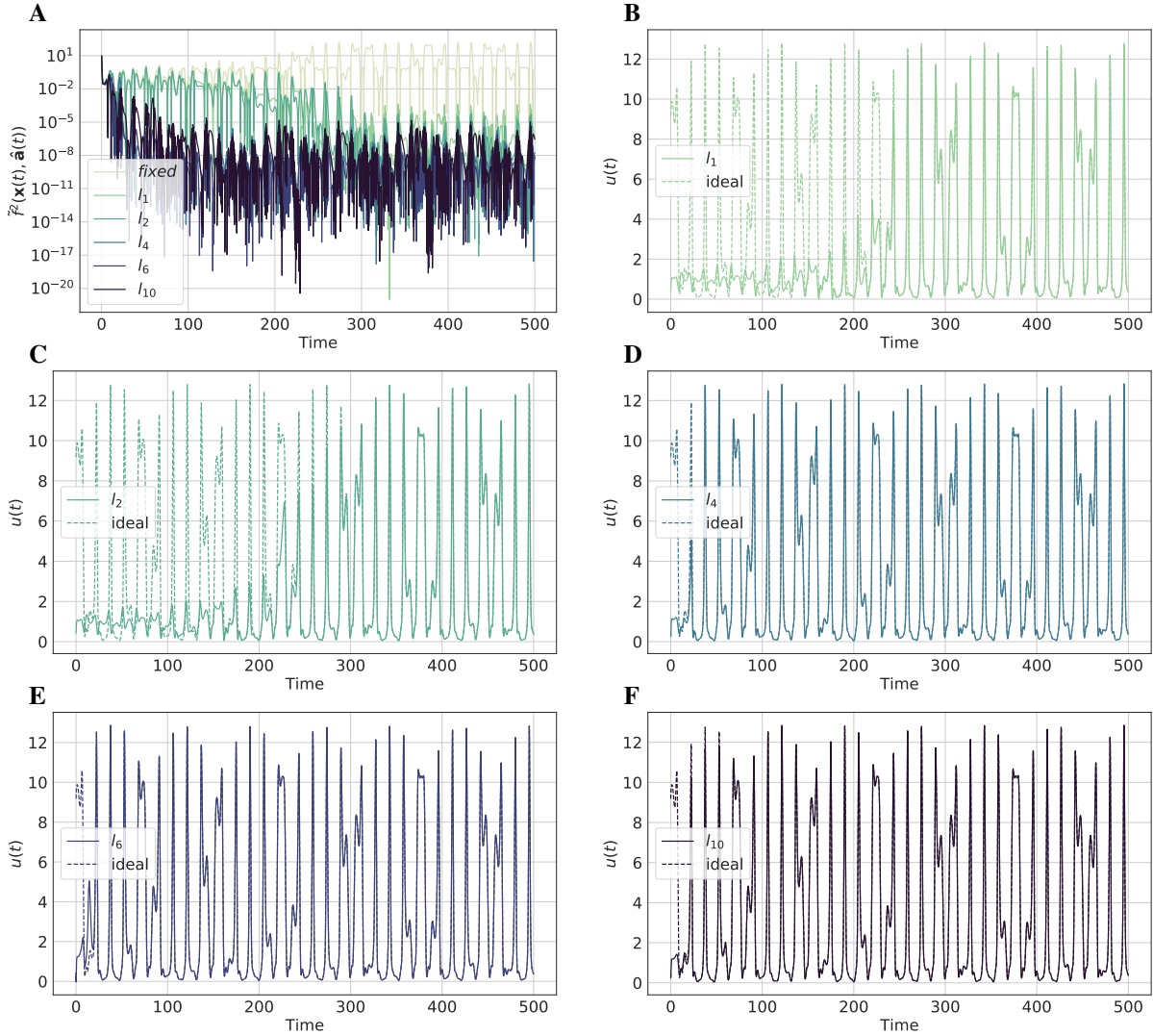


Figure 3: (A) The function approximation error $\tilde{f}^2(\mathbf{x}(t), \hat{\mathbf{a}}(t))$. All algorithms drive the error to zero. (B)-(F) Comparison of the control input $u^\psi(t)$ to the “ideal” control $u(t) = \ddot{x}_d(t) + f(\mathbf{x}_d(t), \mathbf{a})$. All algorithms converge to the ideal control, though at a different rate. The control magnitude is kept to a reasonable level in every case.

Throughout the paper, for simplicity of exposition, we focused on the n^{th} order system (1). As discussed in Remark 2.2, our results extend to more general systems which have an error model similar to (6), in the sense that the proof technique summarized by Lemma A.1 is roughly preserved. The n^{th} order system makes the employed proportional-integral forms simple, in that they can be written down explicitly as in (31)-(34). As summarized in Remark 3.6, in the general case, a PDE needs to be solved, and solutions to this PDE may be hard to find, or may not exist at all. Solution of the PDE can be avoided by the dynamic scaling technique (Karagiannis et al., 2009) or a similar embedding technique (I. Tyukin, 2011).

There are many possible directions for future research. A first is to rigorously test and understand the advantages of our various proposed algorithms. For example, can we understand how to choose the convex function ψ , or if any choices of ψ lead to gain-independent faster adaptation or more robust parameters? Can we prove when the higher-order algorithms will excel over their first-order counterparts, or theoretically analyze the robustness properties of our proposed modifications? A second is to understand the role of these algorithms in practical applications, for example in the robotic setting, or for learning the weights in a recurrent network. A third is to use our analogy with the Alphatron algorithm to create higher-order algorithms for generalized linear model regression, and to understand their computational and statistical efficiency in the p-concept model (Kearns & Schapire, 1994). A fourth is to search for time-dependent learning rate update laws tailor-made to the monotonicity setting of Assumption 3.3, rather than

the approach based on linear least squares presented in Sec. 3.5. Finally, we are interested in understanding if the higher-order formalism may help with more general nonlinear parameterizations, such as multiple layers of nonlinearity or a sum of single layer functions.

A Omitted proofs

A.1 Miscellaneous results

Lemma A.1. *If $\tilde{f}(\mathbf{x}, \hat{\mathbf{a}}, t) \in \mathcal{L}_2$, $\hat{\mathbf{a}} \in \mathcal{L}_\infty$, and \tilde{f} is locally bounded in \mathbf{x} and $\hat{\mathbf{a}}$ uniformly in t , then $s \in \mathcal{L}_2 \cap \mathcal{L}_\infty$, $s \rightarrow 0$ and $\mathbf{x} \rightarrow \mathbf{x}_d$.*

Proof. By (6), we can write explicitly

$$s(t) = \int_0^t e^{-\eta(t-\tau)} \tilde{f}(\mathbf{x}(\tau), \hat{\mathbf{a}}(\tau), \tau) d\tau \quad (104)$$

By the Cauchy-Schwarz inequality,

$$s^2(t) \leq \left(\int_0^t e^{-2\eta(t-\tau)} d\tau \right) \left(\int_0^t \tilde{f}^2(\tau) d\tau \right) \leq \frac{1}{2\eta} \|\tilde{f}\|_{\mathcal{L}_2} (1 - e^{-2\eta t}) \leq \frac{1}{2\eta} \|\tilde{f}\|_{\mathcal{L}_2}$$

so that $s \in \mathcal{L}_\infty$. Similarly, Parseval's theorem applied to the low-pass filter (104) shows that $s \in \mathcal{L}_2$. Because $s \in \mathcal{L}_\infty$, we conclude that $\mathbf{x} \in \mathcal{L}_\infty$ (J.-J. Slotine & Li, 1991). Because $\mathbf{x} \in \mathcal{L}_\infty$ and $\hat{\mathbf{a}} \in \mathcal{L}_\infty$, and because \tilde{f} is locally bounded in \mathbf{x} and $\hat{\mathbf{a}}$ uniformly in t , $\tilde{f} \in \mathcal{L}_\infty$. By (6), $\dot{s} \in \mathcal{L}_\infty$, and hence by Barbalat's lemma, $s \rightarrow 0$. By definition of s , we then conclude that $\mathbf{x} \rightarrow \mathbf{x}_d$. \square

A.2 Proof of Proposition 3.4

Proof. Consider the Lyapunov function

$$V = \frac{1}{2} s^2 + \frac{1}{2\gamma} (\|\tilde{\mathbf{v}}\|^2 + \|\hat{\mathbf{a}} - \tilde{\mathbf{v}}\|^2)$$

which has time derivative

$$\begin{aligned} \dot{V} &= -\eta s^2 + s \tilde{f} + \frac{1}{\gamma} \left[\tilde{\mathbf{v}}^T \left(-\kappa \tilde{f} - \gamma s \right) \mathbf{Y}^T + (\hat{\mathbf{a}} - \tilde{\mathbf{v}})^T \left(\beta \mathcal{N}(\tilde{\mathbf{v}} - \hat{\mathbf{a}}) + \gamma s \mathbf{Y}^T + \kappa \tilde{f} \mathbf{Y}^T \right) \right] \\ &= -\eta s^2 - \frac{\kappa}{\gamma} \tilde{f}^2 - \frac{\beta}{\gamma} \|\hat{\mathbf{a}} - \tilde{\mathbf{v}}\|^2 - \frac{\beta\mu}{\gamma} \|\hat{\mathbf{a}} - \tilde{\mathbf{v}}\| \|\mathbf{Y}\|^2 + 2s(\hat{\mathbf{a}} - \tilde{\mathbf{v}})^T \mathbf{Y}^T + 2\frac{\kappa}{\gamma} \tilde{f} (\hat{\mathbf{a}} - \tilde{\mathbf{v}})^T \mathbf{Y}^T \\ &\leq -\eta s^2 - \frac{\kappa}{\gamma} \tilde{f}^2 - \frac{\beta}{\gamma} \|\hat{\mathbf{a}} - \tilde{\mathbf{v}}\|^2 - \frac{\beta\mu}{\gamma} \|\hat{\mathbf{a}} - \tilde{\mathbf{v}}\| \|\mathbf{Y}\|^2 + 2|s| \|\hat{\mathbf{a}} - \tilde{\mathbf{v}}\| \|\mathbf{Y}\| + 2\frac{\kappa}{\gamma} |\tilde{f}| \|\hat{\mathbf{a}} - \tilde{\mathbf{v}}\| \|\mathbf{Y}\| \\ &\leq -\epsilon_1 \eta s^2 - \epsilon_2 \frac{\kappa}{\gamma} \tilde{f}^2 - \left(\sqrt{(1 - \epsilon_1)\eta} |s| - \frac{1}{\sqrt{(1 - \epsilon_1)\eta}} \|\hat{\mathbf{a}} - \tilde{\mathbf{v}}\| \|\mathbf{Y}\| \right)^2 \\ &\quad - \left(\sqrt{\frac{(1 - \epsilon_2)\kappa}{\gamma}} |\tilde{f}| - \frac{\kappa}{\gamma} \sqrt{\frac{\gamma}{(1 - \epsilon_2)\kappa}} \|\hat{\mathbf{a}} - \tilde{\mathbf{v}}\| \|\mathbf{Y}\| \right)^2 - \frac{\beta}{\gamma} \|\hat{\mathbf{a}} - \tilde{\mathbf{v}}\|^2 \end{aligned}$$

where $0 < \epsilon_1 < 1$ and $0 < \epsilon_2 < 1$ are arbitrary and where we have taken $\mu = \frac{\gamma}{\beta} \left(\frac{1}{(1 - \epsilon_1)\eta} + \frac{\kappa}{(1 - \epsilon_2)\gamma} \right)$. Because ϵ_1 and ϵ_2 are arbitrary, this shows that \dot{V} is negative semi-definite for $\mu > \frac{\gamma}{\beta} \left(\frac{1}{\eta} + \frac{\kappa}{\gamma} \right)$. Hence $\tilde{\mathbf{v}} \in \mathcal{L}_\infty$, $\hat{\mathbf{a}} \in \mathcal{L}_\infty$, and $s \in \mathcal{L}_\infty$. Because $s \in \mathcal{L}_\infty$, we automatically have $\mathbf{x} \in \mathcal{L}_\infty$, which shows that $\dot{s} \in \mathcal{L}_\infty$ by local boundedness of \tilde{f} in \mathbf{x} and $\hat{\mathbf{a}}$ uniformly in t . Integrating \dot{V} shows that $s \in \mathcal{L}_2$ and hence by Barbalat's Lemma $s \rightarrow 0$ and $\mathbf{x} \rightarrow \mathbf{x}_d$. \square

A.3 Proof of Proposition 3.6

Proof. Consider the Lyapunov function candidate

$$V = \frac{1}{2\gamma} \|\tilde{\mathbf{v}}\|^2 + \frac{1}{2\gamma} \|\hat{\mathbf{a}} - \tilde{\mathbf{v}}\|^2$$

which has time derivative

$$\begin{aligned}
\dot{V} &= \frac{1}{\gamma} \tilde{\mathbf{v}}^T \left(-\gamma \tilde{f} \boldsymbol{\alpha} \right) + \frac{1}{\gamma} (\hat{\mathbf{a}} - \hat{\mathbf{v}})^T \left(\beta \mathcal{N} (\hat{\mathbf{v}} - \hat{\mathbf{a}}) + \gamma \tilde{f} \boldsymbol{\alpha} \right) \\
&= -(\tilde{\mathbf{a}}^T \boldsymbol{\alpha}) \tilde{f} - \frac{\beta}{\gamma} \mathcal{N} \|\hat{\mathbf{a}} - \hat{\mathbf{v}}\|^2 + 2(\hat{\mathbf{a}} - \hat{\mathbf{v}})^T \boldsymbol{\alpha} \tilde{f} \\
&\leq -\frac{\tilde{f}^2}{D_1} - \frac{\beta}{\gamma} \|\hat{\mathbf{a}} - \hat{\mathbf{v}}\|^2 - \frac{\beta \mu}{\gamma} \|\hat{\mathbf{a}} - \hat{\mathbf{v}}\|^2 \|\boldsymbol{\alpha}\|^2 + 2\|\boldsymbol{\alpha}\| \|\hat{\mathbf{a}} - \hat{\mathbf{v}}\| |\tilde{f}| \\
&\leq -\frac{\epsilon}{D_1} \tilde{f}^2 - \beta \|\hat{\mathbf{a}} - \hat{\mathbf{v}}\|^2 - \left(\sqrt{\frac{1-\epsilon}{D_1}} |\tilde{f}| - \sqrt{\frac{D_1}{1-\epsilon}} \|\boldsymbol{\alpha}\| \|\hat{\mathbf{a}} - \hat{\mathbf{v}}\| \right)^2
\end{aligned}$$

where where $0 < \epsilon < 1$ is arbitrary and we have chosen $\mu = \frac{\gamma D_1}{(1-\epsilon)\beta}$. Because ϵ is arbitrary, this shows that $\hat{\mathbf{v}}$ and $\hat{\mathbf{a}}$ remain bounded for $\mu > \frac{\gamma D_1}{\beta}$. By integrating \dot{V} , we see that $\tilde{f} \in \mathcal{L}_2$. Application of Lemma A.1 completes the proof. \square

A.4 Proof of Proposition 3.9

Proof. The Lyapunov-like function

$$V = \frac{1}{2\gamma} (\|\tilde{\mathbf{v}}\|^2 + \|\hat{\mathbf{a}} - \hat{\mathbf{v}}\|^2 + \|\bar{\mathbf{a}} - \hat{\mathbf{a}}\|^2)$$

has time derivative

$$\begin{aligned}
\dot{V} &= -(\tilde{\mathbf{a}}^T \boldsymbol{\alpha}) \tilde{f} - \frac{\beta}{\gamma} \mathcal{N} \|\hat{\mathbf{a}} - \hat{\mathbf{v}}\|^2 + \frac{k\beta}{\gamma} \mathcal{N} (\hat{\mathbf{a}} - \hat{\mathbf{v}})^T (\bar{\mathbf{a}} - \hat{\mathbf{a}}) + 2\tilde{f} (\hat{\mathbf{a}} - \hat{\mathbf{v}})^T \boldsymbol{\alpha} - 2\frac{k\beta}{\gamma} \mathcal{N} \|\hat{\mathbf{a}} - \bar{\mathbf{a}}\|^2 + \frac{\beta}{\gamma} \mathcal{N} (\hat{\mathbf{a}} - \bar{\mathbf{a}})^T (\hat{\mathbf{v}} - \hat{\mathbf{a}}) \\
&\leq -\frac{\tilde{f}^2}{D_1} - \frac{\beta \mathcal{N}}{2\gamma} (1-k) \|\hat{\mathbf{a}} - \hat{\mathbf{v}}\|^2 - \frac{\beta \mathcal{N}}{2\gamma} \|\hat{\mathbf{a}} - \bar{\mathbf{a}}\|^2 (3k-1) + 2|\tilde{f}| \|\hat{\mathbf{a}} - \hat{\mathbf{v}}\| \|\boldsymbol{\alpha}\| \\
&\leq -\frac{\tilde{f}^2}{D_1} - \frac{\beta}{2\gamma} (1-k) \|\hat{\mathbf{a}} - \hat{\mathbf{v}}\|^2 - \frac{\beta \mu}{2\gamma} (1-k) \|\hat{\mathbf{a}} - \hat{\mathbf{v}}\|^2 \|\boldsymbol{\alpha}\|^2 - \frac{\beta \mathcal{N}}{2\gamma} \|\hat{\mathbf{a}} - \bar{\mathbf{a}}\|^2 (3k-1) + 2|\tilde{f}| \|\hat{\mathbf{a}} - \hat{\mathbf{v}}\| \|\boldsymbol{\alpha}\| \\
&\leq -\frac{\epsilon}{D_1} \tilde{f}^2 - \left(\sqrt{\frac{1-\epsilon}{D_1}} |\tilde{f}| - \sqrt{\frac{D_1}{1-\epsilon}} \|\boldsymbol{\alpha}\| \|\hat{\mathbf{a}} - \hat{\mathbf{v}}\| \right)^2 - \frac{\beta}{2\gamma} (1-k) \|\hat{\mathbf{a}} - \hat{\mathbf{v}}\|^2 - \frac{\beta \mathcal{N}}{2\gamma} (3k-1) \|\hat{\mathbf{a}} - \bar{\mathbf{a}}\|^2
\end{aligned}$$

where $0 < \epsilon < 1$ is arbitrary and we have chosen $\mu = \frac{2\gamma D_1}{\beta(1-\epsilon)(1-k)}$. From above, we conclude $\hat{\mathbf{v}}$, $\hat{\mathbf{a}}$, and $\bar{\mathbf{a}}$ remain bounded for $\frac{1}{3} \leq k < 1$. By integrating \dot{V} , we see that $\tilde{f} \in \mathcal{L}_2$, $(\hat{\mathbf{a}} - \bar{\mathbf{a}}) \in \mathcal{L}_2$, and $(\hat{\mathbf{a}} - \hat{\mathbf{v}}) \in \mathcal{L}_2$. Application of Lemma A.1 completes the proof. \square

A.5 Proof of Proposition 3.10

Proof. The Lyapunov-like function

$$V = \frac{1}{\gamma} (\|\tilde{\mathbf{v}}\|^2 + \|\bar{\mathbf{v}}\|^2 + \|\hat{\mathbf{a}} - \bar{\mathbf{v}}\|^2)$$

has time derivative

$$\begin{aligned}
\dot{V} &= -(\tilde{\mathbf{a}}^T \boldsymbol{\alpha}) \tilde{f} + 2\tilde{f} (\hat{\mathbf{a}} - \hat{\mathbf{v}})^T \boldsymbol{\alpha} - \frac{\beta \mathcal{N}}{\gamma} \|\hat{\mathbf{a}} - \hat{\mathbf{v}}\|^2 - \frac{\rho}{\gamma} \|\hat{\mathbf{v}} - \bar{\mathbf{v}}\|^2 - \frac{\rho}{\gamma} (\hat{\mathbf{a}} - \hat{\mathbf{v}})^T (\bar{\mathbf{v}} - \hat{\mathbf{v}}) \\
&\leq -\frac{\tilde{f}^2}{D_1} + 2|\tilde{f}| \|\hat{\mathbf{a}} - \hat{\mathbf{v}}\| \|\boldsymbol{\alpha}\| - \left(\frac{\beta}{\gamma} - \frac{\rho}{2\gamma} \right) \|\hat{\mathbf{a}} - \hat{\mathbf{v}}\|^2 - \frac{\beta \mu}{\gamma} \|\hat{\mathbf{a}} - \hat{\mathbf{v}}\|^2 \|\boldsymbol{\alpha}\|^2 - \frac{\rho}{2\gamma} \|\hat{\mathbf{v}} - \bar{\mathbf{v}}\|^2 \\
&\leq -\frac{\epsilon}{D_1} \tilde{f}^2 - \left(\sqrt{\frac{1-\epsilon}{D_1}} |\tilde{f}| - \sqrt{\frac{D_1}{1-\epsilon}} \|\boldsymbol{\alpha}\| \|\hat{\mathbf{a}} - \hat{\mathbf{v}}\| \right)^2 - \frac{\rho}{2\gamma} \|\bar{\mathbf{v}} - \hat{\mathbf{v}}\|^2 - \frac{1}{2\gamma} (2\beta - \rho) \|\hat{\mathbf{v}} - \hat{\mathbf{a}}\|^2
\end{aligned}$$

where $0 < \epsilon < 1$ is arbitrary and we have chosen $\mu = \frac{\gamma D_1}{\beta(1-\epsilon)}$. From above, we conclude $\hat{\mathbf{v}}$, $\bar{\mathbf{v}}$, and $\hat{\mathbf{a}}$ remain bounded for $\rho < 2\beta$. Integrating \dot{V} shows that $\tilde{f} \in \mathcal{L}_2$, $(\hat{\mathbf{v}} - \bar{\mathbf{v}}) \in \mathcal{L}_2$, and $(\hat{\mathbf{v}} - \hat{\mathbf{a}}) \in \mathcal{L}_2$. Application of Lemma A.1 completes the proof. \square

A.6 Proof of Proposition 3.11

Proof. The Lyapunov-like function

$$V = \frac{1}{2\gamma} (\|\hat{\mathbf{a}} - \hat{\mathbf{v}}\|^2 + \|\hat{\mathbf{a}} - \bar{\mathbf{a}}\|^2 + \|\tilde{\mathbf{v}}\|^2 + \|\tilde{\mathbf{v}}\|^2)$$

has time derivative

$$\begin{aligned} \dot{V} &= -(\tilde{\mathbf{a}}^T \boldsymbol{\alpha}) \tilde{f} - \frac{\beta \mathcal{N}}{\gamma} \|\hat{\mathbf{a}} - \hat{\mathbf{v}}\|^2 - \frac{2k\beta \mathcal{N}}{\gamma} \|\bar{\mathbf{a}} - \hat{\mathbf{a}}\|^2 + 2\tilde{f}(\hat{\mathbf{a}} - \hat{\mathbf{v}})^T \boldsymbol{\alpha} + \beta N (\hat{\mathbf{a}} - \bar{\mathbf{a}})^T (\hat{\mathbf{v}} - \hat{\mathbf{a}}) \\ &\quad + \frac{k\beta \mathcal{N}}{\gamma} (\hat{\mathbf{a}} - \hat{\mathbf{v}})^T (\bar{\mathbf{a}} - \hat{\mathbf{a}}) - \frac{\rho}{\gamma} \|\hat{\mathbf{v}} - \bar{\mathbf{v}}\|^2 - \frac{\rho}{\gamma} (\hat{\mathbf{a}} - \hat{\mathbf{v}})^T (\bar{\mathbf{v}} - \hat{\mathbf{v}}) \\ &\leq -\frac{1}{D_1} \tilde{f}^2 - \frac{1}{2\gamma} (\beta(1-k) - \rho) \|\hat{\mathbf{a}} - \hat{\mathbf{v}}\|^2 - \frac{1}{2\gamma} (\beta\mu(1-k)) \|\hat{\mathbf{a}} - \hat{\mathbf{v}}\|^2 \|\boldsymbol{\alpha}\|^2 \\ &\quad - \frac{\mathcal{N}\beta}{2\gamma} (3k-1) \|\bar{\mathbf{a}} - \hat{\mathbf{a}}\|^2 - \frac{\rho}{2\gamma} \|\hat{\mathbf{v}} - \bar{\mathbf{v}}\|^2 + 2|\tilde{f}|\|\hat{\mathbf{a}} - \hat{\mathbf{v}}\| \|\mathbf{Y}\| \\ &\leq -\frac{\epsilon}{D_1} \tilde{f}^2 - \left(\sqrt{\frac{1-\epsilon}{D_1}} |\tilde{f}| - \sqrt{\frac{D_1}{1-\epsilon}} \|\hat{\mathbf{a}} - \hat{\mathbf{v}}\| \|\boldsymbol{\alpha}\| \right)^2 - \frac{\rho}{2\gamma} \|\bar{\mathbf{v}} - \hat{\mathbf{v}}\|^2 \\ &\quad - \frac{\beta \mathcal{N}}{2\gamma} (3k-1) \|\hat{\mathbf{a}} - \bar{\mathbf{a}}\|^2 - \frac{1}{2\gamma} ((1-k)\beta - \rho) \|\hat{\mathbf{a}} - \hat{\mathbf{v}}\|^2 \end{aligned}$$

where $0 < \epsilon < 1$ is arbitrary and we have chosen $\mu = \frac{2\gamma D_1}{\beta(1-k)(1-\epsilon)}$. This immediately shows that $\hat{\mathbf{a}}, \hat{\mathbf{v}}, \bar{\mathbf{a}}$, and $\bar{\mathbf{v}}$ remain bounded for $\frac{1}{3} \leq k < 1$ and $\rho < \beta(1-k)$. Integrating \dot{V} shows that $\tilde{f} \in \mathcal{L}_2$, $(\bar{\mathbf{v}} - \hat{\mathbf{v}}) \in \mathcal{L}_2$, $(\hat{\mathbf{a}} - \bar{\mathbf{a}}) \in \mathcal{L}_2$, and $(\hat{\mathbf{a}} - \hat{\mathbf{v}}) \in \mathcal{L}_2$. Application of Lemma A.1 completes the proof. \square

A.7 Proof of Proposition 3.13

Proof. Consider the Lyapunov-like function

$$V = \frac{1}{2} s^2 + \frac{1}{2} \tilde{\mathbf{v}}^T \mathbf{P}^{-1} \tilde{\mathbf{v}} + \frac{1}{2} (\hat{\mathbf{v}} - \hat{\mathbf{a}})^T \mathbf{P}^{-1} (\hat{\mathbf{v}} - \hat{\mathbf{a}})$$

which has time derivative

$$\begin{aligned} \dot{V} &= -\eta s^2 + s\tilde{f} - (\hat{\mathbf{v}} - \hat{\mathbf{a}} + \tilde{\mathbf{a}})^T (s + \tilde{f}) \mathbf{Y}^T + \frac{1}{2} (\tilde{\mathbf{v}}^T \mathbf{Y}^T)^2 - \frac{\lambda(t)}{2} \tilde{\mathbf{v}}^T \mathbf{P}^{-1} \tilde{\mathbf{v}} \\ &\quad + (\hat{\mathbf{v}} - \hat{\mathbf{a}})^T \left(-\beta \mathcal{N} (\hat{\mathbf{v}} - \hat{\mathbf{a}}) - (s + \tilde{f}) \mathbf{Y}^T \right) + \frac{1}{2} \left[(\hat{\mathbf{v}} - \hat{\mathbf{a}})^T \mathbf{Y}^T \right]^2 - \frac{\lambda(t)}{2} (\hat{\mathbf{v}} - \hat{\mathbf{a}})^T \mathbf{P}^{-1} (\hat{\mathbf{v}} - \hat{\mathbf{a}}) \\ &= -\eta s^2 - \tilde{f}^2 - 2(\hat{\mathbf{v}} - \hat{\mathbf{a}})^T (s + \tilde{f}) \mathbf{Y}^T - \beta \mathcal{N} \|\hat{\mathbf{v}} - \hat{\mathbf{a}}\|^2 + \frac{1}{2} (\tilde{\mathbf{v}}^T \mathbf{Y}^T)^2 + \frac{1}{2} \left[(\hat{\mathbf{v}} - \hat{\mathbf{a}})^T \mathbf{Y}^T \right]^2 \\ &\quad - \frac{\lambda(t)}{2} \left(\tilde{\mathbf{v}}^T \mathbf{P}^{-1} \tilde{\mathbf{v}} + (\hat{\mathbf{v}} - \hat{\mathbf{a}})^T \mathbf{P}^{-1} (\hat{\mathbf{v}} - \hat{\mathbf{a}}) \right) \end{aligned}$$

Now we use that $\tilde{\mathbf{v}}^T \mathbf{Y}^T = (\hat{\mathbf{v}} - \hat{\mathbf{a}})^T \mathbf{Y}^T + \tilde{f}$ to say that $\frac{1}{2} (\tilde{\mathbf{v}}^T \mathbf{Y}^T)^2 = \frac{1}{2} \left[(\hat{\mathbf{v}} - \hat{\mathbf{a}})^T \mathbf{Y}^T \right]^2 + (\hat{\mathbf{v}} - \hat{\mathbf{a}})^T \mathbf{Y}^T \tilde{f} + \frac{1}{2} \tilde{f}^2$. Hence,

$$\begin{aligned}
\dot{V} &= -\eta s^2 - \frac{1}{2} \tilde{f}^2 - 2s (\hat{\mathbf{v}} - \hat{\mathbf{a}})^T \mathbf{Y}^T - \tilde{f} (\hat{\mathbf{v}} - \hat{\mathbf{a}})^T \mathbf{Y}^T - \beta \mathcal{N} \|\hat{\mathbf{v}} - \hat{\mathbf{a}}\|^2 + \left[(\hat{\mathbf{v}} - \hat{\mathbf{a}})^T \mathbf{Y}^T \right]^2 \\
&\quad - \frac{\lambda(t)}{2} \left(\tilde{\mathbf{v}}^T \mathbf{P}^{-1} \tilde{\mathbf{v}} + (\hat{\mathbf{v}} - \hat{\mathbf{a}})^T \mathbf{P}^{-1} (\hat{\mathbf{v}} - \hat{\mathbf{a}}) \right) \\
&= -\eta s^2 - \frac{1}{2} \tilde{f}^2 - 2s (\hat{\mathbf{v}} - \hat{\mathbf{a}})^T \mathbf{Y}^T - \tilde{f} (\hat{\mathbf{v}} - \hat{\mathbf{a}})^T \mathbf{Y}^T - \beta \|\hat{\mathbf{v}} - \hat{\mathbf{a}}\|^2 - \beta \mu \|\mathbf{Y}\|^2 \|\hat{\mathbf{v}} - \hat{\mathbf{a}}\|^2 + \left[(\hat{\mathbf{v}} - \hat{\mathbf{a}})^T \mathbf{Y}^T \right]^2 \\
&\quad - \frac{\lambda(t)}{2} \left(\tilde{\mathbf{v}}^T \mathbf{P}^{-1} \tilde{\mathbf{v}} + (\hat{\mathbf{v}} - \hat{\mathbf{a}})^T \mathbf{P}^{-1} (\hat{\mathbf{v}} - \hat{\mathbf{a}}) \right) \\
&\leq -\eta s^2 - \frac{1}{2} \tilde{f}^2 + 2s \|\hat{\mathbf{v}} - \hat{\mathbf{a}}\| \|\mathbf{Y}^T\| + \|\tilde{f}\| \|\hat{\mathbf{v}} - \hat{\mathbf{a}}\| \|\mathbf{Y}^T\| - \beta \|\hat{\mathbf{v}} - \hat{\mathbf{a}}\|^2 - (\beta \mu - 1) \|\mathbf{Y}\|^2 \|\hat{\mathbf{v}} - \hat{\mathbf{a}}\|^2 \\
&\quad - \frac{\lambda(t)}{2} \left(\tilde{\mathbf{v}}^T \mathbf{P}^{-1} \tilde{\mathbf{v}} + (\hat{\mathbf{v}} - \hat{\mathbf{a}})^T \mathbf{P}^{-1} (\hat{\mathbf{v}} - \hat{\mathbf{a}}) \right) \\
&\leq -\eta \epsilon_1 s^2 - \frac{\epsilon_2}{2} \tilde{f}^2 - \left(\sqrt{(1 - \epsilon_1) \eta} |s| - \frac{1}{\sqrt{(1 - \epsilon_1) \eta}} \|\hat{\mathbf{v}} - \hat{\mathbf{a}}\| \|\mathbf{Y}\| \right)^2 - \left(\sqrt{\frac{1 - \epsilon_2}{2}} |\tilde{f}| - \frac{1}{2} \sqrt{\frac{2}{1 - \epsilon_2}} \|\hat{\mathbf{v}} - \hat{\mathbf{a}}\| \|\mathbf{Y}^T\| \right)^2 \\
&\quad - \beta \|\hat{\mathbf{v}} - \hat{\mathbf{a}}\|^2 - \frac{\lambda(t)}{2} \left(\tilde{\mathbf{v}}^T \mathbf{P}^{-1} \tilde{\mathbf{v}} + (\hat{\mathbf{v}} - \hat{\mathbf{a}})^T \mathbf{P}^{-1} (\hat{\mathbf{v}} - \hat{\mathbf{a}}) \right)
\end{aligned}$$

where $0 < \epsilon_1 < 1$ and $0 < \epsilon_2 < 1$ are both arbitrary and where we have chosen $\mu = \frac{1}{\beta} \left(1 + \frac{1}{\eta(1 - \epsilon_1)} + \frac{1}{2(1 - \epsilon_2)} \right)$. This shows that s , $\hat{\mathbf{v}}$, and $\hat{\mathbf{a}}$ remain bounded. Because s remains bounded, \mathbf{x} remains bounded. Integrating \dot{V} shows that $s \in \mathcal{L}_2$ and $\tilde{f} \in \mathcal{L}_2$. By local boundedness of \tilde{f} in \mathbf{x} and $\hat{\mathbf{a}}$ uniformly in t , \tilde{f} remains bounded and hence \dot{s} remains bounded. By Barbalat's Lemma, $s \rightarrow 0$ and $\mathbf{x} \rightarrow \mathbf{x}_d$. \square

A.8 Proof of Proposition 3.15

Proof. Consider the Lyapunov-like function

$$V = \frac{1}{2} \left(\tilde{\mathbf{v}}^T \mathbf{P}^{-1} \tilde{\mathbf{v}} + (\hat{\mathbf{a}} - \hat{\mathbf{v}})^T \mathbf{P}^{-1} (\hat{\mathbf{a}} - \hat{\mathbf{v}}) \right),$$

which has time derivative

$$\begin{aligned}
\dot{V} &= -\tilde{\mathbf{v}}^T \boldsymbol{\alpha} \tilde{f} + \frac{1}{2} \tilde{\mathbf{v}}^T (-\lambda \mathbf{P}^{-1} + \boldsymbol{\alpha} \boldsymbol{\alpha}^T) \tilde{\mathbf{v}} + (\hat{\mathbf{a}} - \hat{\mathbf{v}})^T \left(\beta \mathcal{N} (\hat{\mathbf{v}} - \hat{\mathbf{a}}) + \boldsymbol{\alpha} \tilde{f} \right) + \frac{1}{2} (\hat{\mathbf{a}} - \hat{\mathbf{v}})^T (-\lambda \mathbf{P}^{-1} + \boldsymbol{\alpha} \boldsymbol{\alpha}^T) (\hat{\mathbf{a}} - \hat{\mathbf{v}}) \\
&\leq -(\tilde{\mathbf{a}}^T \boldsymbol{\alpha}) \tilde{f} + \frac{1}{2} (\tilde{\mathbf{v}}^T \boldsymbol{\alpha})^2 + \frac{1}{2} \left((\hat{\mathbf{a}} - \hat{\mathbf{v}})^T \boldsymbol{\alpha} \right)^2 - \beta \mathcal{N} \|\hat{\mathbf{a}} - \hat{\mathbf{v}}\|^2 + 2\tilde{f} (\hat{\mathbf{a}} - \hat{\mathbf{v}})^T \boldsymbol{\alpha} \\
&\leq -D_2 (\boldsymbol{\alpha}^T \tilde{\mathbf{a}})^2 + \frac{1}{2} (\tilde{\mathbf{v}}^T \boldsymbol{\alpha})^2 + \frac{1}{2} \left((\hat{\mathbf{a}} - \hat{\mathbf{v}})^T \boldsymbol{\alpha} \right)^2 - \beta \mathcal{N} \|\hat{\mathbf{a}} - \hat{\mathbf{v}}\|^2 + 2|\tilde{f}| \|\hat{\mathbf{a}} - \hat{\mathbf{v}}\| \|\boldsymbol{\alpha}\|
\end{aligned}$$

Now, we use the fact that $\frac{1}{2} (\tilde{\mathbf{v}}^T \boldsymbol{\alpha})^2 = \frac{1}{2} \left[(\hat{\mathbf{v}} - \hat{\mathbf{a}})^T \boldsymbol{\alpha} \right]^2 + (\hat{\mathbf{v}} - \hat{\mathbf{a}})^T \boldsymbol{\alpha} (\boldsymbol{\alpha}^T \tilde{\mathbf{a}}) + \frac{1}{2} (\tilde{\mathbf{a}}^T \boldsymbol{\alpha})^2$ to rewrite

$$\begin{aligned}
\dot{V} &\leq - \left(D_2 - \frac{1}{2} \right) (\boldsymbol{\alpha}^T \tilde{\mathbf{a}})^2 + \left[(\hat{\mathbf{a}} - \hat{\mathbf{v}})^T \boldsymbol{\alpha} \right]^2 - \beta \mathcal{N} \|\hat{\mathbf{a}} - \hat{\mathbf{v}}\|^2 + \|\hat{\mathbf{v}} - \hat{\mathbf{a}}\| \|\boldsymbol{\alpha}\| |\boldsymbol{\alpha}^T \tilde{\mathbf{a}}| (2D_1 + 1) \\
&\leq - \left(D_2 - \frac{1}{2} \right) (\boldsymbol{\alpha}^T \tilde{\mathbf{a}})^2 - \beta \|\hat{\mathbf{a}} - \hat{\mathbf{v}}\|^2 - (\beta \mu - 1) \|\hat{\mathbf{a}} - \hat{\mathbf{v}}\|^2 \|\boldsymbol{\alpha}\|^2 + \|\hat{\mathbf{v}} - \hat{\mathbf{a}}\| \|\boldsymbol{\alpha}\| |\boldsymbol{\alpha}^T \tilde{\mathbf{a}}| (2D_1 + 1) \\
&\leq -\epsilon \left(D_2 - \frac{1}{2} \right) (\boldsymbol{\alpha}^T \tilde{\mathbf{a}})^2 - \left(\sqrt{(1 - \epsilon) \left(D_2 - \frac{1}{2} \right)} |\boldsymbol{\alpha}^T \tilde{\mathbf{a}}| - \frac{2D_1 + 1}{2\sqrt{(1 - \epsilon) (D_2 - \frac{1}{2})}} \|\hat{\mathbf{v}} - \hat{\mathbf{a}}\| \|\boldsymbol{\alpha}\| \right)^2 - \beta \|\hat{\mathbf{a}} - \hat{\mathbf{v}}\|^2
\end{aligned}$$

where $0 < \epsilon < 1$ is arbitrary and where we have chosen $\mu = \frac{1}{\beta} \left(1 + \frac{(2D_1 + 1)^2}{(1 - \epsilon)(4D_2 - 2)} \right)$. \dot{V} is clearly negative semi-definite for $D_2 < \frac{1}{2}$, which shows that $\hat{\mathbf{v}}$ and $\hat{\mathbf{a}}$ remain bounded. Integrating \dot{V} shows that $(\boldsymbol{\alpha}^T \tilde{\mathbf{a}}) \in \mathcal{L}_2$ which implies that $\tilde{f} \in \mathcal{L}_2$ by Assumption 3.3. By Lemma A.1, the proposition is proven. \square

A.9 Proof of Prop. 4.1

Proof. Consider the Lyapunov-like function candidate

$$\begin{aligned} V &= \frac{1}{2}s^2 + \frac{1}{\gamma} \left(d_\psi(\mathbf{a}, \hat{\mathbf{v}}) + \frac{1}{2}\|\hat{\mathbf{a}} - \hat{\mathbf{v}}\|^2 \right) \\ &= \frac{1}{2}s^2 + \frac{1}{\gamma} \left(\psi(\mathbf{a}) - \psi(\hat{\mathbf{v}}) - \nabla\psi(\hat{\mathbf{v}})^T(\mathbf{a} - \hat{\mathbf{v}}) + \frac{1}{2}\|\hat{\mathbf{a}} - \hat{\mathbf{v}}\|^2 \right) \end{aligned}$$

This function has time derivative

$$\begin{aligned} \dot{V} &= -\eta s^2 + s \mathbf{Y} \tilde{\mathbf{a}} + \frac{1}{\gamma} \left((\hat{\mathbf{v}} - \mathbf{a})^T \nabla^2 \psi(\hat{\mathbf{v}}) \hat{\mathbf{v}} + (\hat{\mathbf{a}} - \hat{\mathbf{v}})^T (\dot{\hat{\mathbf{a}}} - \dot{\hat{\mathbf{v}}}) \right) \\ &= -\eta s^2 + s \mathbf{Y} \tilde{\mathbf{a}} + (\mathbf{a} - \hat{\mathbf{v}})^T \mathbf{Y}^T s + \frac{1}{\gamma} (\hat{\mathbf{a}} - \hat{\mathbf{v}})^T \left(\beta \mathcal{N}(\hat{\mathbf{v}} - \hat{\mathbf{a}}) + \gamma \nabla^2 \psi(\hat{\mathbf{v}})^{-1} \mathbf{Y}^T s \right) \\ &= -\eta s^2 - \frac{\beta \mathcal{N}}{\gamma} \|\hat{\mathbf{a}} - \hat{\mathbf{v}}\|^2 + (\hat{\mathbf{a}} - \hat{\mathbf{v}})^T \left([\nabla^2 \psi(\hat{\mathbf{v}})]^{-1} + \mathbf{I} \right) \mathbf{Y}^T s \end{aligned}$$

By l -strong convexity of ψ , $(\nabla^2 \psi(\hat{\mathbf{v}}))^{-1} \leq l^{-1} \mathbf{I}$. Hence, using that $\mathcal{N} = 1 + \mu \|\mathbf{Y}\|^2$,

$$\dot{V} \leq -\eta s^2 - \frac{\beta}{\gamma} \|\hat{\mathbf{a}} - \hat{\mathbf{v}}\|^2 - \frac{\beta \mu}{\gamma} \|\hat{\mathbf{a}} - \hat{\mathbf{v}}\|^2 \|\mathbf{Y}\|^2 + \left(\frac{l+1}{l} \right) |s| \|\hat{\mathbf{a}} - \hat{\mathbf{v}}\| \|\mathbf{Y}\| \quad (105)$$

$$\leq -\epsilon \eta s^2 - \left(\sqrt{(1-\epsilon)\eta} |s| - \frac{l+1}{2l\sqrt{(1-\epsilon)\eta}} \|\hat{\mathbf{a}} - \hat{\mathbf{v}}\| \|\mathbf{Y}\| \right)^2 - \frac{\beta}{\gamma} \|\hat{\mathbf{a}} - \hat{\mathbf{v}}\|^2 \quad (106)$$

where $0 < \epsilon < 1$ is arbitrary and we have chosen $\mu = \frac{\gamma(l+1)^2}{4\beta l^2(1-\epsilon)\eta}$. This shows that \dot{V} is negative semi-definite, so that $\hat{\mathbf{a}}, \hat{\mathbf{v}}$, and s remain bounded. Because s remains bounded, \mathbf{x} remains bounded. Integrating \dot{V} shows that $s \in \mathcal{L}_2$, so that $s \in \mathcal{L}_2 \cap \mathcal{L}_\infty$. By local boundedness of \mathbf{Y} in \mathbf{x} , \dot{s} remains bounded, and hence by Barbalat's lemma $s \rightarrow 0$. Then $\mathbf{x} \rightarrow \mathbf{x}_d$ by definition of s . \square

A.10 Proof of Prop. 4.2

Proof. Consider the Lyapunov-like function candidate

$$\begin{aligned} V &= \frac{1}{2}s^2 + \frac{1}{\gamma} (d_\psi(\mathbf{a}, \hat{\mathbf{v}}) + d_\psi(\hat{\mathbf{v}}, \hat{\mathbf{a}})) \\ &= \frac{1}{2}s^2 + \frac{1}{\gamma} (\psi(\mathbf{a}) - \psi(\hat{\mathbf{v}}) - \nabla\psi(\hat{\mathbf{v}})^T(\mathbf{a} - \hat{\mathbf{v}}) + \psi(\hat{\mathbf{v}}) - \psi(\hat{\mathbf{a}}) - \nabla\psi(\hat{\mathbf{a}})^T(\hat{\mathbf{v}} - \hat{\mathbf{a}})) \end{aligned}$$

These individual terms satisfy

$$\begin{aligned} \frac{d}{dt} \frac{1}{2}s^2 &= -\eta s^2 + \mathbf{Y} \tilde{\mathbf{a}} s \\ \frac{1}{\gamma} \frac{d}{dt} d_\psi(\mathbf{a}, \hat{\mathbf{v}}) &= -\mathbf{Y} \tilde{\mathbf{a}} s + (\hat{\mathbf{a}} - \hat{\mathbf{v}})^T \mathbf{Y}^T s \\ \frac{1}{\gamma} \frac{d}{dt} d_\psi(\hat{\mathbf{v}}, \hat{\mathbf{a}}) &= -\frac{1}{\gamma} (\hat{\mathbf{v}} - \hat{\mathbf{a}})^T \nabla^2 \psi(\hat{\mathbf{a}}) \dot{\hat{\mathbf{a}}} - s \mathbf{Y} (\nabla^2 \psi(\hat{\mathbf{v}}))^{-1} (\nabla\psi(\hat{\mathbf{v}}) - \nabla\psi(\hat{\mathbf{a}})) \end{aligned}$$

Note that, by l -strong convexity and L -smoothness, the second term in the last line above can be bounded as

$$-s \mathbf{Y} (\nabla^2 \psi(\hat{\mathbf{v}}))^{-1} (\nabla\psi(\hat{\mathbf{v}}) - \nabla\psi(\hat{\mathbf{a}})) \leq \frac{\gamma L}{l} |s| \|\mathbf{Y}\| \|\hat{\mathbf{a}} - \hat{\mathbf{v}}\|.$$

First consider (90). Then, by l -strong convexity of ψ ,

$$-\frac{1}{\gamma} (\hat{\mathbf{v}} - \hat{\mathbf{a}})^T \nabla^2 \psi(\hat{\mathbf{a}}) \dot{\hat{\mathbf{a}}} \leq -\frac{l\beta\mathcal{N}}{\gamma} \|\hat{\mathbf{a}} - \hat{\mathbf{v}}\|^2$$

For (92) we obtain

$$-\frac{1}{\gamma} (\hat{\mathbf{v}} - \hat{\mathbf{a}})^T \nabla^2 \psi(\hat{\mathbf{a}}) \dot{\hat{\mathbf{a}}} \leq -\frac{\beta\mathcal{N}}{\gamma} \|\hat{\mathbf{a}} - \hat{\mathbf{v}}\|^2$$

Hence, for (89) & (90),

$$\dot{V} \leq -\eta s^2 - \frac{l\beta}{\gamma} \|\hat{\mathbf{a}} - \hat{\mathbf{v}}\|^2 - \frac{l\beta\mu}{\gamma} \|\mathbf{Y}\|^2 \|\hat{\mathbf{a}} - \hat{\mathbf{v}}\|^2 + \frac{l + \gamma L}{l} |s| \|\mathbf{Y}\| \|\hat{\mathbf{a}} - \hat{\mathbf{v}}\|$$

Similarly, for (91) & (92),

$$\dot{V} \leq -\eta s^2 - \frac{\beta}{\gamma} \|\hat{\mathbf{a}} - \hat{\mathbf{v}}\|^2 - \frac{\beta\mu}{\gamma} \|\mathbf{Y}\|^2 \|\hat{\mathbf{a}} - \hat{\mathbf{v}}\|^2 + \frac{l + \gamma L}{l} |s| \|\mathbf{Y}\| \|\hat{\mathbf{a}} - \hat{\mathbf{v}}\|$$

In both cases,

$$\dot{V} \leq -\epsilon \eta s^2 - \left(\sqrt{(1-\epsilon)\eta} |s| - \frac{l + \gamma L}{2l\sqrt{(1-\epsilon)\eta}} \|\mathbf{Y}\| \|\hat{\mathbf{a}} - \hat{\mathbf{v}}\| \right)^2$$

In former case, we have chosen $\mu = \frac{\gamma(l+\gamma L)^2}{4\beta\eta(1-\epsilon)l^3}$ and in the latter we have chosen $\mu = \frac{\gamma(l+\gamma L)^2}{4\beta\eta(1-\epsilon)l^2}$. This shows that \dot{V} is negative semi-definite, so that $\hat{\mathbf{a}}, \hat{\mathbf{v}}$, and s remain bounded. Because s remains bounded, \mathbf{x} remains bounded. Integrating \dot{V} shows that $s \in \mathcal{L}_2$, so that $s \in \mathcal{L}_2 \cap \mathcal{L}_\infty$. By local boundedness of \mathbf{Y} in \mathbf{x} , \dot{s} remains bounded, and hence by Barbalat's lemma $s \rightarrow 0$. Then $\mathbf{x} \rightarrow \mathbf{x}_d$ by definition of s . \square

References

Ai-Poh Loh, Annaswamy, A. M., & Skantze, F. P. (1999, Sep.). Adaptation in the presence of a general nonlinear parameterization: an error model approach. *IEEE Transactions on Automatic Control*, 44(9), 1634-1652. doi: 10.1109/9.788531

Alemi, A., Machens, C., Deneve, S., & Slotine, J.-J. (2018). Learning nonlinear dynamics in efficient, balanced spiking networks using local plasticity rules. *AAAI Conference on Artificial Intelligence*.

A. L. Fradkov, V. O. N., I. V. Miroshnik. (1999). *Nonlinear and adaptive control of complex systems*. Springer Netherlands.

Amari, S.-i. (1998). Natural gradient works efficiently in learning. *Neural Computation*, 10(2), 251-276. Retrieved from <https://doi.org/10.1162/089976698300017746> doi: 10.1162/089976698300017746

Annaswamy, A. M., Skantze, F. P., & Loh, A.-P. (1998). Adaptive control of continuous time systems with convex/concave parametrization. *Automatica*, 34(1), 33 - 49. doi: [https://doi.org/10.1016/S0005-1098\(97\)00159-3](https://doi.org/10.1016/S0005-1098(97)00159-3)

Astolfi, A., & Ortega, R. (2003). Immersion and invariance: a new tool for stabilization and adaptive control of nonlinear systems. *IEEE Transactions on Automatic Control*, 48(4), 590-606.

Attouch, H., Goudou, X., & Redont, P. (2000). The heavy ball with friction method, i. the continuous dynamical system: global exploration of the local minima of a real-valued function by asymptotic analysis of a dissipative dynamical system. *Communications in Contemporary Mathematics*, 02(01), 1-34. doi: <https://doi.org/10.1142/S0219199700000025>

Azizan, N., & Hassibi, B. (2019). Stochastic gradient/mirror descent: Minimax optimality and implicit regularization. In *International conference on learning representations*.

Azizan, N., Lale, S., & Hassibi, B. (2019). *Stochastic mirror descent on overparameterized nonlinear models: Convergence, implicit regularization, and generalization*.

Bartlett, P. L., Long, P. M., Lugosi, G., & Tsigler, A. (2019). *Benign overfitting in linear regression*.

Beck, A., & Teboulle, M. (2003). Mirror descent and nonlinear projected subgradient methods for convex optimization. *Operations Research Letters*, 31(3), 167 - 175. doi: [https://doi.org/10.1016/S0167-6377\(02\)00231-6](https://doi.org/10.1016/S0167-6377(02)00231-6)

Belkin, M., Hsu, D., Ma, S., & Mandal, S. (2019). Reconciling modern machine-learning practice and the classical bias-variance trade-off. *Proceedings of the National Academy of Sciences*, 116(32), 15849–15854. doi: 10.1073/pnas.1903070116

Betancourt, M., Jordan, M. I., & Wilson, A. C. (2018). *On symplectic optimization*.

Boffi, N. M., & Slotine, J.-J. E. (2020). A continuous-time analysis of distributed stochastic gradient. *Neural Computation*, 32(1), 36-96. doi: https://doi.org/10.1162/neco_a_01248

Chung, S.-J., & Slotine, J.-J. E. (2009, June). Cooperative robot control and concurrent synchronization of lagrangian systems. *Trans. Rob.*, 25(3), 686–700. doi: <https://doi.org/10.1109/TRO.2009.2014125>

Diakonikolas, J., & Jordan, M. I. (2019). *Generalized momentum-based methods: A hamiltonian perspective*.

Fradkov, A. L. (1979). A scheme of speed gradient and its application in problems of adaptive control. *Automation and Remote Control*, 40, 1333-1342.

França, G., Sulam, J., Robinson, D. P., & Vidal, R. (2019). *Conformal symplectic and relativistic optimization*.

Gaudio, J. E., Gibson, T. E., Annaswamy, A. M., & Bolender, M. A. (2019). *Provably correct learning algorithms in the presence of time-varying features using a variational perspective*.

Gentile, C. (2003). The robustness of the p-norm algorithms. *Machine Learning*, 53(3), 265-299. Retrieved from <https://doi.org/10.1023/A:1026319107706> doi: 10.1023/A:1026319107706

Gilra, A., & Gerstner, W. (2017, nov). Predicting non-linear dynamics by stable local learning in a recurrent spiking neural network. *eLife*, 6, e28295. Retrieved from <https://doi.org/10.7554/eLife.28295> doi: 10.7554/eLife.28295

Goel, S., & Klivans, A. (2017). *Learning neural networks with two nonlinear layers in polynomial time*.

Goel, S., Klivans, A., & Meka, R. (2018). *Learning one convolutional layer with overlapping patches*.

Gunasekar, S., Lee, J., Soudry, D., & Srebro, N. (2018a). *Characterizing implicit bias in terms of optimization geometry*.

Gunasekar, S., Lee, J. D., Soudry, D., & Srebro, N. (2018b). Implicit bias of gradient descent on linear convolutional networks. In S. Bengio, H. Wallach, H. Larochelle, K. Grauman, N. Cesa-Bianchi, & R. Garnett (Eds.), *Advances in neural information processing systems 31* (pp. 9461–9471). Curran Associates, Inc.

Ioannou, P. A., & Sun, J. (2012). *Robust adaptive control*. Dover Publications.

Jin, C., Netrapalli, P., & Jordan, M. I. (2017). *Accelerated gradient descent escapes saddle points faster than gradient descent*.

Jouffroy, J., & Slotine, J. . E. (2004, Dec). Methodological remarks on contraction theory. In *2004 43rd ieee conference on decision and control (cdc) (ieee cat. no.04ch37601)* (Vol. 3, p. 2537-2543 Vol.3). doi: 10.1109/CDC.2004.1428824

Kakade, S., Kalai, A. T., Kanade, V., & Shamir, O. (2011). *Efficient learning of generalized linear and single index models with isotonic regression*.

Karagiannis, D., Sassano, M., & Astolfi, A. (2009). Dynamic scaling and observer design with application to adaptive control. *Automatica*, 45(12), 2883 - 2889. doi: <https://doi.org/10.1016/j.automatica.2009.09.013>

Kearns, M. J., & Schapire, R. E. (1994). Efficient distribution-free learning of probabilistic concepts. *Journal of Computer and System Sciences*, 48(3), 464 - 497. doi: [https://doi.org/10.1016/S0022-0000\(05\)80062-5](https://doi.org/10.1016/S0022-0000(05)80062-5)

Kojić, A., & Annaswamy, A. M. (2002). Adaptive control of nonlinearly parameterized systems with a triangular structure. *Automatica*, 38(1), 115 - 123. Retrieved from <http://www.sciencedirect.com/science/article/pii/S000510980100173X> doi: [https://doi.org/10.1016/S0005-1098\(01\)00173-X](https://doi.org/10.1016/S0005-1098(01)00173-X)

Krichene, W., Bayen, A., & Bartlett, P. L. (2015). Accelerated mirror descent in continuous and discrete time. In C. Cortes, N. D. Lawrence, D. D. Lee, M. Sugiyama, & R. Garnett (Eds.), *Advances in neural information processing systems 28* (pp. 2845–2853). Curran Associates, Inc.

Lee, T., Kwon, J., & Park, F. C. (2018, Oct). A natural adaptive control law for robot manipulators. In *2018 ieee/rsj international conference on intelligent robots and systems (iros)* (p. 1-9). doi: 10.1109/IROS.2018.8593727

Lee, T., Wensing, P. M., & Park, F. C. (2019). Geometric robot dynamic identification: A convex programming approach. *IEEE Transactions on Robotics*, 1-18. doi: 10.1109/TRO.2019.2926491

Liu, X., Ortega, R., Su, H., & Chu, J. (2010). Immersion and invariance adaptive control of nonlinearly parameterized nonlinear systems. *IEEE Transactions on Automatic Control*, 55(9), 2209-2214.

Lohmiller, W., & Slotine, J.-J. E. (1998, June). On contraction analysis for non-linear systems. *Automatica*, 34(6), 683–696. doi: [http://dx.doi.org/10.1016/S0005-1098\(98\)00019-3](http://dx.doi.org/10.1016/S0005-1098(98)00019-3)

Luenberger, D. G. (1979). *Introduction to dynamic systems*. John Wiley & Sons.

Maddison, C. J., Paulin, D., Teh, Y. W., O'Donoghue, B., & Doucet, A. (2018). *Hamiltonian descent methods*.

Morse, A. S. (1992). High-order parameter tuners for the adaptive control of linear and nonlinear systems. In A. Isidori & T.-J. Tarn (Eds.), *Systems, models and feedback: Theory and applications: Proceedings of a u.s.-italy workshop in honor of professor antonio ruberti, capri, 15–17. june 1992* (pp. 339–364). Boston, MA: Birkhäuser Boston. doi: https://doi.org/10.1007/978-1-4612-2204-8_23

Muehlebach, M., & Jordan, M. I. (2019). *A dynamical systems perspective on nesterov acceleration*.

Muthukumar, V., Vodrahalli, K., & Sahai, A. (2019, July). Harmless interpolation of noisy data in regression. In *2019 ieee international symposium on information theory (isit)* (p. 2299-2303). doi: 10.1109/ISIT.2019.8849614

Narendra, K. S., & Annaswamy, A. M. (2005). *Stable adaptive systems*. Dover Publications.

Nemirovski, A., & Yudin, D. (1983). *Problem complexity and method efficiency in optimization*. Wiley.

Nesterov, Y. (1983). A Method for Solving a Convex Programming Problem with Convergence Rate $O(1/k^2)$. *Soviet Mathematics Doklady*, 26, 367-372.

O'Neill, M., & Wright, S. (2017, 06). Behavior of accelerated gradient methods near critical points of nonconvex problems. *Mathematical Programming*. doi: 10.1007/s10107-018-1340-y

Ortega, R. (1996). Some remarks on adaptive neuro-fuzzy systems. *International Journal of Adaptive Control and Signal Processing*, 10(1), 79-83.

Ortega, R., Gromov, V., Nuño, E., Pyrkin, A., & Romero, J. G. (2019). *Parameter estimation of nonlinearly parameterized regressions without overparameterization nor persistent excitation: Application to system identification and*

adaptive control.

Polyak, B. (1964). Some methods of speeding up the convergence of iteration methods. *USSR Computational Mathematics and Mathematical Physics*, 4(5), 1 - 17. doi: [https://doi.org/10.1016/0041-5553\(64\)90137-5](https://doi.org/10.1016/0041-5553(64)90137-5)

Polyak, B. T., & Juditsky, A. B. (1992). Acceleration of stochastic approximation by averaging. *SIAM Journal on Control and Optimization*, 30(4), 838-855. doi: <https://doi.org/10.1137/0330046>

Russo, G., & Slotine, J.-J. E. (2011, Oct). Symmetries, stability, and control in nonlinear systems and networks. *Phys. Rev. E*, 84, 041929. doi: [10.1103/PhysRevE.84.041929](https://doi.org/10.1103/PhysRevE.84.041929)

Sanner, R. M., & Slotine, J. . E. (1992, Nov). Gaussian networks for direct adaptive control. *IEEE Transactions on Neural Networks*, 3(6), 837-863. doi: [10.1109/72.165588](https://doi.org/10.1109/72.165588)

Shi, B., Du, S. S., Su, W. J., & Jordan, M. I. (2019). *Acceleration via symplectic discretization of high-resolution differential equations*.

Slotine, J.-J., & Coetsee, J. (1986). Adaptive sliding controller synthesis for non-linear systems. *International Journal of Control*, 43(6), 1631-1651. doi: <https://doi.org/10.1080/00207178608933564>

Slotine, J.-J., & Li, W. (1991). *Applied nonlinear control*. Prentice Hall.

Slotine, J.-J. E., & Li, W. (1987). On the adaptive control of robot manipulators. *The International Journal of Robotics Research*, 6(3), 49-59. doi: <https://doi.org/10.1177/027836498700600303>

Soudry, D., Hoffer, E., Nacson, M. S., Gunasekar, S., & Srebro, N. (2018, January). The implicit bias of gradient descent on separable data. *J. Mach. Learn. Res.*, 19(1), 2822-2878.

Su, W., Boyd, S., & Candès, E. J. (2016). A differential equation for modeling nesterov's accelerated gradient method: Theory and insights. *Journal of Machine Learning Research*, 17(153), 1-43.

Sussillo, D., & Abbott, L. F. (2009, Aug). Generating coherent patterns of activity from chaotic neural networks. *Neuron*, 63(4), 544-557.

Tabareau, N., Slotine, J.-J., & Pham, Q.-C. (2010, 01). How synchronization protects from noise. *PLOS Computational Biology*, 6(1), 1-9. doi: <https://doi.org/10.1371/journal.pcbi.1000637>

Tyukin, I. (2011). *Adaptation in dynamical systems*. Cambridge University Press.

Tyukin, I. Y. (2003, Jun 01). Adaptation algorithms in finite form for nonlinear dynamic objects. *Automation and Remote Control*, 64(6), 951-974. doi: <https://doi.org/10.1023/A:1024141700331>

Tyukin, I. Y., Prokhorov, D. V., & van Leeuwen, C. (2007, Sep.). Adaptation and parameter estimation in systems with unstable target dynamics and nonlinear parametrization. *IEEE Transactions on Automatic Control*, 52(9), 1543-1559. doi: [10.1109/TAC.2007.904448](https://doi.org/10.1109/TAC.2007.904448)

Wang, W., & Slotine, J.-J. E. (2005, January). On partial contraction analysis for coupled nonlinear oscillators. *Biol. Cybern.*, 92(1), 38-53. doi: <https://doi.org/10.1007/s00422-004-0527-x>

Wensing, P. M., Kim, S., & Slotine, J. E. (2018). Linear matrix inequalities for physically consistent inertial parameter identification: A statistical perspective on the mass distribution. *IEEE Robotics and Automation Letters*, 3(1), 60-67. doi: [10.1109/LRA.2017.2729659](https://doi.org/10.1109/LRA.2017.2729659)

Wensing, P. M., & Slotine, J.-J. E. (2017). *Cooperative adaptive control for cloud-based robotics*.

Wensing, P. M., & Slotine, J.-J. E. (2018). *Contraction analysis of geodesically convex optimization*.

Wibisono, A., Wilson, A. C., & Jordan, M. I. (2016). A variational perspective on accelerated methods in optimization. *Proceedings of the National Academy of Sciences*, 113(47), E7351-E7358. doi: [10.1073/pnas.1614734113](https://doi.org/10.1073/pnas.1614734113)

Wilson, A. C., Recht, B., & Jordan, M. I. (2016). *A lyapunov analysis of momentum methods in optimization*.

Zhang, S., Choromanska, A., & LeCun, Y. (2014). *Deep learning with elastic averaging sgd*.